The Meteoritical Society

Meteoritics & Planetary Science 47, Nr 8, 1365–1402 (2012)
doi: 10.1111/j.1945-5100.2012.01393.x

Invited Review

Lunar meteorites from Oman

Randy L. KOROTEV

Department of Earth and Planetary Sciences and McDonnell Center for the Space Sciences, Washington University, Saint Louis, Missouri 63130, USA
E-mail: korotev@wustl.edu

(Received 06 February 2012; revision accepted 13 June 2012)

Abstract–Sixty named lunar meteorite stones representing about 24 falls have been found in Oman. In an area of 10.7×10^3 km^2 in southern Oman, lunar meteorite areal densities average 1 g km^{-2}. All lunar meteorites from Oman are breccias, although two are dominated by large igneous clasts (a mare basalt and a crystalline impact-melt breccia). Among the meteorites, the range of compositions is large: 9–32% Al_2O_3, 2.5–21.1% FeO, 0.3–38 μg g^{-1} Sm, and <1 to 22.5 ng g^{-1} Ir. The proportion of nonmare lunar meteorites is higher among those from Oman than those from Antarctica or Africa. Omani lunar meteorites extend the compositional range of lunar rocks as known from the Apollo collection and from lunar meteorites from other continents. Some of the feldspathic meteorites are highly magnesian (high MgO/[MgO + FeO]) compared with most similarly feldspathic Apollo rocks. Two have greater concentrations of incompatible trace elements than all but a few Apollo samples. A few have moderately high abundances of siderophile elements from impacts of iron meteorites on the Moon. All lunar meteorites from Oman are contaminated, to various degrees, with terrestrial Na, K, P, Zn, As, Se, Br, Sr, Sb, Ba, U, carbonates, or sulfates. The contamination is not so great, however, that it seriously compromises the scientific usefulness of the meteorites as samples from randomly distributed locations on the Moon.

INTRODUCTION

At this writing, 2649 named meteorite stones found in the Sultanate of Oman are listed in the database of the Meteoritical Society (*Meteoritical Bulletin Database*, 2012). By comparison, only 38 and 21 meteorites are listed for Italy and Poland, which are each about the same size as Oman. Remarkably, a total of 60 named stones from Oman representing, as reasoned in this paper, 17–25 meteorites are from the Moon (Figs. 1 and 2). The fraction of lunar meteorites among all meteorites reported from Oman, 2.3% (by stone name), vastly overestimates the proportion of lunar meteorites among all meteorites having fallen in Oman (or, on Earth) in part because finders seek the rare achondrites and many of the ordinary chondrites from Oman are never (or have not yet been; Hofmann et al. 2011) classified and named. In comparison, 33 lunar meteorite stones representing about 20 falls have been found in Antarctica by expeditions sponsored by various governments and only 0.11% of all meteorite stones found in Antarctica are of lunar origin. Thus, the country of Oman has provided a treasure trove of lunar meteorites comparable to that of the continent of Antarctica. (For Martian meteorites, 13 stones representing about 4 falls have been found in Oman.)

The geology and climate of Oman, as they relate to meteorite finds, are reviewed by Al-Kathiri et al. (2005). Briefly, the area of meteorite concentration (Dhofar stones) is a flat Tertiary limestone plain with little vegetation. All meteorites discussed here were found at elevations ranging from 109 m (Sayh al Uhaymir in the northeast; Fig. 1) to 295 m (Shişr 160 in the southwest). Summer temperatures can reach 50 °C and the mean annual precipitation is <10 cm. Most precipitation in

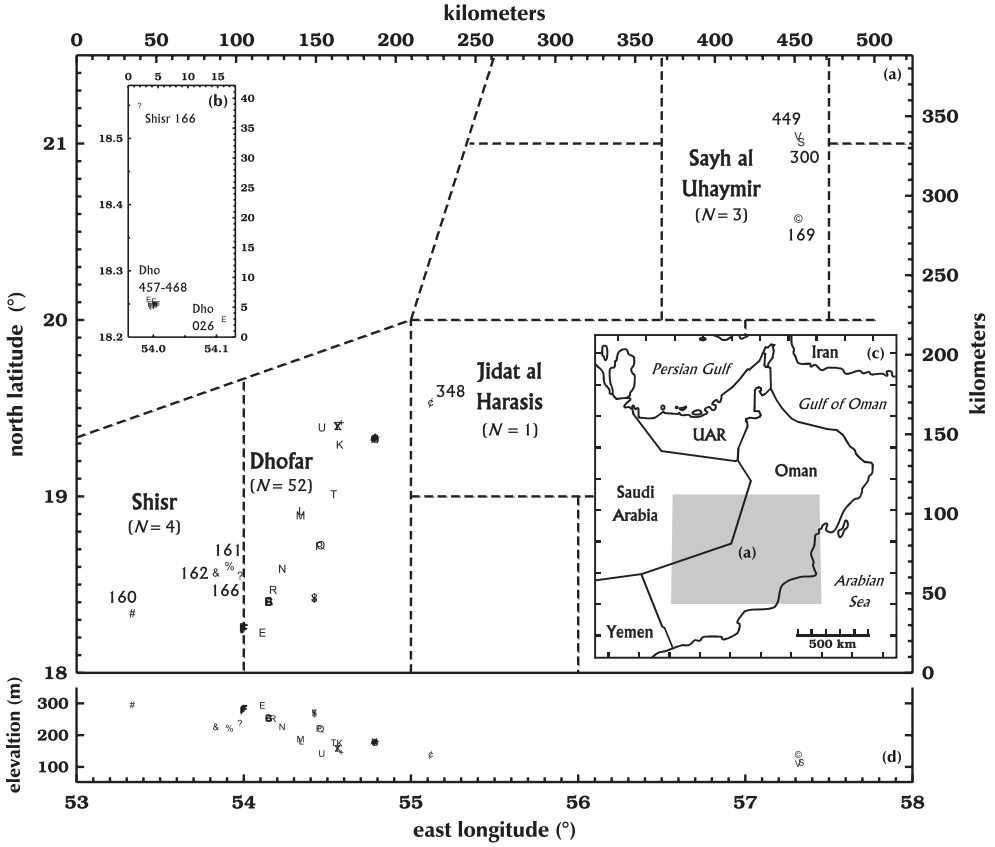

Fig. 1. (a) Reported locations of lunar meteorite finds from Oman. Name boundaries are from the Meteoritical Society (Al-Kathiri et al. 2005). The number in parentheses is the number of named stones. A minimum area, convex polygon enclosing the lunar meteorite find sites has an area of 3.0×10^4 km^2, about the size of Belgium or the state of Maryland. (b) Relationship of paired stones Dhofar 026 and Dhofar 457–468 with possibly paired stone Shişr 166. (c) Regional map. The gray rectangle is the location of map (a). (d) Elevations above sea level of find locations range over only 186 m.

southern Oman is from monsoons from the Indian Ocean to the south.

This work summarizes and synthesizes information about the lunar meteorites from Oman. The emphasis is mainly on composition because there are more compositional data available for the meteorites than there are geochronological, CRE (cosmic-ray exposure), or detailed petrographic data. The paper builds on works of Nazarov et al. (2004) and Demidova et al. (2007) and incorporates new data presented here, data that I and colleagues have published in earlier works (Table 1), and data from other published studies. Some of the new data presented here have been presented in preliminary reports (Bunch et al. 2006; Korotev 2006; Korotev and Zeigler 2007; Foreman et al. 2008, 2009; Korotev et al. 2008, 2009a, 2012).

This review comes with two caveats. (1) Although the compositional data presented here are self-consistent because they were all obtained in one laboratory, available petrographic descriptions are not self-consistent because they have been made by many persons. In Table 1, I oversimplify and put all the brecciated meteorites into four bins, regolith breccia, fragmental breccia, granulitic breccia, and impact-melt breccia, following the "recommended classification" of Stöffler et al. (1980) and my interpretation of the petrographic descriptions. Some of these classifications may be wrong. See Cohen et al. (2004) and Warren et al. (2005) for discussions of some of the gray areas and pitfalls associated with petrographic classification of lunar breccias. (2) The discussion assumes that find locations and masses, as reported in *The Meteoritical Bulletin*, are accurate. Because lunar meteorites are valuable commodities, it is possible that at least some of the reported find locations and masses are inaccurate.

SAMPLES AND ANALYSIS

Most of the samples of this study (Table 1) the author purchased from dealers. Some were donated, and a few are subsamples of the type specimens (Dhofar 1180, Dhofar 1428, Dhofar 1627, JaH [Jiddat al Harasis] 348, SaU [Sayh al Uhaymir] 169, SaU 300, Shişr 161, Shişr 162, and Shişr 166). Most of the samples were received in the form of sawn slices 1–2 mm thick.

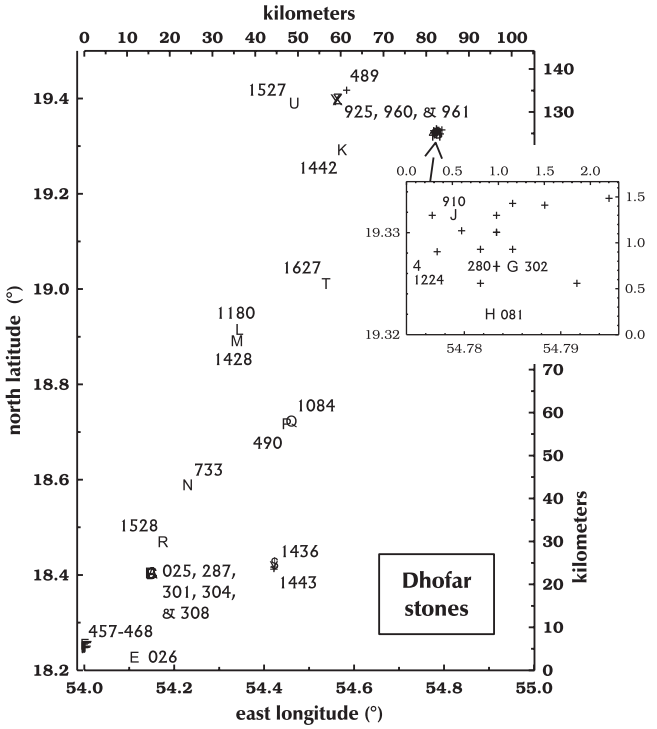

Fig. 2. Reported locations of Dhofar lunar meteorite finds. In the inset, the + symbol represents 14 paired stones: Dhofar 303, 305, 306, 307, 309, 310, 311, 730, 731, 908, 909, 911, 950, and 1085. Symbol "4" represents Dhofar 1224. The key to other symbols is in Table 1. After fig. 14 of Korotev et al. (2006), but with a corrected kilometer scales.

The analytical procedures are the same as those described in Korotev et al. (2009b). Briefly, after photographing samples, I break them into multiple subsamples typically of 20–35 mg each and obtain data for 29 mostly trace elements by INAA (instrumental neutron activation analysis). The data presented here and in previous papers (Table 1) were collected from samples irradiated in 18 different neutron irradiations between 2001 and 2011. For meteorites for which there are no previously published data from my laboratory, mass-weighted mean concentrations from all INAA subsamples of each stone or meteorite are presented in Table 2; data for individual subsamples are presented in figures and tabulated in the electronic annex (Data S1). After radioassay, some of the INAA samples were pulverized, fused to glass, and analyzed by EPMA (electron probe microanalysis) for concentrations of major and minor elements. Mean results are presented in Table 3.

PRESENTATION

A major focus of this paper is establishing compositional similarities and differences among meteorites. For this purpose, some elements are more useful than others. Six features account for most of the compositional variation among lunar meteorites: (1) the ratio of plagioclase to pyroxene plus olivine (Al_2O_3/[FeO + MgO]); (2) the ratio of olivine to pyroxene, which increases with increasing whole-rock Mg' (mole percent MgO/[MgO + FeO]; Korotev et al. 2003); (3) the albite content of the plagioclase (correlates with Na_2O and Eu concentrations); (4) the relative abundance of KREEP lithologies (correlates with K, rare earth elements, P, Th, U, etc., abundances); (5) for basaltic meteorites, the relative abundance of ilmenite (TiO_2); and (6) the fraction of asteroidal meteorite material (siderophile elements). Unfortunately, the INAA procedure used here does not provide data for TiO_2, Al_2O_3, or MgO, but some "INAA elements" provide useful proxies for these elements. For example, Sc correlates with pyroxene abundance. As a consequence, the Al_2O_3 concentrations of Table 3 anticorrelate with the corresponding Sc concentrations of Table 2 (R^2 = 0.966), which allows for the "approximately Al_2O_3" alternate axis of Fig. 3. Also, unlike for Fe, the Sc concentration is not significantly affected by the presence of asteroidal meteoritic material (Fig. 4). As noted below, a large fraction of the total iron in some subsamples is metallic (52% in one subsample of Dhofar 1527). High Sc concentrations in feldspathic lunar breccias are often a result of the presence of mare basalt or glass, which range from 40 to 100 μg g^{-1} in Sc. Cr/Sc (Fig. 5), which varies by a factor of three among the meteorites, serves as proxy for MgO/FeO or Mg' (Korotev et al. 1996; Fig. 6). Small differences in the albite content of plagioclase are reflected by bulk concentrations of Na and Eu, both of which are determined with high precision in INAA (Figs. 7 and 8). Samarium is a representative element associated with KREEP, one also determined precisely by INAA. Sm-Sc diagrams (Fig. 3) have long been useful for classification and depiction of mixing relationships for lunar samples (e.g., Korotev 1982, 1987, 1996, 1997; McKay et al. 1986; Jolliff et al. 1996). FeO-Th (Fig. 4) provides a similar picture and has the comparative advantage that both elements have been measured on the lunar surface from orbit (e.g., Korotev et al. 2009). The diagonal trend of data on Figs. 3 and 4 is mainly a mixing effect between anorthosite materials with low concentrations of FeO, Sc, Sm, and Th of the Feldspathic Highlands Terrane and noritic material with moderately high concentrations of FeO and Sc and high concentrations of Sm and Th such as that from the Procellarum KREEP Terrane (Korotev 2005). Among siderophile elements, Ni, Ir, and Au are determined adequately by INAA (Table 2) and Ni/Ir provided some information about the identity of the extralunar material contained in the lunar meteorite.

METEORITE REVIEW

This section reviews the Omani lunar meteorites in alphanumeric order of the lowest numbered stone in

Table 1. Lunar meteorites from Oman and samples analyzed by INAA in this laboratory.

S/N	Plot symbol	Meteorite	Mass (g)	INAA mass (mg)	*N* of INAA subsamples	Rock type	Data sources
1	A/B/C	Dho 025/301/304/308	772	73/205/74/0	3/8/3/0	RB	1,5
2	E/F	Dho 026/461 (457–468)	709	176/38	6/2	IMB or GB	4,5
3	H/I/J	Dho 081/280/910/1224	571.8	252/103/227/0	8/4/10/0	FB or RB	5
4	D	Dho 287	154	196	6	MB & RB	5
5	G	Dho 302	3.8	87	3	IMB	5
6	+	Dho 303/305/306/307/ 308/309/310/311/489/730/ 731/908/911/950/1085	1037	1200	2/8/3/0 0/2/6/0/9/0 0/4/4/0/4 = 42	IMB	2
7	P/Q	Dho 490/1084	124	98/135	4/5	FB	5
8	N	Dho 733	98	32	2	GB	4,5
9	X/Y/Z	Dho 925/960/961	106	51/138/256	2/6/10	RB	3,5
10	L	Dho 1180	115.2	196	9	RB	3
11	M	Dho 1428	213	224	8	RB	5
12	$/¥	Dho 1436/1443	60.9	269/250	8/8	IMB	5
13	K	Dho 1442	106.5	324	16	RB	3,5
14	U	Dho 1527	42.6	168	7	IMB	5
15	R	Dho 1528	213.2	174	7	IMB	5
16	T	Dho 1627	86.14	394	13	IMB	5
17	¢	JaH 348	18.4	238	8	IMB	5
18	©/®	SaU 169 IMB/RB	206.45	394	17	IMB & RB	3
19	S	SaU 300	152.6	321	11	IMB	3
20	V	SaU 449	16.5	237	8	RB	3,5
21	#	Shişr 160	100.86	170	6	RB	5
22	%	Shişr 161	57.2	294	10	RB	5
23	&	Shişr 162	5525	368	12	IMB	5
24	?	Shişr 166	128.8	241	8	IMB	5
		Total	10533	7613	280		

"mass" = total reported mass of all stones of the meteorite. FB = fragmental breccia, GB = granulitic breccia, IMB = impact-melt breccia, MB = mare basalt, RB = regolith breccia. Sources of data: (1) Korotev et al. (2003a), (2) Korotev et al. (2006), (3) Korotev et al. (2009), (4) Hudgins et al. (2011), and (5) this work.

each pairing group. In the headers, the letters, numbers, or symbols in square brackets refer to the plot symbols in figures (also presented in Table 1 and Fig. 3).

Dhofar 025 [A], 301 [B], 304 [C], and 308

Dhofar 025, one of the largest lunar meteorite stones from Oman (751 g), is well described by Cahill et al. (2004) and Warren et al. (2005). Demidova et al. (2003a) and Nazarov et al. (2003, 2004) hypothesize that small Dhofar stones 301 (9 g) and 304 (10 g) are probably paired with Dhofar 025 because of proximity of find locations and similarity of mineral chemistry and matrix composition. Tiny Dhofar 308 (2 g) is also assumed to be part of the pairing group on the basis of proximity and composition (Russell et al. 2003; Demidova et al. 2007).

Data for Dhofar 301 (eight subsamples) and Dhofar 304 (three subsamples) are consistent with the pairing hypothesis in that the compositions of the two stones are more similar to that of Dhofar 025 (three subsamples; Korotev et al. 2003a) than any other Dhofar stones (Figs. 4, 5, and 7). The meteorite is characterized by having moderately high concentrations of ITEs (incompatible trace elements) among feldspathic lunar meteorites from Oman (Fig. 3). I have not studied Dhofar 308; for most INAA elements, the data of Demidova et al. (2007) are in the range of the data for Dhofar 025, 301, and 304 presented here. Concentrations they report for Na_2O, FeO, Co, Zr, and Ir are outside the range of data presented here, however, and all are higher.

Dhofar 025 is a regolith breccia, but with much lower concentrations (approximately 0.01×) of solar noble gasses than the most gas-rich lunar meteorites (Shukolyukov et al. 2001). Leont'eva et al. (2005) obtained U-Pb data from a zircon in Dhofar 025. They interpret the data to indicate that the zircon crystallized from a "felsic" melt 4360 ± 27 Ma ago and that breccia formation occurred about 2000 Myr ago. The most precise ^{40}Ar-^{39}Ar age for a clast of impact-melt breccia in Dhofar 025 obtained by Fernandes et al. (2004) is 3310 ± 240 Ma.

As noted by Nazarov et al. (2003), the meteorite is the most seriously enriched in Sr and Ba from terrestrial

Table 2. Mass-weighted mean results of neutron activation analysis.

Meteorite	Na_2O %	CaO %	Sc μg g^{-1}	Cr μg g^{-1}	FeO_T %	Co μg g^{-1}	Ni μg g^{-1}	As[a] μg g^{-1}	Se[a] μg g^{-1}	Br[a] μg g^{-1}
Dhofar 026/461[b]	0.326	16.4	7.73	607	4.28	15.5	162	< 0.3	< 0.3	0.13
± 1	0.003	0.2	0.08	8	0.04	0.2	9	–	–	0.07
± 2	0.004	0.1	0.37	37	0.14	0.6	14	–	–	0.04
Dhofar 301	0.336	15.5	8.82	804	4.70	16.6	125	0.65	0.39	0.46
Dhofar 304	0.337	15.6	9.26	747	4.57	17.0	116	1.03	0.32	0.38
Dhofar 025/301/304	0.338	15.5	9.12	784	4.69	16.4	124	0.63	0.56	0.58
± 1	0.003	0.2	0.09	8	0.05	0.2	9	0.08	0.10	0.06
± 2	0.006	0.2	0.59	52	0.17	1.0	16	0.31	0.08	0.06
Dhofar 081	0.326	16.8	4.80	372	2.75	8.48	77	< 0.4	< 0.5	0.08
Dhofar 910	0.328	17.6	4.45	323	2.50	6.90	49	< 0.3	< 0.3	0.13
Dhofar 081/910	0.327	17.2	4.62	346	2.62	7.65	63	< 0.3	0.06	0.11
± 1	0.003	0.2	0.05	3	0.03	0.08	5	–	0.05	0.07
± 2	0.003	0.2	0.05	3	0.03	0.08	5	–	0.05	0.07
Dhofar 280	0.352	17.8	6.92	460	3.57	10.96	103	< 0.6	0.24	0.23
± 1	0.004	0.2	0.09	6	0.04	0.12	6	–	0.10	0.16
± 2	0.004	0.2	0.54	45	0.30	1.06	13	–	0.03	0.03
Dhofar 081/280/910	0.331	17.3	5.03	366	2.79	8.23	70	< 0.6	0.10	0.13
Dhofar 287	0.490	10.5	39.5	4260	21.1	53.3	115	< 2	< 0.4	0.7
± 1	0.005	0.5	0.4	45	0.2	0.5	32	–	–	0.3
± 2	0.022	0.7	2.0	540	0.4	2.9	14	–	–	0.2
Dhofar 302	0.341	16.4	5.22	485	3.16	11.38	92	0.29	0.16	0.21
± 1	0.003	0.2	0.05	5	0.03	0.11	6	0.06	0.07	0.05
± 2	0.021	0.5	0.51	158	0.39	1.93	29	0.23	0.09	0.06
Dhofar 490	0.323	19.9[a]	6.61	488	3.73	18.5	246	0.59	0.39	0.34
Dhofar 1084	0.344	18.4[a]	6.93	525	4.00	18.6	251	0.14	0.43	0.34
Dhofar 490/1084	0.335	19.0[a]	6.79	509	3.89	18.6	249	0.33	0.41	0.34
± 1	0.003	0.2	0.07	5	0.04	0.2	8	0.14	0.11	0.08
± 2	0.011	0.8	0.19	18	0.14	0.6	13	0.19	0.08	0.06
Dhofar 960	0.334	14.3	16.83	1406	7.86	39.1	434	0.8	< 1	0.3
Dhofar 925/960	0.329	14.5	16.76	1390	7.74	37.0	410	0.65	0.38	0.30
± 1	0.003	0.3	0.17	15	0.08	0.4	35	0.14	0.25	0.13
± 2	0.011	0.4	1.10	40	0.38	6.7	111	0.20	0.16	0.12
Dhofar 961	0.377	13.6	27.4	1960	11.04	53.6	630	0.70	0.71	0.55
± 1	0.004	0.4	0.3	20	0.11	0.5	20	0.24	0.30	0.28
± 2	0.035	0.5	3.1	190	0.97	15.6	210	0.13	0.21	0.08
Dhofar 925/960/961	0.334	14.4	18.88	1494	8.30	38.5	433	0.57	0.39	0.39
Dhofar 1428	0.369	16.1	8.06	596	4.20	15.87	180	0.26	0.30	0.88
± 1	0.004	0.2	0.08	6	0.04	0.16	9	0.09	0.10	0.11
± 2	0.013	0.2	0.88	27	0.22	1.57	35	0.07	0.06	0.17
Dhofar 1436	0.357	15.4	12.7	1004	5.62	15.5	120	0.4	0.3	0.5
Dhofar 1443	0.368	15.9	12.25	881	5.52	14.4	93	< 0.4	–	0.42
Dhofar 1436/1443	0.362	15.6	12.46	945	5.57	14.94	110	0.34	–	0.48
± 1	0.004	0.3	0.13	9	0.06	0.15	20	0.11	0.05	0.09
± 2	0.005	0.2	0.34	87	0.11	0.62	20	0.09	0.10	0.07
Dhofar 1442	0.800	11.9	31.3	1660	13.74	48.6	664	< 2	< 4	< 2
Dhofar 1527	0.336	14.4	14.00	1176	7.95	80.4	1192	0.56	0.48	0.42
± 1	0.003	0.3	0.14	12	0.08	0.8	22	0.14	0.22	0.10
± 2	0.006	0.4	0.55	47	1.78	61.8	956	0.18	0.26	0.05
Dhofar 1528	0.405	13.5	11.66	1277	6.05	27.1	264	0.53	0.29	1.36
± 1	0.004	0.2	0.12	13	0.06	0.3	15	0.12	0.26	0.18
± 2	0.012	0.4	0.58	90	0.26	1.8	22	0.12	0.11	0.13
Dhofar 1627	0.570	14.4	9.60	848	5.74	33.3	526	0.60	0.3	0.19
± 1	0.006	0.3	0.10	8	0.06	0.3	20.5	0.22	0.3	0.16
± 2	0.023	0.3	0.14	37	0.14	2.0	44.7	0.08	0.1	0.06

Table 2. *Continued*. Mass-weighted mean results of neutron activation analysis.

Meteorite	Na_2O %	CaO %	Sc μg g^{-1}	Cr μg g^{-1}	FeO_T %	Co μg g^{-1}	Ni μg g^{-1}	As[a] μg g^{-1}	Se[a] μg g^{-1}	Br[a] μg g^{-1}
JaH 348	0.340	16.2	12.31	853	5.51	12.86	74	< 0.5	0.32	0.17
± 1	0.003	0.2	0.12	9	0.06	0.13	10	–	0.11	0.10
± 2	0.004	0.2	0.30	96	0.10	0.62	27	–	0.08	0.05
Shişr 160	0.339	17.2	7.17	560	3.90	16.27	212	0.26	0.42	0.33
± 1	0.003	0.3	0.07	6	0.04	0.16	9	0.06	0.10	0.06
± 2	0.010	0.6	0.60	124	0.19	0.73	14	0.04	0.03	0.05
Shişr 161	0.319	15.0	13.05	1118	5.94	16.81	88	0.64	0.30	0.52
± 1	0.003	0.3	0.13	11	0.06	0.17	11	0.10	0.11	0.12
± 2	0.005	0.2	0.73	42	0.19	0.98	10	0.08	0.09	0.06
Shişr 162	0.408	15.3	5.32	428	3.15	14.74	151	0.21	0.05	0.12
± 1	0.004	0.2	0.05	4	0.03	0.15	11	0.08	0.02	0.08
± 2	0.013	0.3	0.24	43	0.31	6.84	98	0.07	0.05	0.04
Shişr 166	0.323	16.5		605	4.13	14.28	141	0.15	0.18	0.28
± 1	0.003	0.3	0.08	6	0.04	0.14	10	0.08	0.11	0.09
± 2	0.006	0.3	0.20	10	0.08	0.52	9	0.06	0.05	0.10

Meteorite	Sr μg g^{-1}	Zr μg g^{-1}	Sb[a] μg g^{-1}	Cs μg g^{-1}	Ba μg g^{-1}	La μg g^{-1}	Ce μg g^{-1}	Nd μg g^{-1}	Sm μg g^{-1}	Eu μg g^{-1}	Tb μg g^{-1}
Dhofar 026/461[b]	208	32	0.01	0.04	65	2.47	6.47	4.1	1.166	0.747	0.245
± 1	8	8	0.01	0.01	3	0.02	0.10	0.7	0.011	0.008	0.006
± 2	88	6	0.04	0.06	45	0.17	0.43	0.4	0.103	0.007	0.020
Dhofar 301	3738	52	0.05	0.04	597	4.03	10.3	6.2	1.765	0.822	0.368
Dhofar 304	3904	35	0.05	0.04	1438	3.11	7.9	4.8	1.382	0.808	0.291
Dhofar 025/301/304	3432	48	0.047	0.039	673	3.68	9.50	5.7	1.687	0.818	0.345
± 1	35	8	0.008	0.017	8	0.04	0.10	0.6	0.017	0.009	0.007
± 2	888	11	0.014	0.008	433	0.58	1.57	1.0	0.266	0.016	0.056
Dhofar 081	178	9	< 0.02	< 0.06	13	0.646	1.7	1	0.324	0.751	0.074
Dhofar 910	169	8	< 0.02	< 0.05	13	0.631	1.7	1.2	0.322	0.761	0.071
Dhofar 081/910	174	9	< 0.2	< 0.06	13	0.639	1.70	1.1	0.323	0.756	0.072
± 1	6	10	–	–	2	0.008	0.05	0.4	0.003	0.008	0.004
± 2	6	10	–	–	2	0.008	0.05	0.4	0.003	0.008	0.004
Dhofar 280	279	25	< 0.3	< 0.08	42	2.026	5.14	3.1	0.900	0.776	0.207
± 1	7	7	–	–	3	0.024	0.07	0.5	0.011	0.008	0.005
± 2	5	2	–	–	1	0.080	0.22	0.2	0.042	0.006	0.009
Dhofar 081/280/910	192	12	0.004	0.013	18	0.884	2.3	1.5	0.425	0.760	0.096
Dhofar 287	800	147	< 1.2	< 0.3	159	12.09	32.3	22.8	7.18	1.41	1.46
± 1	30	28	–	–	11	0.12	1.0	2.6	0.07	0.03	0.03
± 2	370	24	–	–	69	1.39	3.7	3.6	0.77	0.11	0.16
Dhofar 302	413	28	0.03	0.033	98	2.14	5.56	3.4	0.969	0.788	0.202
± 1	6	5	0.01	0.008	2	0.02	0.07	0.4	0.010	0.008	0.005
± 2	277	9	0.01	0.010	45	0.49	1.25	0.7	0.208	0.060	0.048
Dhofar 490	432	39	< 0.04	0.04	90	2.78	7.2	4.5	1.285	0.754	0.265
Dhofar 1084	775	37	< 0.04	0.03	39	2.86	7.5	4.6	1.325	0.787	0.279
Dhofar 490/1084	631	38	0.012	0.037	61	2.82	7.4	4.5	1.323	0.773	0.273
± 1	9	7	0.010	0.017	3	0.03	0.1	0.5	0.013	0.009	0.006
± 2	223	3	0.009	0.006	23	0.09	0.2	0.2	0.043	0.020	0.010
Dhofar 960	458	61	< 0.1	< 0.4	180	5.16	14.0	7.3	2.285	0.723	0.479
Dhofar 925/960	435	61	0.040	0.08	157	4.86	13.0	7.2	2.18	0.718	0.47
± 1	35	32	0.016	0.07	9	0.05	0.4	1.7	0.02	0.029	0.03
± 2	75	8	0.019	0.02	49	1.00	2.9	1.4	0.38	0.017	0.07
Dhofar 961	1220	240	0.024	0.23	338	16.73	43.5	25.1	7.47	0.844	1.55
± 1	30	30	0.021	0.03	8	0.17	0.5	1.6	0.08	0.018	0.02

Table 2. *Continued*. Mass-weighted mean results of neutron activation analysis.

Meteorite	Sr μg g^{-1}	Zr μg g^{-1}	Sb[a] μg g^{-1}	Cs μg g^{-1}	Ba μg g^{-1}	La μg g^{-1}	Ce μg g^{-1}	Nd μg g^{-1}	Sm μg g^{-1}	Eu μg g^{-1}	Tb μg g^{-1}
±2	441	100	0.011	0.08	101	6.51	16.9	9.6	2.85	0.138	0.57
Dhofar 925/960/961	574	97	0.05	0.12	172	7.00	18.3	10.7	3.168	0.739	0.674
Dhofar 1428	543	33	0.004	0.042	48	2.55	6.71	3.9	1.252	0.733	0.273
±1	9	8	0.010	0.013	3	0.03	0.10	0.7	0.013	0.009	0.007
±2	63	5	0.003	0.007	4	0.36	0.97	0.8	0.228	0.013	0.054
Dhofar 1436	1407	30	< 0.05	< 0.1	269	2.37	6.2	3.8	1.160	0.812	0.257
Dhofar 1443	1319	34	< 0.05	< 0.1	130	2.31	6.2	3.8	1.131	0.842	0.242
Dhofar 1436/1443	1360	32	0.019	0.029	202	2.34	6.2	3.8	1.146	0.826	0.250
±1	30	21	0.014	0.022	7	0.02	0.2	1.2	0.011	0.020	0.013
±2	170	3	0.008	0.008	61	0.12	0.3	0.3	0.051	0.014	0.013
Dhofar 1442	1125	1220	< 0.2	0.76	928	83.7	220.	124.	38.4	2.61	7.77
Dhofar 1527	514	40	0.070	0.073	79	2.28	6.27	3.8	1.092	0.693	0.244
±1	16	23	0.011	0.043	6	0.02	0.18	1.3	0.011	0.015	0.012
±2	80	13	0.007	0.012	12	0.08	0.23	0.4	0.045	0.018	0.012
Dhofar 1528	603	62	0.010	0.134	91	4.99	13.0	6.9	2.19	0.766	0.486
±1	16	14	0.013	0.022	5	0.05	0.2	1.1	0.02	0.013	0.014
±2	94	6	0.004	0.012	10	0.40	1.0	0.6	0.16	0.011	0.045
Dhofar 1627	1363	234	0.027	0.19	291	16.9	44.3	25.4	7.75	1.293	1.52
±1	22.5	17	0.019	0.03	8	0.2	0.4	1.7	0.08	0.021	0.02
±2	598	14	0.009	0.02	31	1.1	2.8	1.8	0.48	0.015	0.09
JaH 348	330	22	0.012	0.027	48	1.68	4.43	2.8	0.855	0.777	0.196
±1	11	14	0.012	0.032	4	0.02	0.12	0.9	0.009	0.010	0.007
±2	75	5	0.006	0.007	15	0.11	0.32	0.4	0.048	0.014	0.013
Shişr 160	248	23	0.015	0.021	68	1.81	4.60	3.2	0.864	0.770	0.176
±1	8	8	0.007	0.018	3	0.02	0.09	0.6	0.009	0.009	0.006
±2	12	9	0.008	0.008	14	0.16	0.41	0.5	0.081	0.014	0.017
Shişr 161	1106	16	0.025	0.025	273	1.186	3.24	1.9	0.642	0.639	0.153
±1	15	20	0.011	0.031	5	0.015	0.14	0.9	0.006	0.010	0.008
±2	137	6	0.007	0.013	95	0.056	0.15	0.3	0.030	0.011	0.010
Shişr 162	961	15	0.005	0.033	47	1.22	3.33	1.9	0.550	0.888	0.119
±1	14	13	0.011	0.020	3	0.01	0.11	0.6	0.005	0.014	0.007
±2	430	4	0.002	0.008	19	0.13	0.40	0.3	0.052	0.014	0.010
Shişr 166	210	38	0.014	0.022	83	2.57	6.74	4.2	1.222	0.744	0.254
±1	8	8	0.012	0.022	4	0.03	0.10	0.8	0.012	0.009	0.008
±2	43	4	0.007	0.017	66	0.10	0.16	0.5	0.027	0.014	0.008

Meteorite	Yb μg g^{-1}	Lu μg g^{-1}	Hf μg g^{-1}	Ta μg g^{-1}	Ir ng g^{-1}	Au ng g^{-1}	Th μg g^{-1}	U[a] μg g^{-1}	mass mg
Dhofar 026/461[b]	0.926	0.130	0.90	0.11	6.4	10.6	0.40	0.13	213.8
±1	0.011	0.002	0.02	0.01	0.5	0.6	0.01	0.03	
±2	0.072	0.011	0.12	0.02	0.6	1.6	0.05	0.02	
Dhofar 301	1.406	0.197	1.38	0.16	3.9	3.8	0.647	0.39	205.2
Dhofar 304	1.123	0.160	1.00	0.12	3.9	6.5	0.447	0.28	74.2
Dhofar 025/301/304	1.320	0.186	1.27	0.14	3.8	5.1	0.579	0.33	352.3
±1	0.014	0.002	0.02	0.01	0.4	0.6	0.012	0.03	
±2	0.216	0.030	0.24	0.03	0.3	1.5	0.113	0.07	
Dhofar 081	1.406	0.197	1.38	0.16	3.9	3.8	0.647	0.39	205.2
Dhofar 910	1.123	0.160	1.00	0.12	3.9	6.5	0.447	0.28	74.2
Dhofar 081/910	0.296	0.0420	0.244	0.030	3.2	0.8	0.1	< 0.11	479.7
±1	0.006	0.0010	0.009	0.006	0.3	0.7	0.0	0.03	
±2	0.006	0.0010	0.009	0.006	0.3	0.7	0.0	0.03	
Dhofar 280	0.770	0.1086	0.662	0.086	9.5	3.6	0.4	0.15	102.8

Table 2. *Continued*. Mass-weighted mean results of neutron activation analysis.

Meteorite	Yb μg g^{-1}	Lu μg g^{-1}	Hf μg g^{-1}	Ta μg g^{-1}	Ir ng g^{-1}	Au ng g^{-1}	Th μg g^{-1}	U[a] μg g^{-1}	mass mg
±1	0.010	0.0017	0.013	0.007	0.4	0.5	0.0	0.02	
±2	0.038	0.0056	0.041	0.005	0.8	0.4	0.0	0.01	
Dhofar 081/280/910	0.380	0.054	0.32	0.04	4.3	1.3	0.14	0.05	582.5
Dhofar 287	4.34	0.604	4.15	0.75	< 4	15[a]	0.89	0.60	195.7
±1	0.05	0.009	0.06	0.04	–	2	0.04	0.09	
±2	0.40	0.052	0.44	0.08	–	13	0.10	0.18	
Dhofar 302	0.755	0.106	0.711	0.090	2.5	4.2	0.331	0.17	86.7
±1	0.009	0.001	0.011	0.007	0.3	0.4	0.008	0.02	
±2	0.145	0.020	0.165	0.017	1.0	4.4	0.074	0.11	
Dhofar 490	0.970	0.137	1.03	0.11	11.2	5.8	0.43	0.33	98.1
Dhofar 1084	1.013	0.143	0.99	0.12	10.9	2.9	0.44	0.14	135.4
Dhofar 490/1084	0.995	0.140	1.005	0.116	11.0	4.1	0.437	0.22	233.5
±1	0.010	0.002	0.015	0.010	0.5	0.5	0.010	0.02	
±2	0.032	0.005	0.060	0.006	0.5	1.3	0.018	0.08	
Dhofar 960	2.00	0.279	1.76	0.24	17.4	13.1	1.02	0.50	137.8
Dhofar 925/960	1.95	0.272	1.72	0.23	17.6	14.6	1.00	0.48	188.9
±1	0.02	0.004	0.05	0.05	1.8	1.1	0.04	0.04	
±2	0.23	0.032	0.27	0.03	5.2	4.0	0.16	0.06	
Dhofar 961	5.87	0.815	5.85	0.67	17.8	12.0	3.08	1.04	255.6
±1	0.06	0.008	0.06	0.04	1.1	1.1	0.04	0.06	
±2	2.00	0.271	2.35	0.27	6.7	3.8	1.18	0.31	
Dhofar 925/960/961	2.71	0.376	2.52	0.32	17.9	15.4	1.40	0.58	444.6
Dhofar 1428	1.022	0.143	0.911	0.110	7.0	2.2	0.407	0.16	224.3
±1	0.012	0.002	0.016	0.009	0.5	0.6	0.013	0.03	
±2	0.209	0.029	0.115	0.006	1.1	0.4	0.042	0.02	
Dhofar 1436	1.026	0.146	0.86	0.11	4.3	1.4	0.366	0.186	269.3
Dhofar 1443	0.971	0.138	0.79	0.11	3.4	1.3	0.354	0.159	249.7
Dhofar 1436/1443	1.00	0.142	0.82	0.11	3.9	1.3	0.36	0.17	519.0
±1	0.02	0.003	0.03	0.02	1.0	1.1	0.02	0.04	
±2	0.04	0.006	0.04	0.01	0.4	0.5	0.02	0.02	
Dhofar 1442	27.7	3.78	30.3	3.78	28.3	10.4	14.8	4.11	333.9
Dhofar 1527	1.113	0.162	0.85	0.127	73.1	89	0.50	0.22	168.2
±1	0.017	0.003	0.03	0.018	1.3	2	0.02	0.03	
±2	0.038	0.008	0.06	0.007	70.4	100.	0.03	0.03	
Dhofar 1528	2.21	0.308	1.89	0.29	11.3	5.4	1.43	0.46	174.4
±1	0.02	0.004	0.03	0.02	0.8	0.8	0.03	0.04	
±2	0.19	0.029	0.18	0.03	1.8	1.6	0.16	0.03	
Dhofar 1627	5.20	0.714	5.81	0.68	14.2	10.9	2.70	0.95	393.5
±1	0.05	0.007	0.06	0.04	1.0	1.2	0.04	0.06	
±2	0.32	0.043	0.35	0.04	1.5	1.2	0.18	0.08	
JaH 348	0.814	0.117	0.63	0.087	2.4	< 4	0.260	0.09	238.4
±1	0.012	0.002	0.02	0.010	0.6	–	0.014	0.04	
±2	0.044	0.006	0.04	0.006	0.5	–	0.022	0.03	
Shişr 160	0.689	0.098	0.63	0.073	9.7	5.9	0.261	0.19	170.4
±1	0.011	0.002	0.01	0.008	0.5	0.5	0.015	0.02	
±2	0.066	0.009	0.09	0.006	1.1	4.4	0.039	0.03	
Shişr 161	0.675	0.10	0.45	0.055	2.6	< 2.5	0.165	0.22	294.0
±1	0.013	0.00	0.02	0.012	0.6	–	0.015	0.03	
±2	0.031	0.00	0.03	0.004	0.4	–	0.013	0.03	
Shişr 162	0.476	0.0674	0.372	0.054	6.8	4.1	0.165	0.05	367.8
±1	0.009	0.0017	0.017	0.011	0.6	0.8	0.012	0.03	
±2	0.040	0.0055	0.041	0.006	4.6	2.4	0.023	0.02	

Table 2. *Continued*. Mass-weighted mean results of neutron activation analysis.

Meteorite	Yb μg g^{-1}	Lu μg g^{-1}	Hf μg g^{-1}	Ta μg g^{-1}	Ir ng g^{-1}	Au ng g^{-1}	Th μg g^{-1}	U[a] μg g^{-1}	mass mg
Shişr 166	0.964	0.14	0.93	0.115	5.2	6.7	0.42	0.14	240.6
±1	0.015	0.00	0.02	0.009	0.5	0.8	0.02	0.03	
±2	0.019	0.00	0.04	0.007	0.2	2.4	0.01	0.01	

FeO_T is the total iron concentration expressed as FeO. The row "±1" is the mean analytical uncertainty (one standard deviation, based on counting statistics) for an individual subsample of the meteorite. The row "±2" is the 95% confidence interval for the mean (STDEV×*t*/SQRT[*N*], where *t* is the Student's *t* factor [function TINV in Excel] for *N*–1 degrees of freedom). For precisely determined elements, row "±2" reflects sampling uncertainty (sample heterogeneity) in that the value is usually greater than two times the standard deviation of row "±1." Rows with / in meteorite name represent mass-weighted means of paired stones and include data of sources listed in Table 1.

[a]Analyses values are high, compared with pre-terrestrial concentrations, as a result of terrestrial weathering; see text.

[b]Updated from Hudgins et al. (2011); see text.

Table 3. Results of major and minor element analysis by EPMA.

Meteorite	SiO_2	TiO_2	Al_2O_3	Cr_2O_3	FeO_T	MnO	MgO	CaO	Na_2O	K_2O	P_2O_5	Σ	*Mg′*
Dhofar 081	44.6	0.11	32.1	0.05	2.75	0.05	2.90	17.59	0.326	0.01	0.02	100.6	65.3
Dhofar 280	44.0	0.19	30.2	0.07	3.57	0.06	3.35	18.06	0.352	0.03	0.03	99.9	62.5
Dhofar 910	44.2	0.08	33.0	0.05	2.50	0.04	2.18	17.95	0.328	0.01	0.01	100.4	60.9
Dhofar 081/280/910	44.3	0.11	32.2	0.05	2.79	0.05	2.67	17.83	0.331	0.01	0.02	100.4	63.0
Dhofar 287	44.8	2.76	8.84	0.62	21.12	0.27	11.50	9.50	0.490	0.06	0.26	100.2	49.2
Dhofar 301	44.4	0.25	27.5	0.12	4.70	0.07	6.45	15.96	0.336	0.04	0.04	99.9	71.0
Dhofar 302	44.1	0.18	30.2	0.07	3.16	0.05	4.92	17.10	0.341	0.03	0.04	100.2	73.5
Dhofar 490	41.5	0.20	28.3	0.07	3.73	0.06	3.84	21.51[a]	0.323	0.03	0.84	99.6	64.8
Dhofar 1084	42.5	0.20	28.7	0.08	4.00	0.06	3.75	20.03[a]	0.344	0.30	0.65	99.8	62.6
Dhofar 490/1084	42.1	0.20	28.5	0.07	3.89	0.06	3.79	20.65[a]	0.335	0.03	0.07	99.7	63.5
Dhofar 490/1084©	44.3	0.21	30.1	0.08	4.10	0.07	3.99	16.35	0.353	0.03	0.08	99.7	63.5
Dhofar 960	44.7	0.33	22.5	0.21	7.87	0.11	9.55	14.10	0.335	0.08	0.08	99.9	68.4
Dhofar 925/960/961	44.9	0.38	22.0	0.22	8.30	0.13	9.18	14.03	0.334	0.08	0.11	99.7	66.4
Dhofar 1428	44.0	0.18	28.9	0.09	4.20	0.05	4.66	16.63	0.369	0.06	0.03	99.2	66.4
Dhofar 1436	44.9	0.33	26.9	0.15	5.62	0.09	5.86	15.62	0.357	0.33	0.41	99.9	65.0
Dhofar 1443	44.9	0.29	27.3	0.13	5.52	0.08	5.69	15.64	0.368	0.36	0.31	99.9	64.8
Dhofar 1436/1443	44.9	0.31	27.1	0.14	5.57	0.09	5.78	15.63	0.362	0.03	0.04	99.9	64.9
Dhofar 1442	48.5	2.75	13.6	0.25	13.74	0.19	8.21	9.75	0.800	0.71	0.66	99.0	51.6
Dhofar 1527	44.1	0.25	24.5	0.17	7.95	0.09	8.23	14.16	0.336	0.06	0.04	99.9	64.9
Dhofar 1528	45.4	0.25	24.4	0.19	6.05	0.08	9.07	13.72	0.405	0.16	0.05	99.8	72.8
JaH 348	45.2	0.27	27.7	0.12	5.51	0.08	4.99	16.01	0.340	0.02	0.03	100.2	61.7
SaU 449	44.7	0.31	23.0	0.20	7.86	0.11	9.06	14.12	0.318	0.07	0.06	99.85	67.3
Shişr 160	44.0	0.17	30.0	0.08	3.90	0.06	3.52	17.66	0.339	0.02	0.08	99.8	61.7
Shişr 161	44.2	0.21	25.2	0.16	5.94	0.09	8.17	14.97	0.319	0.04	0.03	99.4	71.0
Shişr 162	44.5	0.16	30.8	0.06	3.15	0.04	3.90	16.82	0.394	0.18[a]	0.02	100.0	68.8
Shişr 166	44.6	0.19	29.3	0.09	4.13	0.05	3.97	17.11	0.323	0.04	0.04	99.9	63.2

All analyses by Ryan Zeigler. Values are in mass % except *Mg′* is mole percent MgO/(MgO + FeO_T). FeO_T is the total iron concentration expressed as FeO. Cr_2O_3, FeO_T, and Na_2O values are from INAA; others are from EPMA of fused glass (Korotev et al. 2009). For paired stones (rows with "/" in meteorite name), the values are mass-weighted means based on INAA mass of Table 1.

[a]Significant contamination from terrestrial weathering (Fig. 21). For Dhofar 490 and 1084, if the lunar CaO concentration is assumed to be 16.35 (from Al_2O_3 concentration and Fig. 21) and the other elements are normalized (×1.054) to yield the same sum, then the corrected (©) composition (preterrestrial) is obtained. Major-elements data for other lunar meteorites from Oman are given in Anand et al. (2003), Cahill et al. (2004), Cohen et al. (2004), Demidova et al. (2007), Gnos et al. (2004), Greshake et al. (2001), Hsu et al. (2008), Hudgins et al. (2011), Korotev et al. (2009), Takeda et al. (2006), and Warren et al. (2005).

alteration among lunar meteorites from Oman (celestite and barite; Figs. 9–12). That distinction still holds. Among all lunar meteorites, Dhofar stones 025, 304, and 308 have the highest Sr concentrations (Figs. 9 and 10). Dhofar 025 has the longest terrestrial residence time, 0.5–0.6 Myr (Nishiizumi and Caffee 2001), of any lunar meteorite from Oman for which the parameter has been reported, and Nazarov et al. (2003) and Al-Kathiri et al. (2005) reasonably conclude that the degree of Sr enrichment correlates with terrestrial age. The meteorite

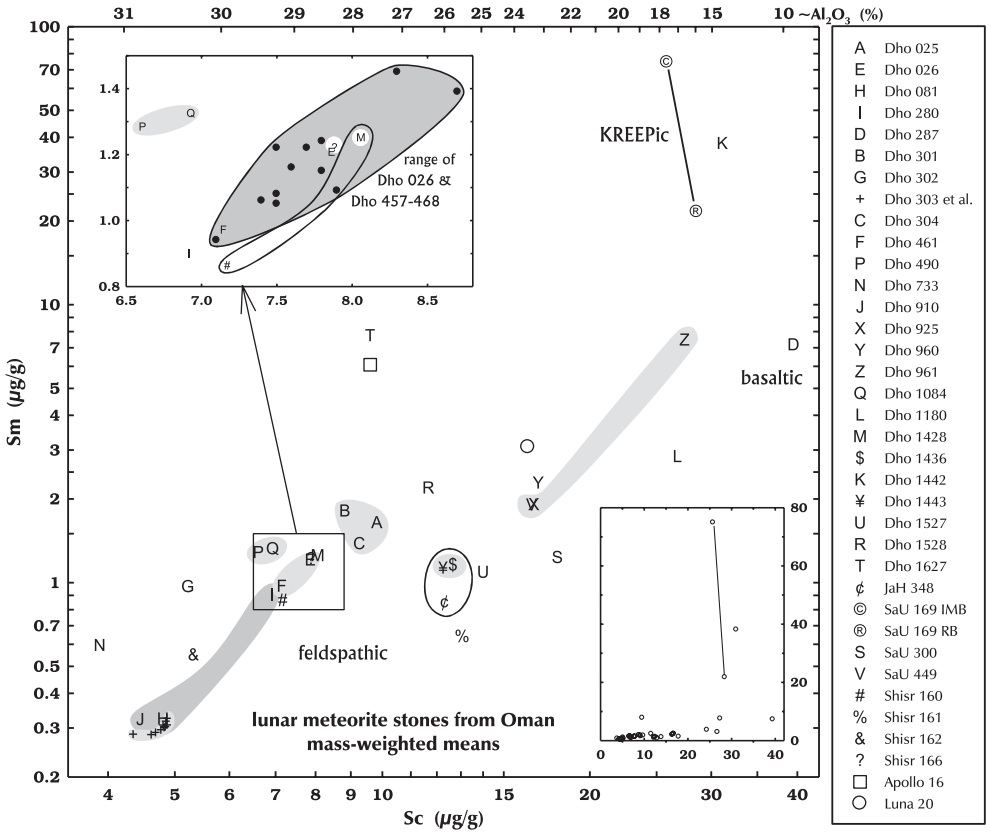

Fig. 3. Lunar meteorites from Oman in Sc-Sm space. Each point represents the mass-weighted mean composition of all analyzed subsamples of a named stone. Two points are plotted for the two lithologies of SaU 169 (impact-melt breccia and regolith breccia). Gray fields encompass stones known to be terrestrially paired; other pairings may exist. Possible source-crater pairings are encircled by unfilled "ellipses." In the upper left inset, the darker gray field is defined by data presented here for Dhofar 026 [E] and Dhofar 461 [F] and the data of Warren et al. (2005) for 12 stones [circles] of the pair group. All other data from this work and references of Table 1. For comparison, the circle represents the soil of Luna 20 and the square represents the typical soil of Apollo 16. The lower right inset shows the meteorite data on linear scales.

is also contaminated with P, presumably from terrestrial sources (Fig. 13).

Dhofar 026 [E], 461 [F], and 457–468

The composition and petrography of Dhofar 026 (148 g, Fig. 14) and its 12 small pairs discovered 12 km away, Dhofar stones 457–468 (19–100 g) are well studied (Cohen et al. 2004; Warren et al. 2005; Demidova et al. 2007; Hudgins et al. 2011; Zhang et al. 2011). Of the 12 stones of Dhofar 457–468, I have studied only one small sample of Dhofar 461 (Table 1). My data (Hudgins et al. 2011) for Dhofar 026 and Dhofar 461 are consistent with those of Warren et al. (2005) (Fig. 3, inset). Cohen et al. (2004) argue that Dhofar 026 is a granulitic breccia, whereas Warren et al. (2005) prefer "an unusual variety of impact-melt breccia." Zhang et al. (2011) report the occurrence of a "polycrystalline zircon" with a $^{207}Pb/^{206}Pb$ age of 3434 ± 15 Ma in Dhofar 458. They interpret the texture of the zircon as the result of "high-pressure shock-induced melting and degassing" and, consequently, favor a classification of "clast-rich impact melt rock." Either interpretation would account for the very low abundances of solar noble gases (Shukolyukov et al. 2001). Fernandes et al. (2004) report ^{40}Ar-^{39}Ar ages for six clasts of impact-melt breccias in Dhofar 026 ranging from 1610 ± 280 Ma to 5070 ± 1750 Ma.

On sawn faces, the meteorite has a low-contrast appearance because clasts are not particularly evident (Fig. 14), a feature more characteristic of granulitic breccias than impact-melt breccias. Hematite staining, which is common on many Dhofar lunar meteorite stones, is scarce (Fig. 15). None of the subsamples of Dhofar 026 or Dhofar 461 analyzed here show the Ir anomaly described by Warren et al. (2005) for Dhofar 026, although we have obtained such anomalies (though not as extreme) in other lunar meteorites (Jolliff et al. 1991) and Apollo regolith samples (Korotev and Morris 1993).

Subsequent to publication of the INAA data (mass-weighted means) in Hudgins et al. (2011), I recognized

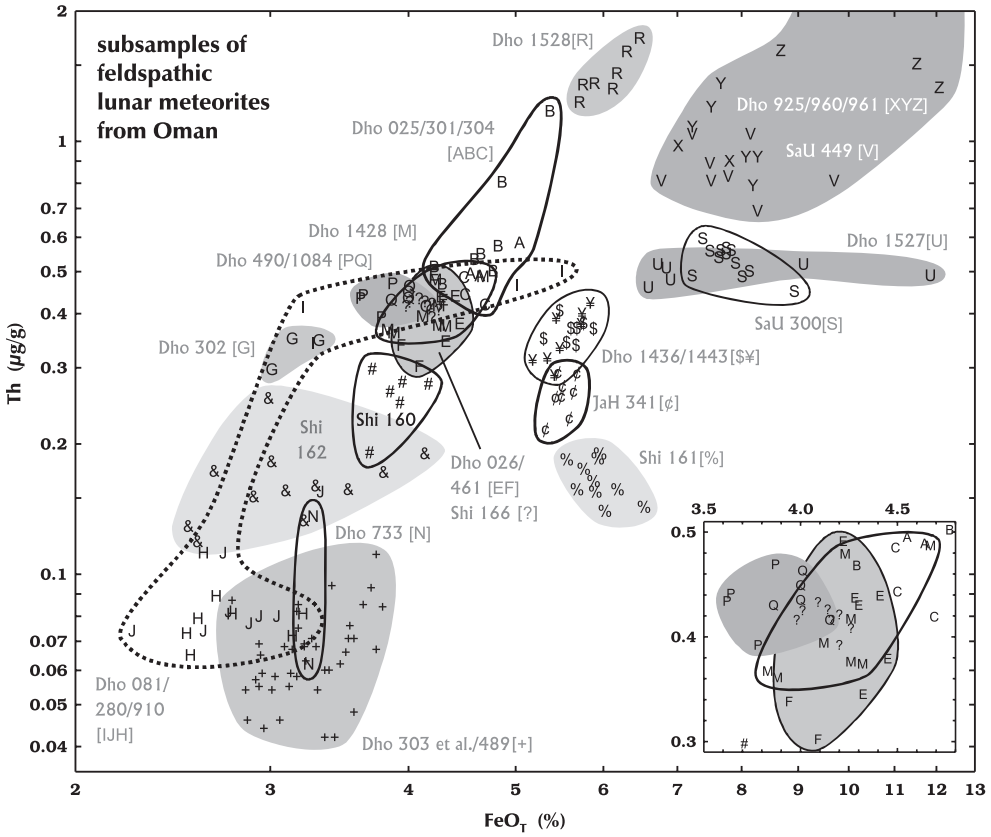

Fig. 4. Subsample data for the feldspathic lunar meteorites from Oman in FeO_T-Th space (total Fe as FeO). Dhofar 1627 (2.3–3.5 μg g^{-1} Th) and some subsamples of Dhofar 961 (1.3–6.3 μg g^{-1} Th) lie off the plot at higher Th concentrations. For Dhofar 1527, note the wide spread in FeO concentrations compared with Sc concentrations in Fig. 5. The "FeO" spread is a result of different abundances of FeNi metal among the subsamples. See Fig. 3 for symbol key.

that one of the subsamples of Dhofar 026 is anomalously rich in Cr (2.9× richer), Fe (1.14×), Co (1.4×), Ni (2.9×), As (11×), W (20×), and Ir (1.5×), but not Sc (0.9×) or Au (1.0×). This anomaly suggests a nonmeteoritic source of metallic contamination. The recalculated weighted means of Table 2 do not include data for this contaminated subsample.

Dhofar 081 [I], 280 [J], 910 [K], and 1224

Dhofar 081 (174 g; Fig. 16) is the first lunar meteorite reported to have been found in Oman (November 1999). Dhofar stones 280 (251 g), 910 (142 g), and 1224 (4.6 g) were later found nearby in the same small area as Dhofar 302 and the 14 Dhofar 303 et al. stones (Fig. 2). Dhofar 081 et al. (081, 280, 910, and 1224) are texturally and compositionally distinct from the others, but similar to each other (Fig. 16). Nishiizumi and Caffee (2006) conclude that Dhofar 081, 280, and 910 are paired on the basis of CRE data. Dhofar 081 is moderately well characterized, and classified as a shocked fragmental breccia with a glassy or devitrified matrix with schlieren (Bischoff 2001; Greshake et al. 2001; Cahill et al. 2004; Warren et al. 2005). M. Nazarov (in Grossman and Zipfel 2001) describe Dhofar 280 as a "clast-rich fragmental breccia containing numerous mineral fragments and clasts of feldspathic rocks embedded in a glass-rich matrix" and hypothesize that the stone is paired with Dhofar 081. Dhofar 910 (Fig. 16) has not been described. Warren et al. (2005) noted that Dhofar 081 "might arguably be classified as an impact-melt breccia" but also that the texture suggests "possible regolith derivation," a hypothesis supported by the moderately high abundances of solar He and Ne (Shukolyukov et al. 2004; Lorenzetti et al. 2005). A number of the breccias discussed here are similarly intermediate between glassy impact-melt breccias and glassy regolith breccias. Many have not been thoroughly studied and some of the "impact-melt breccias" of Table 1 and Fig. 17b may be reclassified as regolith breccias after further petrographic study.

The INAA data for Dhofar 910 (Table 2) derive from two different samples that are indistinguishable in

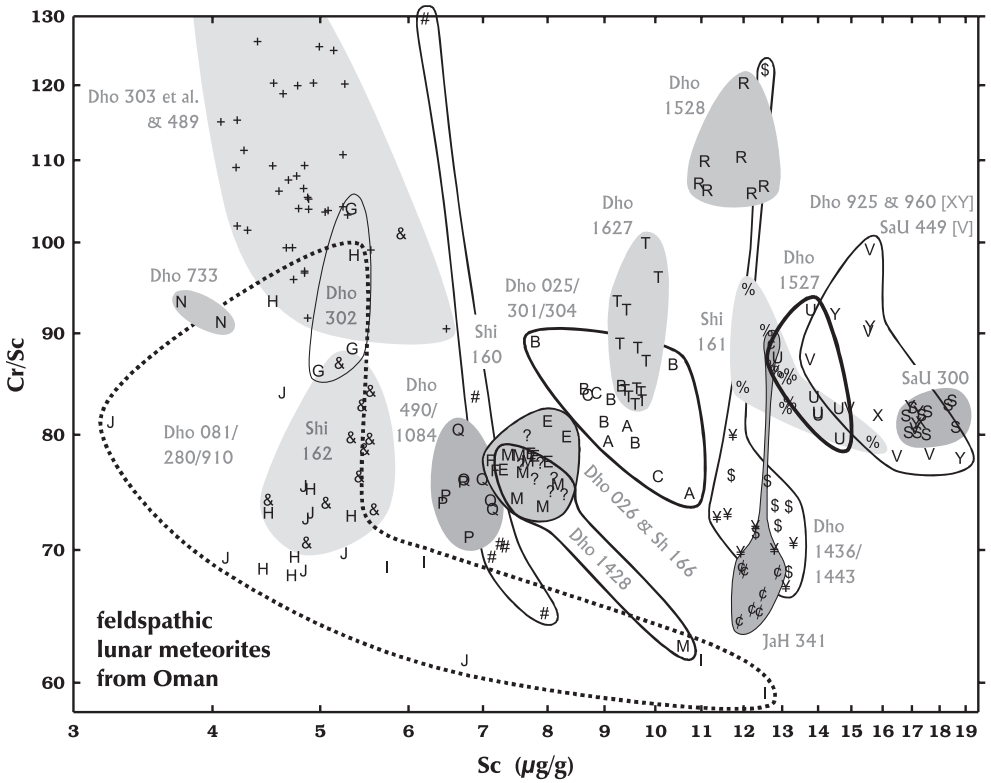

Fig. 5. Data for subsamples. Cr/Sc, which proxies for Mg/Fe (Fig. 6), is useful for discriminating among feldspathic lunar meteorites. For example, in Fig. 4, Dhofar 1528 [R] appears to be an extension of a trend defined by Dhofar 025/301/304 [A/B/C] and Dhofar 1428 [M], but Cr/Sc is highly different, suggesting that the meteorites are unrelated. Subsamples with anomalously high Cr probably contain chromite nuggets. See Fig. 3 for symbol key.

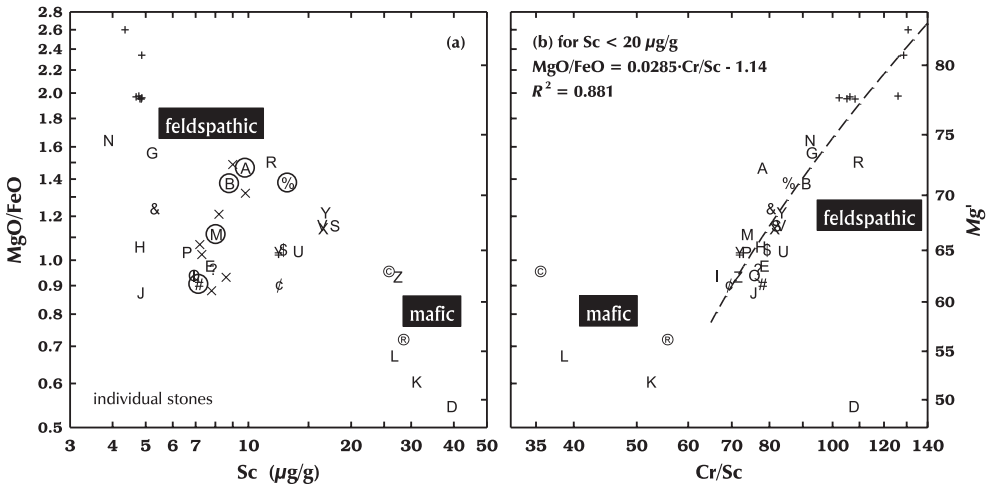

Fig. 6. Data for mass-weighted means of each analyzed stone. The left vertical axis of both plots is MgO/FeO; the right axis is *Mg′* (whole-rock mole % MgO/[MgO + FeO_T]; Table 3). (a) Feldspathic lunar meteorites from Oman (<20 μg g^{-1} Sc, or >22% Al_2O_3) have a wide range in MgO/FeO. There is no correlation, however, between Sc concentration and MgO/FeO (R^2 = 0.03). The × symbols represent the "KREEP-poor highlands regolith samples" of fig. 12 of Warren et al. (2005) and the circled symbols are similar meteorites of this work. For these two subsets of data, R^2 = 0.42. (b) For the feldspathic meteorites from Oman, MgO/FeO correlates with Cr/Sc (Korotev 2005). The dashed line (curved in this log-log plot) is as a simple linear regression of MgO/FeO against Cr/Sc. See Fig. 3 for symbol key.

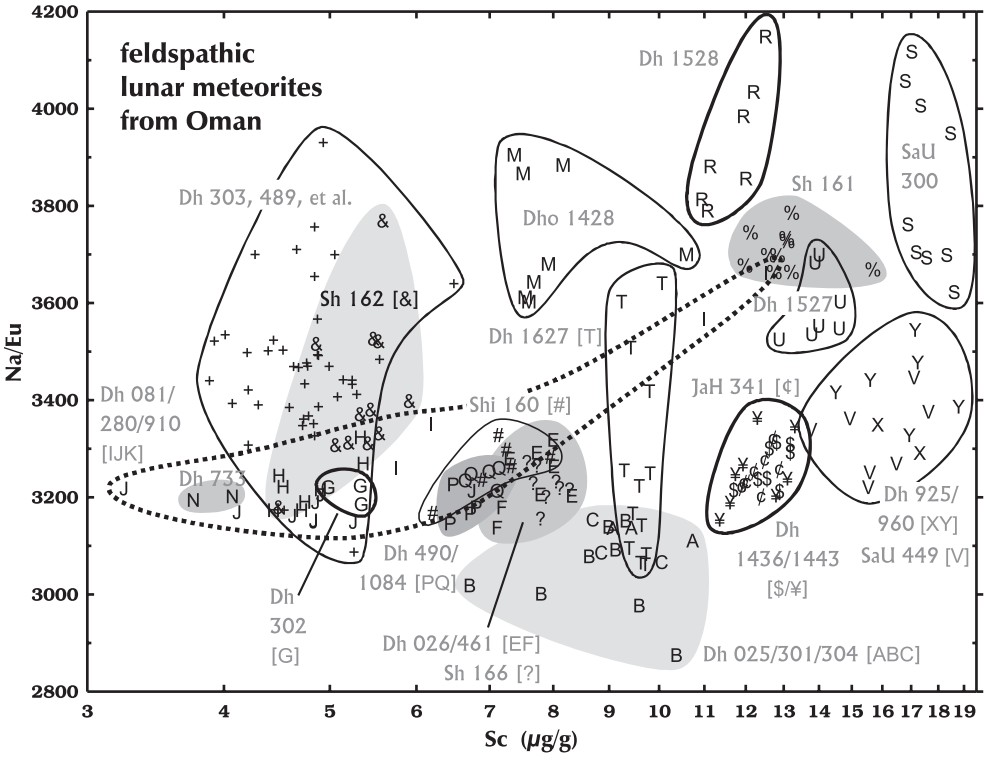

Fig. 7. Data for subsamples. Although both Na and Eu are carried mainly by plagioclase in the meteorites, the ratio of Na to Eu varies and is useful for discriminating among the meteorites. For example, Dhofar 1428 [M] and Dhofar 025/301/304 [ABC] overlap in Fig. 4, but are widely separated on this plot. See Fig. 3 for symbol key.

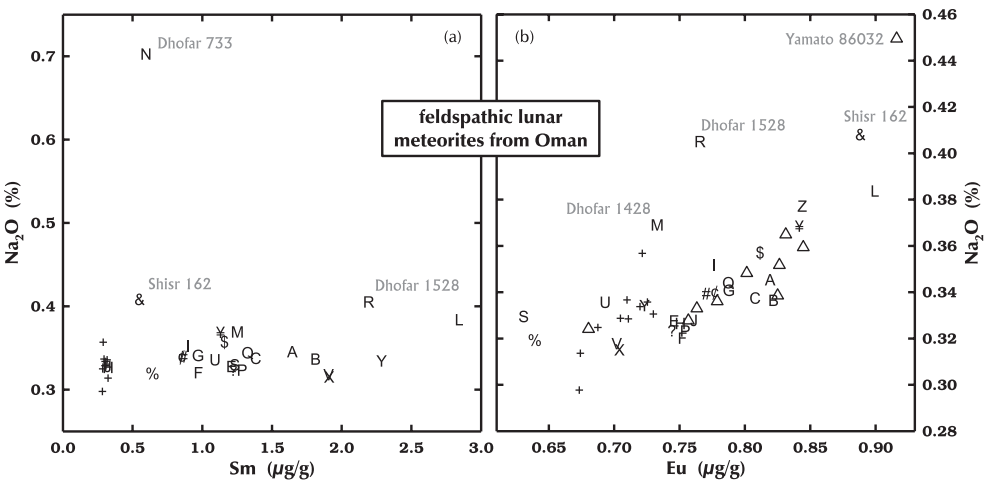

Fig. 8. (a) Concentrations of Na_2O in feldspathic lunar meteorites are typically in the range 0.3–0.4% because the anorthite content of the plagioclase is typically $An_{96–97}$. Dhofar 733 has a troctolitic anorthosite composition (84% normative plagioclase, 12% normative olivine), but the plagioclase is twice as sodic (normative An_{93}) as is typical. (b) Na_2O and Eu are carried mainly by plagioclase in feldspathic lunar rocks. Triangles represent lunar meteorites from Antarctica. Some lunar meteorites from Oman have an excess of sodium compared with Antarctic meteorites with similar Eu concentrations. Dhofar 733 and 1627 plot off the chart. See Fig. 3 for symbol key.

composition. Irving and Kuehner (in Russell et al. 2005) hypothesize that the small stone, Dhofar 1224, is part of the pairing group, but classify the stone as a regolith breccia. I have not studied this stone. In hand specimen, samples of the three larger stones are distinctive and unusual for lunar breccias in each containing several

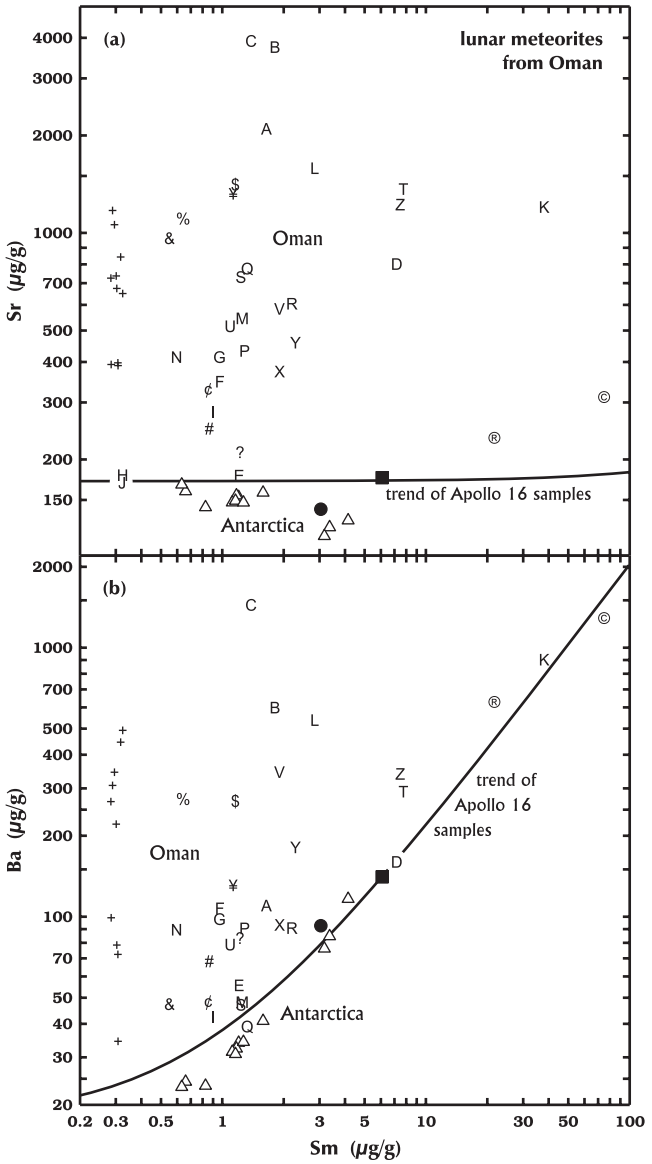

Fig. 9. Lunar meteorites from Oman are contaminated by terrestrial Sr and Ba to varying extents (Korotev et al. 2003, 2009; Nazarov et al. 2004; Warren et al. 2005). Stone means are plotted here. The curved lines are least-squares fits to data for Apollo 16 samples (Korotev et al. 2009). The triangles represent lunar meteorites from Antarctica. For reference, the filled circle represents the soil of Luna 20 and the filled square represents the typical soil of Apollo 16. See Fig. 3 for symbol key.

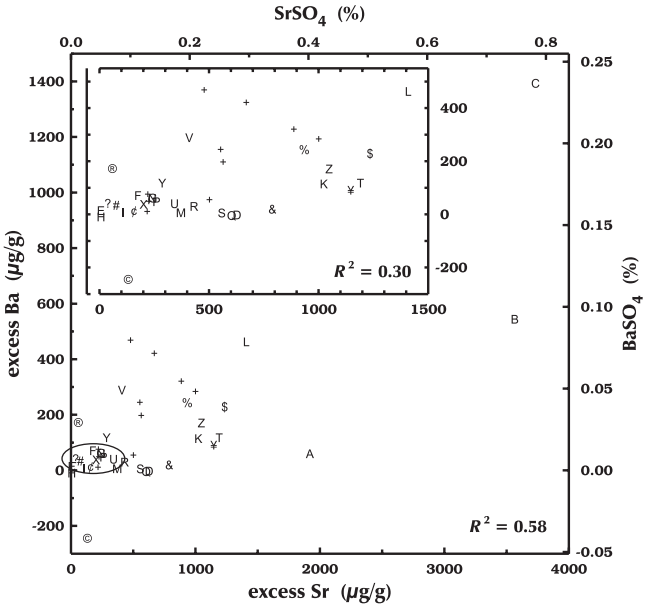

Fig. 10. There is only a weak correlation between concentrations of terrestrial Ba and terrestrial Sr among lunar meteorites from Oman. "Excess" (terrestrial) Sr and Ba is defined as the difference in concentration between the meteorite and a point on the corresponding Apollo 16 line of Fig. 9 with the same Sm concentration. For comparison, the ellipse represents equivalent data (mean ± 1 standard deviation) for 39 ordinary chondrites from Oman in the study of Al-Kathiri et al. (2005). The inset includes all meteorites except the highly contaminated, paired stones Dhofar 025, 301, and 304 [A, B, C]. The fraction of terrestrial celestite ($SrSO_4$) and barite ($BaSO_4$) required to cause the enrichments is shown on the alternate axes. See Fig. 3 for symbol key.

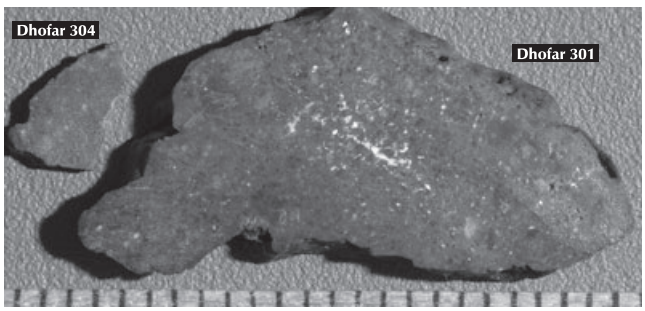

Fig. 11. Paired Dhofar stones 025, 301, and 304 are the most seriously contaminated with terrestrial celestite and barite (white areas in Dhofar 301; Fig. 9). Tick marks are millimeters.

percent vugs; the larger ones are typically elongated (Fig. 16).

Dhofar 081 and Dhofar 910 are among the most feldspathic, poorest in ITEs (Figs. 3 and 4), and most ferroan (Fig. 6) of the lunar meteorites from Oman. However, the meteorite is also one of the most compositionally heterogeneous (Figs. 4, 5, and 18). Samples of both Dhofar 081 and Dhofar 910 analyzed here are more feldspathic and poorer in ITEs than the samples of Dhofar 081 and 280 of Cahill et al. (2004), Warren et al. (2005), and Demidova et al. (2007). In contrast, the sample of Dhofar 280 is more mafic and richer in ITEs than any of the other analyzed samples of the Dhofar 081 et al. stones (Fig. 18). La/Th is anomalously low in Dhofar 280 (Fig. 19). Siderophile-element concentrations are moderately low, but all three

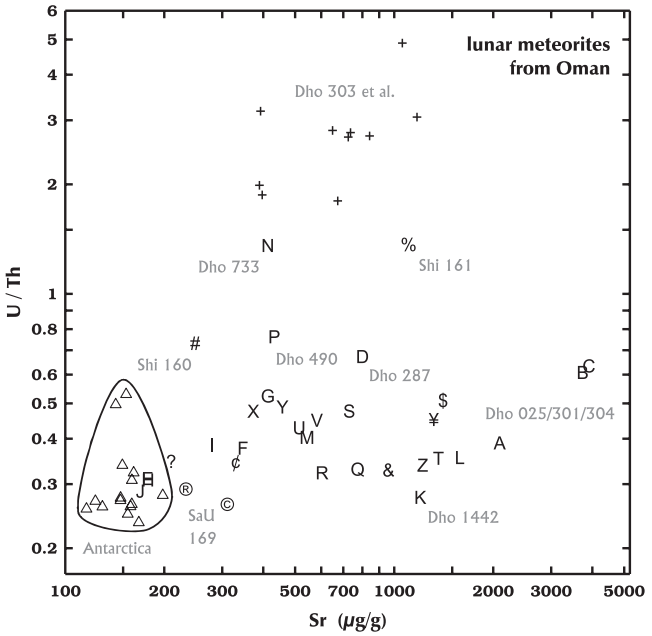

Fig. 12. Sr concentrations are relatively constant in feldspathic lunar meteorites from Antarctica (triangles, 3–13% FeO). Because U correlates with Th, U/Th is also relatively constant, so lunar meteorites from Antarctica span only a small region in the lower left corner of this plot. (The two with high U/Th are Allan Hills 81005 and Larkman Nunatak 06638.) Most lunar meteorites from Oman are enriched in Sr from terrestrial alteration. Most are also contaminated with U, leading to U/Th ratios well outside the range of the Antarctic meteorites. The effect is particularly severe for the Sm- and U-poor meteorites Dhofar 303 et al., Dhofar 733, and Shişr 161, but not as severe for Sm- and Th-poor Dhofar 026/461 [E,F], Dhofar 081 et al. [H,I,J], Shişr 162 [&], and Shişr 166 [?]. Expectedly, the relative contamination of U in Th- and U-rich SaU 169 [©, ®] and Dhofar 1442 [K] is minimal. There is no correlation between degree of U contamination and Sr contamination. See Fig. 3 for symbol key.

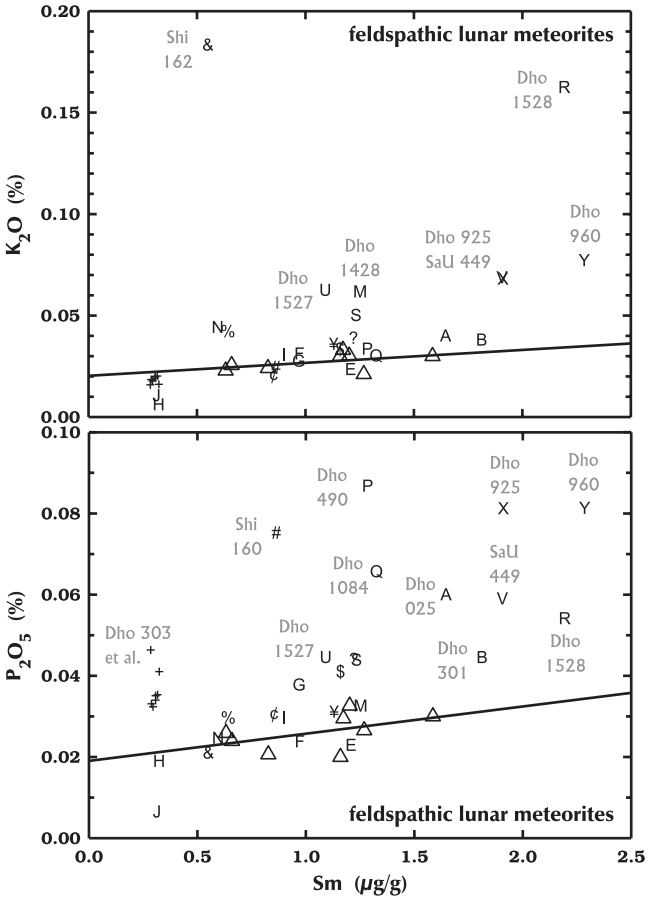

Fig. 13. K_2O and P_2O_5 increase with Sm in feldspathic lunar breccias. Several of the Omani lunar meteorites are enriched in both elements compared with meteorites from Antarctica (triangles). For Dhofar 925/960 and presumed launch pair SaU 449, the high K_2O and P_2O_5 may be intrinsic to the part of the Moon from which they derive (Korotev et al. 2009). See Fig. 3 for symbol key.

stones have low Ni/Ir compared with other feldspathic lunar meteorites from Oman (Fig. 17a).

As noted by Nazarov et al. (2004), Dhofar 081 et al. is among the least contaminated with terrestrial Sr and Ba of the lunar meteorites from Oman (Figs. 9 and 10). There is no evidence for contamination with K, P, Na, or U (Figs. 8, 12, and 13). The meteorite has a low terrestrial residence age 40 ± 20 kyr (Nishiizumi et al. 2004).

Dhofar 287 [D]

Dhofar 287 (154 g) is the only basaltic lunar meteorite from Oman (Fig. 20). The meteorite "consists in large part (95%) of low-Ti mare basalt (Dho 287A) and a minor, attached portion (approximately 5%) of regolith breccia (Dho 287B)" (Demidova et al. 2003b). Like SaU 169, Dhofar 287 could be characterized as a regolith breccia with one anomalously large igneous clast (Korotev 2005). The basalt portion of Dhofar 287 has been moderately well characterized (Shih et al. 2002; Anand et al. 2003; Terada et al. 2008). Anand et al. (2003) note that their sample of the meteorite has high modal abundance of olivine (20.6% olivine phenocrysts) compared with other lunar basalts. The data of Table 3 are similar to those of Anand et al. (2003) except that (FeO + MgO)/SiO_2 (0.73) and Mg' (49.2) are less than that of Anand et al. (0.82 and 51.6). Sc concentrations are greater and the ratios of light to heavy REE (rare earth elements) are less in the sample analyzed here compared with that of Anand et al. (2003). These differences all correspond to a greater proportion of normative olivine in the sample of Anand et al. (2003). Anand et al. (2003) note that the composition of their 1 g sample requires cumulate olivine and they assume 15% (Fo_{70}) for their petrogenetic model. On average, the

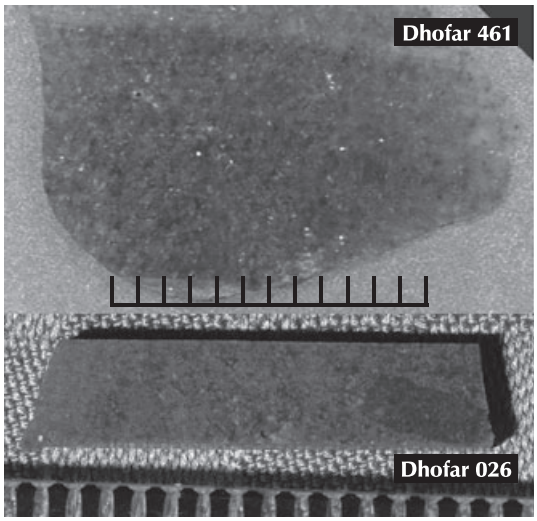

Fig. 14. Paired stones Dhofar 026 and 461 are granulitic breccias (Cohen et al. 2004) or impact-melt breccias (Warren et al. 2005). Clasts are not distinct in this meteorite. Tick marks are millimeters.

Fig. 15. Paired Dhofar stones of the Dhofar 303 et al. clan (305, 309, 310, 489, 911, and 1085; labels white on black, all impact-melt breccias) vary considerably in appearance, but are compositionally identical (Korotev et al. 2006). Dhofar 302 found in the same area (Fig. 2) is darker and compositionally distinct. Clasts are not obvious in the small sample of Dhofar 733, a feature that is characteristic of granulitic breccias. Tick marks are millimeters.

major-element composition of the sample of Table 3 (0.2 g) corresponds to that of the sample of Anand et al. (2003) minus 8% olivine (Fo_{70}). Clearly, mineral proportions are not uniform at the scale of the sampling size.

In detail, the Dhofar 287 basalt is dissimilar to any other basaltic lunar meteorite or any Apollo or Luna basalt. Dhofar 287 is distinct in having low Sc (Fig. 20) and high Cr, leading to the highest Cr/Sc (108; Fig. 6) of which I am aware among lunar mare basalts, although Cr/Sc is not significantly greater than that of the olivine basalts of Apollo 12 and 15. Anand et al. (2003) refer to Dhofar 287 as "KREEPy," but with 7.2 μg g^{-1} Sm (Table 2), it is not unusually rich in REE. All Apollo 11 basalts and some basalts from Apollo 14 and Apollo 17, as well as lunar meteorite LaPaz Icefield 02005, have greater concentrations of Sm (BVSP [Basaltic Volcanism Study Project] 1981; Neal et al. 1988; Zeigler et al. 2005). Shih et al. (2002) obtained a Sm-Nd crystallization age of 3.46 ± 0.03 Ga and Terada et al. (2008) obtained a Pb/U isochron age of 3.34 ± 0.20 Ga and a $^{207}Pb/^{206}Pb$ age of 3.35 ± 0.13 Ga for the basalt.

Sr concentrations in low-Ti mare basalts from Antarctica and the Apollo collection do not exceed 200 μg g^{-1}, thus with 800 μg g^{-1} Sr, Dhofar 287 is significantly contaminated. The 15 ng g^{-1} of Au (Table 2) is also a contaminant (3–33 ng g^{-1} range among six subsamples).

The only information about the regolith-breccia portion of Dhofar 287 is provided in the petrographic study of Demidova et al. (2003b). No bulk composition data are available and I have been unable to obtain a sample. In a preliminary report we stated, "The 'regolith breccia' lithology of Dhofar 287 … is highly dissimilar in composition to the basalt lithology … and, in fact, to any Apollo regolith" (Korotev and Zeigler 2007). The statement is correct, but is based on a sample sold to me as Dhofar 287B, but which, compositionally, is a howardite.

The reported find location of Dhofar 287 (Grossman 2000) is 0.53 km from that for Dhofar 025 and 0.25 km from Dhofar 301 (Russell et al. 2002). Kalahari 008 and 009 notwithstanding (Sokol et al. 2008), the meteorites are unlikely pairs as the Dhofar 025 clan is a feldspathic breccia and Dhofar 287 is a mare basalt. No CRE data have been reported for Dhofar 287.

Dhofar 302 [G]

Dhofar 302, which constitutes the smallest lunar meteorite from Oman (3.8 g), was found with Dhofar 081 et al. (0.18 km from Dhofar 280) and Dhofar 303 et al. (0.17 km from Dhofar 311; Fig. 2). Sawn faces of hand specimens resemble Dhofar 303 et al. more so than

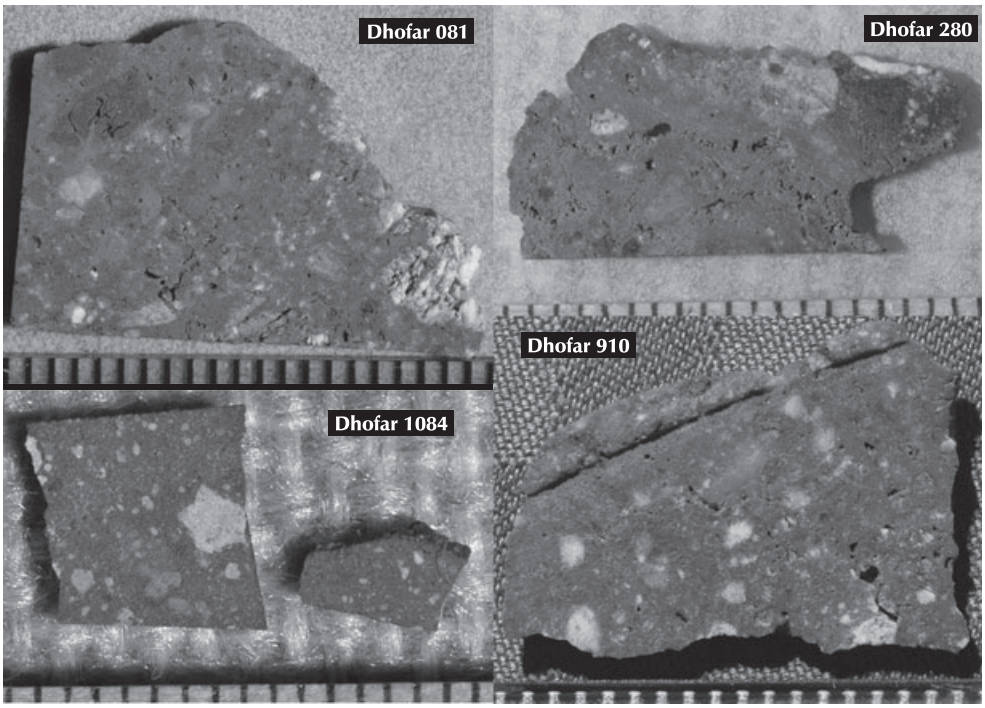

Fig. 16. Dhofar 081 is a clast-rich fragmental breccia with a glassy and fine-grained, devitrified crystalline matrix with schlieren (Bischoff 2001; Greshake et al. 2001; Warren et al. 2005). Paired stones Dhofar 280 and 910 are similar. The meteorite is one of the most vuggy lunar breccias of which the author is aware. The dark area on the right side of Dhofar 280 yielded the two subsamples with anomalously high concentrations of Sc and Sm in Fig. 18. Dhofar 1084 is texturally distinct from, and not nearly as vesicular as, the Dhofar 081 et al. stones.

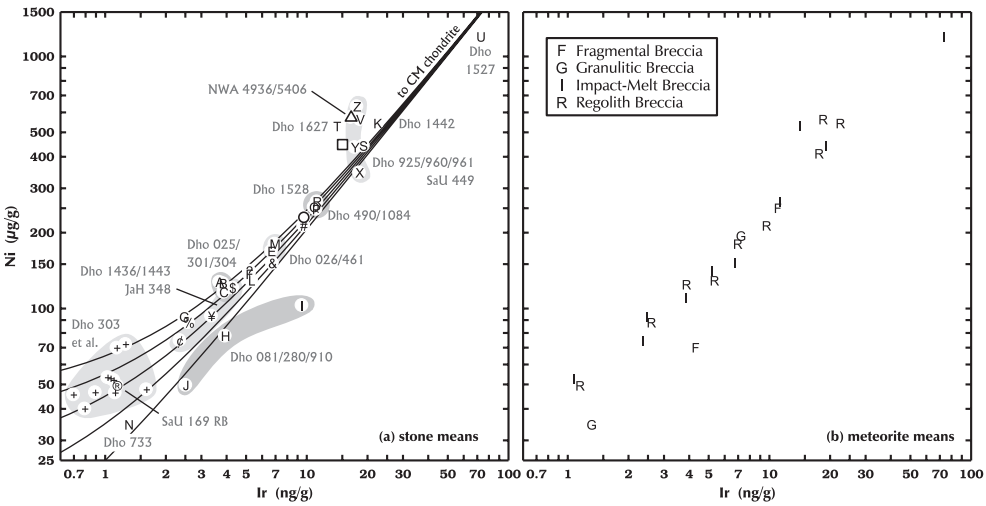

Fig. 17. Concentrations of siderophile elements Ni and Ir in brecciated lunar meteorites from Oman. (a) Mean concentrations for each stone are plotted. See Fig. 3 for symbol key. The curved lines are mixing lines between CM chondrites (595 ng g^{-1} Ir, 12000 μg g^{-1} Ni; Wasson and Kallemeyn 1988) and low-Ir, low-Ni points (off scale) representing lunar silicates. Five lines are shown representing compositions at 0.01 μg g^{-1} Ir and 5, 15, 25, 35, and 45 μg g^{-1} Ni. The spread for the Dhofar 303 et al. stones reflects analytical uncertainty (±0.5 ng g^{-1} Ir, ±8 μg g^{-1} Ni; 2σ). For reference, the circle represents the soil of Luna 20, the square represents the typical soil of Apollo 16, and the triangle represents NWA 4936/5406, a lunar meteorite that has a lithophile-element composition similar to Apollo 16 soil (Korotev et al. 2009). (b) Mean concentrations for all Omani lunar meteorites are plotted; symbols represent the type of breccia (column 7 of Table 1). There is no correlation between breccia type and siderophile-element concentrations.

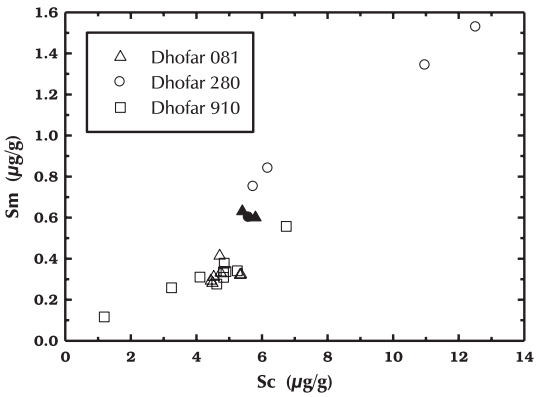

Fig. 18. Subsamples (typically 25–30 mg) of paired stones Dhofar 081, 280, and 910 analyzed for this study scatter over the entire low-Sm portion of Fig. 3. The filled points represent the data of Warren et al. (2005) for Dhofar 081 (0.408 g), Cahill et al. (2004) for Dhofar 081 (1 g), and Demidova et al. (2007) for Dhofar 280 (1 g).

Dhofar 081 et al. in having the texture of a crystalline impact-melt breccia with some clasts stained reddish (Fig. 15). The matrix of Dhofar 302, however, is darker than that of the Dhofar 303 et al. stones. Nazarov et al. (2002) describe Dhofar 302 as a clast-rich impact-melt breccia having a poorly crystallized, glassy matrix with some KREEP glass fragments. They regard it as petrographically distinct from Dhofar 081 et al. and Dhofar 303 et al. (Nazarov et al. 2002, 2003; Demidova et al. 2003a).

Dhofar 302 is compositionally distinct from Dhofar 303 et al. in being less magnesian, three times richer in ITEs (Figs. 4 and 6), and about two times richer in Ni and Ir (Fig. 17a). In Fig. 4, none of the numerous subsamples of Dhofar 303 et al. approach Dhofar 302 in composition, so there is no reason to suspect that Dhofar 302 is a clast from the Dhofar 303 et al. meteorite. Compositional and petrographic data suggest that Dhofar 302 represents a fall distinct from the other two meteorites found in the same location (Fig. 2, inset). No CRE data are available.

Nazarov et al. (2002) state that, petrographically, Dhofar 302 is "virtually free of terrestrial weathering." Compositionally, however, the meteorite is moderately contaminated with Sr and Ba, with concentrations at the low end of the range for the Dhofar 303 et al. stones (Figs. 9 and 10).

Dhofar 303 et al. and Dhofar 489 [+]

Fourteen paired stones, Dhofar 303, 305, 306, 307, 309, 310, 311, 730, 731, 908, 909, 911, 950, and 1085, ranging in mass from 2 to 245 g, were found within 2 km of each other (Fig. 2, inset). Sawn faces of the stones are distinctive in having varying degrees of pinkish iron oxide or hydroxide staining (Fig. 15). I refer to the meteorite here as "Dhofar 303 et al." because Dhofar 303 is the lowest numbered stone and the first of the 14 to be described (M. Nazarov and L. Taylor in Russell et al. 2002). We have studied 9 of the 14 stones (Table 1; Korotev et al. 2006). All are feldspathic impact-melt breccias (approximately 79% normative plagioclase) having the lowest concentrations of ITEs among lunar meteorites from Oman (Figs. 3 and 4). They also have the greatest Mg' (Fig. 6) because they derive from a magnesian troctolitic-anorthosite precursor (Demidova et al. 2003; Arai et al. 2007). Many of the stones have been well described in Demidova et al. (2003a, 2007), Nazarov et al. (2002, 2003, 2004), Korotev et al. (2006), Takeda et al. (2007, 2008, 2009, 2010), and Treiman et al. (2010). For four of the stones, there are no petrographic descriptions (908, 909, 911, and 1085). Shukolyukov et al. (2004) argue on the basis of CRE data from noble gases that Dhofar 303 is from a different fall than Dhofar stones 305, 307, and 731. I return to this issue below in the discussion of Dhofar 733.

Dhofar 489 is reported to have been found 23 km distance from Dhofar 303 et al. (Fig. 2) and was first described at the same time as Dhofar 303 (H. Takeda et al., in Russell et al. 2002). Despite the distance, Nishiizumi and Caffee (2006) conclude that Dhofar 489 is paired with Dhofar 908, 911, and 1085 on the basis of CRE data. The terrestrial age is about 300 kyr. In all compositional and petrographic respects, Dhofar 489 is indistinguishable from Dhofar 303 et al. (e.g., Korotev et al. 2006; Takeda et al. 2007, 2008; Fig. 15) and the designation "Dhofar 489 et al." has been used to refer to all 15 stones assuming that they are all terrestrially paired (Korotev et al. 2006; Arai et al. 2007). The meteorite is of special interest because in addition to being magnesian it contains some very old clasts (Fernandes et al. 2004; Nyquist et al. 2010).

The Dhofar 489 et al. stones are all seriously contaminated with terrestrial Sr and Ba (Figs. 9 and 10). They are also among several lunar meteorites from Oman that are contaminated with uranium, probably associated with terrestrial calcite, as there is no correlation between excess U and Sr (Fig. 12). Concentrations of U are about 10 times those of otherwise similar feldspathic lunar meteorites from Antarctica (Fig. 12). Concentrations of P average two times those of meteorites from Antarctica (Fig. 13).

Dhofar 490 [P] and 1084 [Q]

There is no petrographic information available for Dhofar stones 490 (34 g) and 1084 (90 g; Fig. 16) other

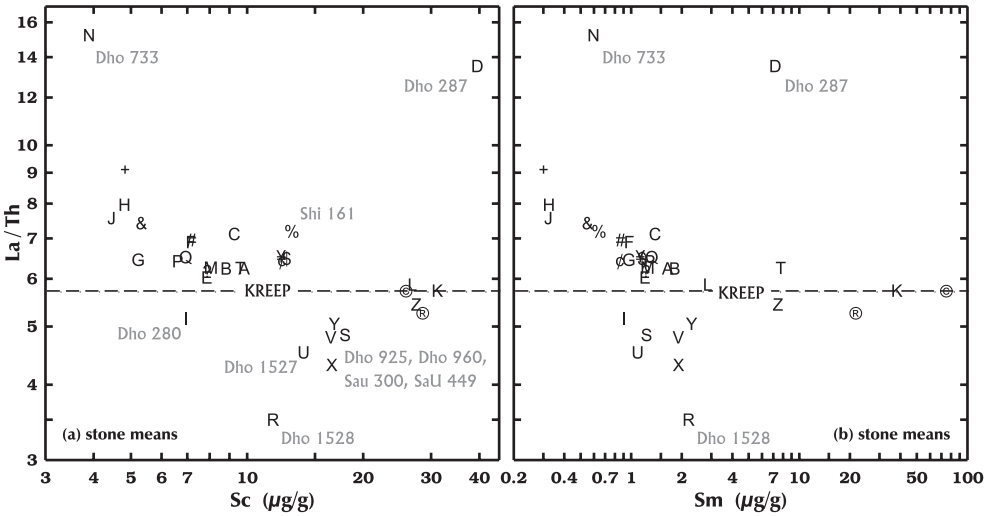

Fig. 19. Among feldspathic lunar meteorites, La/Th tends to decrease with increasing Sc concentration and, to a lesser extent, REE concentrations, represented here by Sm. Dhofar 287 is anomalous because it is a mare basalt. The small sample of Dhofar 280 [I] analyzed here is anomalous compared with the trends and, particularly, compared with paired stones Dhofar 081 [H] and Dhofar 910 [J]. La/Th is anomalously low in Dhofar 1528, but the "REE pattern" (Fig. 22) is not at all unusual, suggesting that, for some unknown reason, Th is anomalously high.

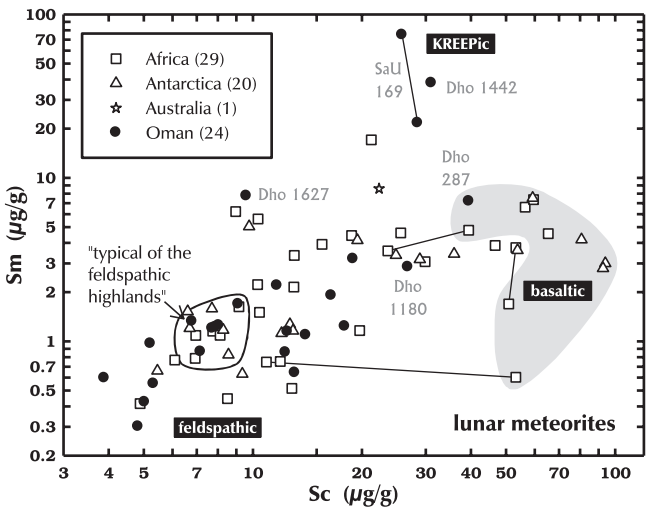

Fig. 20. Compositional comparison of lunar meteorites from Oman with those found elsewhere. Each point represents the mean composition of a meteorite, except that two points, connected by a line, are used for dilithologic meteorites. Meteorites in gray field are unbrecciated mare basalts. The field at 7–10 μg g^{-1} Sc represents the 16 meteorites named in the text with compositions "typical of the feldspathic highlands." Data from this work, Fagan et al. (2002); Haloda et al. (2009); Jolliff et al. (1993); Korotev and Zeigler (2007); Korotev et al. (2003, 2006, 2008, 2009, 2011a, 2012), and works cited therein; Kuehner et al. (2010), and Zeigler et al. (2007).

than the initial description of Dhofar 490 in *The Meteoritical Bulletin* (A. Greshake and M. Kürz, in Russell et al. 2003). That work classifies the stone as an "anorthositic fragmental breccia consisting of clasts of various lithologies embedded into a glassy, partly devitrified fine-grained matrix; the clast size is generally below 3 mm; vesicles are abundant." That work also states "Dhofar 490 may be paired with Dhofar 280 since they were found nearby and have similar mineralogical characteristics." Despite the similar description to Dhofar 081, neither of the samples of Dhofar 490 and 1084 studied here is as vuggy as the Dhofar 081 et al. pairs (Fig. 16). Also, the reported find locations are not "nearby," but separated by 76 km (Fig. 2). Dhofar 490 and Dhofar 1084 were found together, but distant from other lunar meteorites. Subsamples of both stones studied here are indistinguishable from each other in composition (Figs. 4 and 5) so the two stones are certainly paired.

The meteorite is described as "moderately weathered; gypsum, celestite and calcite occur in cracks and holes" (A. Greshake and M. Kürz in Russell et al. 2003). Of the lunar meteorites from Oman, Dhofar 490/1084 is the most seriously contaminated with calcium. On average, the two stones contain 4.8% "CaO" in excess of that expected based on the CaO/Al_2O_3 ratio of feldspathic lunar meteorites of otherwise similar composition (Fig. 21), an amount that corresponds to 8.6% calcite or 10.3% gypsum. The meteorite is also one of the most contaminated with P (Fig. 13). It is not, however, significantly more contaminated with Sr or Ba than other lunar meteorites from Oman (Fig. 9). The Dhofar 490 sample is more contaminated with Ca, P, and U than is the Dhofar 1084 sample (Figs. 12 and 21). This difference may simply reflect the location (unknown) of the small samples with respect to the surface of the stones.

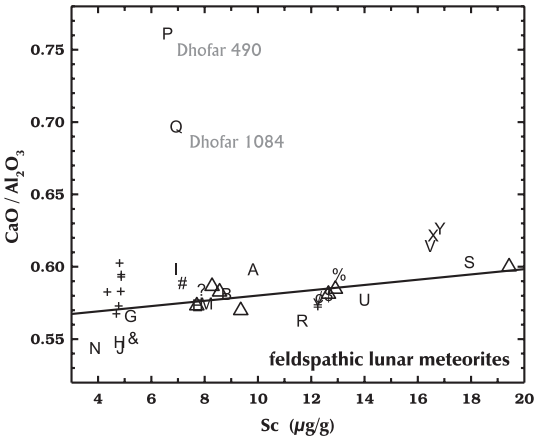

Fig. 21. The triangles represent feldspathic lunar meteorites from Antarctica, which are not significantly contaminated with terrestrial Ca. The line is a simple least-squares fit to the Antarctic data. CaO/Al_2O_3 increases slightly with FeO + MgO in feldspathic lunar breccias because the more mafic rocks contain a greater proportion of Ca-bearing pyroxene. Paired stones Dhofar 490 [P] and 1084 [Q] are anomalously rich in Ca from terrestrial alteration (gypsum and calcite). See Fig. 3 for symbol key.

Dhofar 733 [N]

Dhofar 733 (98 g) was found distant from other Dhofar lunar stones. The meteorite, a granulitic breccia (S. Demidova and G. Kurat, in Russell et al. 2003; Foreman et al. 2008), is one of the most feldspathic of the meteorites discussed here (84% normative plagioclase; Fig. 3). Slices exposing the interior of the meteorite are distinct in being uniformly pink (Fig. 15). Like breccias Dhofar 026 and Dhofar 461 (Fig. 14), clasts are not evident on sawn faces (Fig. 15). My analytical results for a 32 mg sample of the stone (Hudgins et al. 2011) are similar to those of Demidova et al. (2007) for a 20 mg fragment. As noted in Korotev et al. (2009), the meteorite is compositionally distinct in having the highest concentrations of Na and Eu among feldspathic lunar meteorites with low concentrations of trivalent REE (rare earth elements), approximately twice the typical values (Fig. 8). The plagioclase has an albite content of 7% (range: 4–9%; Foreman et al. 2008), about twice that typical of anorthosite from the lunar highlands. Like Dhofar 303 et al., it is at the magnesian (high Mg') end of the range of feldspathic lunar meteorites (Fig. 6) and apparently derives from a troctolitic anorthosite assemblage. Concentrations of siderophile elements are low (Fig. 17), in contrast to many granulitic breccias in the Apollo collection (Hudgins et al. 2008, 2011). Relative concentrations of trivalent REE differ from other lunar meteorites of similar absolute REE concentrations in having the highest La/Lu ratio (Fig. 22). Some rocks in the Apollo 16 regolith have similarly high La/Lu, but they are more feldspathic (< 1% FeO, e.g., Jolliff and Haskin 1995). The meteorite is also distinctive in having the highest La/Th ratio (Fig. 19), but Lu/Th is typical of other feldspathic lunar meteorites, suggesting that it is the light REE that are anomalously high.

Shukolyukov et al. (2004) studied nuclides of noble gases in Dhofar stones 303, 305, 307, 731, and 733. For several parameters, most notably concentrations and ratios of Ne isotopes and $^{40}Ar/^{36}Ar$, data for Dhofar 303 are substantially different from that for Dhofar stones 305, 307, and 731, for which data are similar to each other. Shukolyukov et al. (2004) conclude that Dhofar 305, 307, and 731 are from a common fall, whereas Dhofar 303 is from a different fall. For most of the same parameters, however, data for Dhofar 733 are similar to those for Dhofar 305, 307, and 731. Shukolyukov et al. (2004) nevertheless conclude that Dhofar 733 is from a different fall than Dhofar 305, 307, and 731 because their derived $^{38}Ar_{cosm}$ is substantially lower (their Table 6), which leads to a lower exposure age (T_{38} = 1.8 Ma compared with 10.4–15 Ma for the other three stones; their Table 8). (The ^{38}Ar concentration for the four stones are all nearly the same, however.) If Shukolyukov et al. (2004) interchanged their samples of Dhofar 303 and Dhofar 733, then most of the noble gas observations reconcile with the petrographic and compositional observations; that is, Dhofar 303, 305, 307, and 731 are similar for all parameters and Dhofar 733 is different.

Compared with other Omani lunar meteorites, Dhofar 733 is moderately contaminated with terrestrial Sr (Figs. 9 and 10), but highly contaminated, in a relative sense, with terrestrial U because of its low intrinsic (lunar) concentration of U (Fig. 12).

Dhofar 925 [X], 960 [Y], and 961 [Z]

In Korotev et al. (2009) we questioned, on the basis of differences in composition (e.g., Figs. 19 and 23), whether Dhofar 961 (22 g) was paired with Dhofar 925 (49 g), for which we have only a small sample, and Dhofar 960 (35 g), for which we did not have a sample. All three stones were found together (Fig. 2) and regarded as paired by Demidova et al. (2005, 2007) based on the find location and petrography. I have subsequently obtained a sample of Dhofar 960. Its composition overlaps (Fig. 23) with that of Dhofar 925 and SaU 489 found 340 km away (Figs. 1 and 2) (erroneously stated as 212 km in Korotev et al. 2009). Table 2 contains an updated weighted-mean composition for Dhofar 961 because it includes data for one additional INAA subsample (Fig. 23).

Demidova et al. (2005) state that "Dhofar 925, 960, and 961 are impact melt breccias with abundant mineral fragments and lithic clasts, which are embedded into a

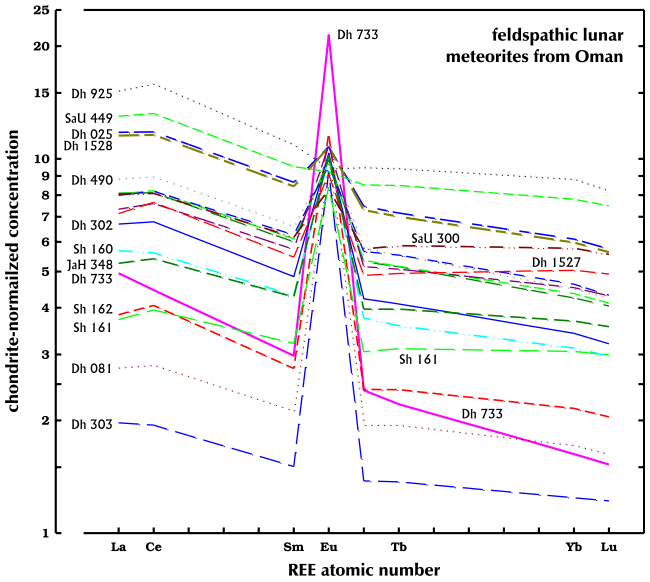

Fig. 22. Chondrite-normalized REE concentrations of feldspathic lunar meteorites from Oman (see fig. 12 of Korotev et al. [2003] for normalization technique). This plot is based on data for the seven REEs of the abscissa, for which the analytical uncertainties are typically 1–4% (Table 2). For paired meteorites, the line represents the weighted mean of all stones, but the label is that of the lowest number of the pair group. "Dh 925" represents only Dhofar 925 and 960. The cluster of unlabeled lines at 7–8 La includes, from lowest to highest La concentration, Dhofar 1527, Dhofar 1436/1443, Dhofar 1428, SaU 300, Shişr 166, and Dhofar 026/461. Data from the sources of Table 1.

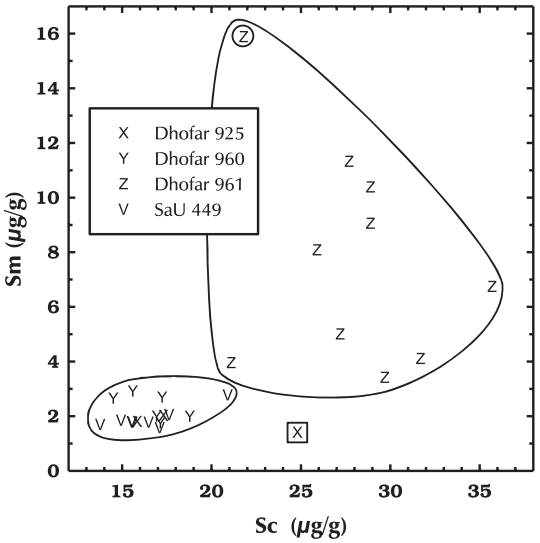

Fig. 23. Although compositionally distinct, Dhofar 961 is probably paired with Dhofar 925 and 960 on the basis of field location and petrography (Demidova et al. in Russell et al. 2004, 2005; Demidova et al. 2007; Zeigler et al. 2010). This figure is updated from fig. 15 of Korotev et al. (2009), with new data for Dhofar 960 and one additional subsample of Dhofar 961 (encircled) that, ironically, lies outside the range of the previously analyzed subsamples. SaU 449 appears to be a launch pair to the Dhofar stones (Korotev et al. 2009b). The square represents the analysis of Dhofar 925 by Demidova et al. (2007).

fine-grained impact melt matrix. In some areas, the meteorites have a fragmental breccia texture. Glass veins and fragments of different composition are common and therefore the meteorites have characteristics of regolith breccias." On the basis of preliminary petrographic study, all four stones are glassy-matrix regolith breccias with a variety of clast types, several of which occur in all four stones (Zeigler et al. 2010). For this reason, I concur with the conclusion of Demidova et al. (2005) that the three stones are paired. Dhofar 961 is compositionally distinct from the other stones because it is dominated by a mafic, ITE-rich impact-melt-breccia component that is largely absent in the other two stones (Zeigler et al. 2010). For this reason and the fact that the analyzed mass of Dhofar 961 is greater than the other two stones (Table 1), the Dhofar 925/960/961 mass-weighted means presented in Tables 2 and 3 are based on stone masses, not INAA subsample masses (Table 1).

Dhofar 1180 [L]

Dhofar 1180 (115 g; Fig. 24), a regolith breccia (Zhang and Hsu 2009), is compositionally distinct from other lunar meteorites from Oman in being moderately mafic and having low concentrations of ITEs and low *Mg′* (Figs. 3 and 6b). With 63% normative feldspar (composition from Korotev et al. 2009), it is nominally a feldspathic breccia, but one bearing mineral clasts derived from low-Ti mare basalt (Zhang and Hsu 2009). The composition corresponds to a 2:1 mixture of typical material of the feldspathic highlands (Korotev et al. 2003a) and very-low-Ti mare basalt with a composition like Asuka-881757 or Miller Range 05035 (Korotev et al. 2009). Although several regolith breccias having subequal proportions of mare material and feldspathic highlands material have been found in Antarctica (Elephant Moraine 87521/96008, Queen Alexandra Range [QUE] 94281, Yamato 793274/981031, Yamato 983885), Dhofar 1180 is the only lunar meteorite from Oman that is such a mixture. The meteorite is strongly contaminated by terrestrial Sr and Ba (Fig. 9). No CRE data are available.

Dhofar 1428 [M]

Dhofar 1428 (213 g; Fig. 24) is a feldspathic lunar meteorite that is similar in composition to several others, most notably Dhofar 025 and pairs, Dhofar 026 and pairs, Dhofar 490/1084, and Shişr 160 (Figs. 3, 4, and 5).

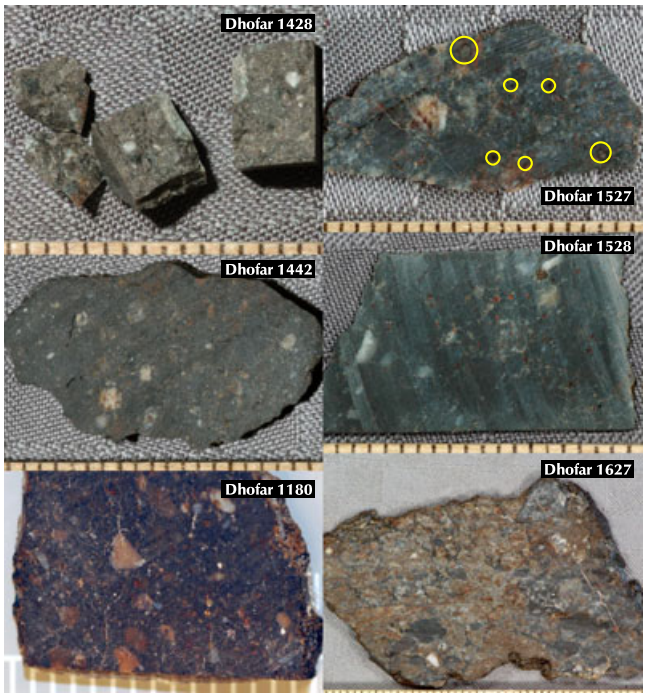

Fig. 24. Chips and sawn faces of Dhofar 1180, 1428, 1442, 1527, 1528, and 1627, all breccias. In Dhofar 1527, the circles indicate large grains of FeNi metal. Tick marks are millimeters.

Of these, it is similar in texture only to Shişr 160 (see below). Although it is distinct on the Na/Eu versus Sc plot of Fig. 7, the Na enrichment is probably a terrestrial weathering effect (below). Dhofar 1428 (213) was found distant from other Dhofar stones except for compositionally and texturally dissimilar Dhofar 1180 (Figs. 3 and 24) reported to have been found 2.7 km away (Fig. 2). The meteorite was originally classified as a "clast-rich, crystalline melt breccia" (Bunch et al. 2006), but Zhang et al. (2009) report that it has "a distinct breccia texture with numerous fragments of rock, mineral, and glass all welded by a glassy matrix. This matrix shows a schlieren texture and contains numerous small rounded vesicles, implying that Dhofar 1428 is a regolith breccia." Liu et al. (2009) postulate that an olivine-rich spherule with a barred texture that they found in Dhofar 1428 is of chondritic origin. Hidaka et al. (2009) provide a short petrographic description. The compositional results of Tables 2 and 3 are similar to those of Hidaka et al. (2009, 2010), who concluded that the meteorite derives mainly from ferroan anorthosite precursor rocks ($Mg' = 66$). With 7.0 ng g^{-1} Ir (Table 2), Dhofar 1428 contains 1.2% equivalent CM chondrite, a typical value for a regolith breccia.

Dhofar 1428 has little staining by hematite. It is moderately contaminated with terrestrial Sr, but not seriously contaminated with Ba (Fig. 9). It is also moderately contaminated with Na (Fig. 8b), K (Fig. 13), and Zn. With INAA, a signal for Zn is obtained, but, for lunar samples, I do not report the derived concentration values because they tend to be systematically high, typically 20–30 μg g^{-1} for feldspathic regolith breccias, as a result of spectral interferences. Nevertheless, the INAA results are sometimes semiquantitatively useful. Low levels of Zn are characteristic of impact-melt breccias, whereas high levels are characteristic of regolith breccias because most of the Zn in lunar materials derives from micrometeorite impacts into the regolith (Baedecker et al. 1972; Haskin and Warren 1991). For example, Zn concentrations are typically 20 μg g^{-1} in Apollo 16 soils, but < 10 in the impact-melt breccias (Haskin and Warren 1991). The derived values for Dhofar 1428 average 87 ± 21 μg g^{-1}, much higher than any Apollo 16 soil. There is no self-evident "lunar explanation," given that siderophile element concentrations are typical. The derived concentration of Zn is also high (41 ± 5 μg g^{-1}) in Dhofar 1180, which was collected 2.7 km away, however. If this similarity is not a coincidence, then there must be some localized source of Zn contamination in the area of Oman where these two stones were found.

Dhofar 1436 [$] and Dhofar 1443 [¥]

Dhofar 1436 (24 g) and Dhofar 1443 (37 g) were collected < 0.8 km from each other, but on different occasions. Both are described as impact-melt breccias with abundant vesicles (C. Lorenz and M. Nazarov, in Connolly et al. 2007; A. Bischoff, in Weisberg et al. 2009). Vesicles are not as self-evident in the samples analyzed here (Fig. 25) as they are in Dhofar 081 et al. (Fig. 16). Korochantseva et al. (2009) describe Dhofar 1436 as "gas-rich" and it may well be a regolith breccia. The meteorite is at the mafic end of the range of feldspathic lunar meteorites (Fig. 3), but neither of the short petrographic descriptions mentions clasts of mare basalt. Compositionally, the stones are identical (Figs. 4, 5, and 7) and are likely paired. Korochantseva et al. (2009) present some preliminary ^{40}Ar-^{39}Ar data for Dhofar 1436. Neither stone is seriously contaminated with Sr, Ba, K, or U.

Dhofar 1442 [K]

Although originally classified as an impact-melt breccia (Ivanova et al., in Weisberg et al. 2009), Dhofar 1442 (106.5 g; Fig. 24) is a clast-rich, glassy-matrix regolith breccia (Zeigler et al. 2011). INAA data are presented in Korotev et al. (2009) and major-element data are presented in Table 3. I have also analyzed three new subsamples from another stone of the meteorite by INAA. Lithophile-element concentrations are essentially the same, but concentrations of Ni and Ir average three

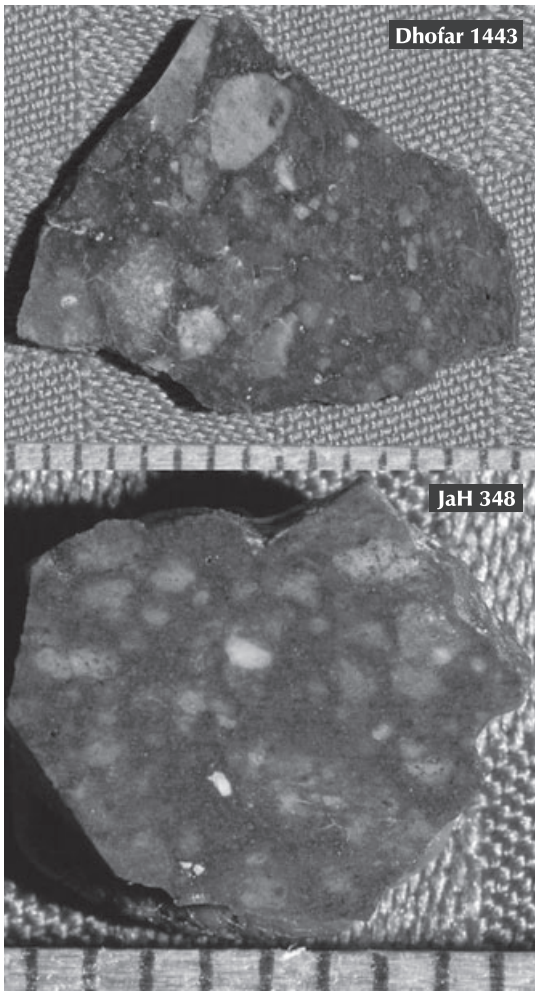

Fig. 25. Dhofar 1443 and JaH 348 are compositionally similar, but collected 143 km apart.

times greater in the new sample than in the previous sample. The recalculated weighted mean is given in Table 2. The meteorite represents the most KREEP-rich regolith in the lunar sample collection and is one of the most mafic breccias among the Omani lunar meteorites. Concentrations of ITEs are 1.1–1.3 times those of Apollo 14 soil and 1.6–1.8 times that of the regolith breccia lithology of SaU 169. Compared with these regoliths, however, Dhofar 1442 is more mafic and more ferroan ($Mg' = 52$; Fig. 6) because it contains a greater proportion of clastic mare basalt (Zeigler et al. 2011). Presumably, the mare component accounts for the moderately high concentration of TiO_2, 2.75%, the same as in basalt Dhofar 287 (Table 3).

Dhofar 1442 has among the greatest concentrations of siderophile elements among Omani lunar meteorites (Fig. 17). The Ni concentration is 14 times greater than that of the other KREEP-rich regolith breccia, SaU 169. Using the same regression procedure described in Fig. 26 for Dhofar 1527, the estimated mean composition of the FeNi metal carrier of the siderophile elements is 89 ± 11% Fe, 10.1 ± 0.4% Ni, 0.467 ± 0.015% Co, 5.4 μg g^{-1} Ir (assumed; Fig. 17), and 1.3 ± 0.13 μg g^{-1} Au (uncertainties are 95% confidence intervals based on the data for replicate subsamples). This composition is consistent with metal in H chondrites (Rambaldi 1977). The mean Ir concentration (23 ng g^{-1}) of the Dhofar 1442 sample analyzed in Korotev et al. (2009) corresponds to 3.0% H chondrite, whereas that (76 ng g^{-1}) of the new sample analyzed here corresponds to 9.9% H chondrite (Wasson and Kallemeyn 1988). On average, 4% of the Fe in the Dhofar 1442 is of chondritic origin.

Dhofar 1527 [U]

Dhofar 1527 (43 g; Fig. 24) is glassy impact-melt breccia (H. Haack, in *The Meteoritical Bulletin*, No. 100, in prep.). For well-behaved lithophile elements, it is most similar in composition to Dhofar 1436/1443. The most distinctive feature of the meteorite, however, is the high abundance of FeNi metal, with grains up to 1 mm in diameter (Fig. 24). As a consequence, Dhofar 1527 has the highest concentrations of Co, Ni, Ir, and Au among the meteorites studied here (Table 2; Fig. 17a) and "FeO_T" concentrations vary by a factor of two among subsamples (Fig. 4). On the basis of correlations of Fe, Ni, Co, and Au against Ir, the mean composition of the metal is 93 ± 8% Fe, 6.5 ± 0.8% Ni, 0.41 ± 0.05% Co, 4.6 μg g^{-1} Ir, and 1.3 ± 0.5 μg g^{-1} Au (Fig. 26). Among common types of iron meteorites, this composition is consistent with group IAB (Wasson and Kallemeyn 2002). The analyzed sample (seven subsamples) contains 1.7 wt% metal. On average, 28% of the total iron in the meteorite is carried by FeNi metal. The meteorite is moderately contaminated with Na, K, and P (Figs. 8 and 13).

Dhofar 1527 was found 10 km east of Dhofar 925/960/961, another metal-rich meteorite. There is no compositional reason to suspect that the meteorites are paired, however, because there is no overlap in FeO-Th space (Fig. 4) and, more importantly, Ni/Ir ratios of the two meteorites are significantly different (Fig. 26c), indicating a different metal component.

Dhofar 1528 [R]

Dhofar 1528 (213 g; Fig. 24) is an impact-melt breccia (H. Haack, in *The Meteoritical Bulletin*, No. 100, in prep.). The meteorite is the most magnesian ($Mg' = 73$) of meteorites having >6 μg g^{-1} Sc (Fig. 6) or $<30\%$ Al_2O_3 (Fig. 3). Dhofar 025 and its pairs, another moderately mafic and magnesian feldspathic

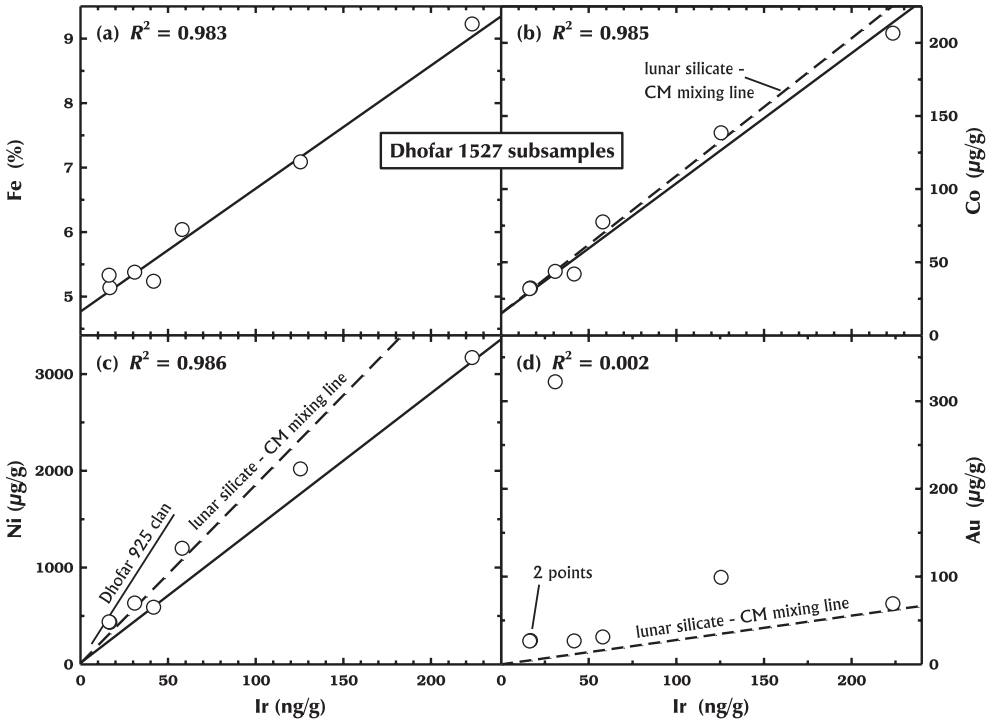

Fig. 26. Siderophile elements in seven subsamples of Dhofar 1527 (the two lowest-Ni samples plot together in b, c, and d). The solid lines are least-squares regressions with both elements weighted by 5% of the concentration value. In (a) and (b), if the regression lines are extrapolated to 4633 ng g^{-1} Ir, Fe is 93.13%, Ni is 6.46%, and Co is 0.41%, and the sum of the three elements is 100.00%. This is the estimated composition of the metal phase causing the correlations. For reference, the dashed lines are mixing lines between the lunar silicates and CM chondrites (Wasson and Kallemeyn 1988). (a) In the most extreme subsample, half of the total iron is metallic. (b) The inferred Ni/Co of the metal is 15.6 ± 0.3, which compares with 20–22 for carbonaceous and ordinary chondrites. (c) The inferred Ni/Ir of the metal is $1.39 \pm 0.17 \times 10^4$, a value 0.7 times that of CM chondrites. The range of and linear regression for 18 subsamples of Dhofar 925/960/961 are also shown. For this meteorite, the inferred metal composition has Ni/Ir of $3.1 \pm 0.3 \times 10^4$, 1.6× that of CM chondrites. (d) The Au/Ir ratios are highly variable among the subsamples, which may be a result of Au contamination. If the most highly anomalous point is omitted, the regression (not shown) extrapolates to 1.3 ± 0.5 μg g^{-1} Au in the metal.

lunar meteorite, were found <8 km south of Dhofar 1528. Fields for the two meteorites nearly overlap on Fig. 4, but the Cr/Sc of Dhofar 1528 is significantly greater than that of Dhofar 025/301/304 (Fig. 5), La/Th is 0.5 times (Fig. 19), and siderophile element concentrations are two to three times greater in Dhofar 1528, so there is no compositional reason to suspect that the two meteorites are paired. La/Th in Dhofar 1528 is significantly less than that of any other Omani lunar meteorite (Fig. 19), a feature that does not appear to correlate with any other compositional parameter. The diagonal trend of the subsamples on Fig. 4 is a mixing effect between feldspathic components and some ITE-rich component, perhaps the clasts of "K-rich rhyolitic glass" described by Haack (in *The Meteoritical Bulletin*, No. 100, in prep.). Dhofar 1528 is significantly contaminated with alkali elements. The Na_2O concentration is about 1.2 times that of Antarctic lunar meteorites of similar Eu concentration (Figs. 7 and 8). The concentration of K_2O is four times (Fig. 13) and that of Cs is about two times greater than expected on the basis of Antarctic meteorite of similar Sm concentration. Sr and Ba are not as seriously enriched (Fig. 10), however (another difference from Dhofar 025/301/304).

Dhofar 1627 [T]

Dhofar 1627 (Fig. 24) is an 86 g feldspathic impact-melt breccia (S. Seddio and B. Jolliff, in *The Meteoritical Bulletin*, No. 100, in prep.) found distant from other Dhofar lunar meteorites (Fig. 1). It is among the most mafic of the nominally feldspathic breccias from Oman, but is three to four times richer in ITEs than other meteorites of similar Sc concentration (Fig. 3). In both regards, the meteorite is similar to regolith from the Apollo 16 site and to lunar meteorite Northwest Africa 4936 (a glassy impact-melt breccia, or possibly regolith breccia; Korotev et al. 2009) and its pair, NWA 5406 (Fig. 27a). Another similarity among the two meteorites

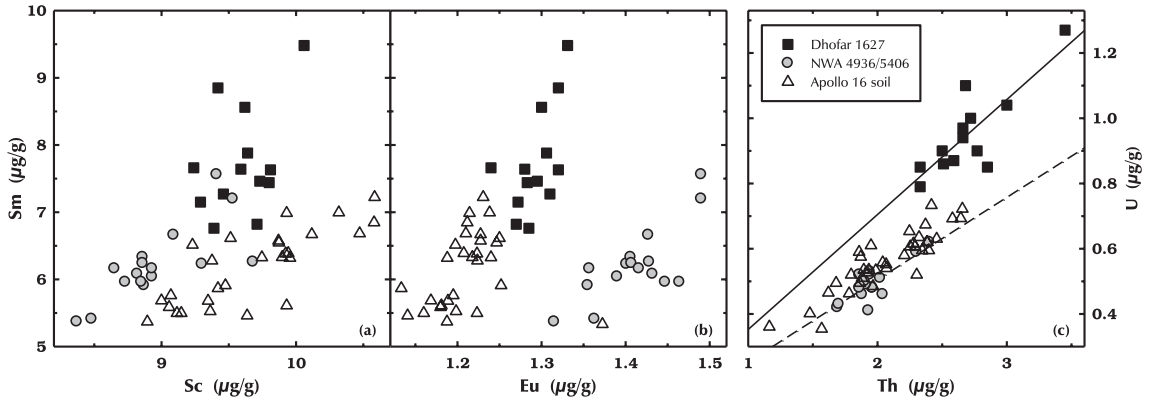

Fig. 27. Dhofar 1627 is similar in composition to NWA 4936/5406 (Korotev et al. 2009). (a) The two meteorites are the only lunar meteorites having bulk compositions similar to soil from the Apollo 16 site (see also Fig. 3). (b) Eu distinguishes Dhofar 1627 from NWA 4936. (c) The mean U/Th of Dhofar 1627 (0.352 ± 0.016; solid line) is different from that of NWA 4936/5406 (0.252 ± 0.009; dashed line). The circles and squares represent subsamples of a meteorite. The triangles represent different 6xxx1 samples of surface and trench soil from Apollo 16 (references of Korotev 1997).

and the Apollo 16 regolith is moderately high concentrations of siderophile elements with nonchondritic Ni/Ir (Fig. 28). In detail, Sm/Na and Th/U distinguish the two meteorites from each other and from the Apollo 16 regolith (Fig. 27b and 27c). We previously speculated that NWA 4936 might originate from near the Apollo 16 site (Korotev et al. 2009) and the same arguments apply to Dhofar 1627. The meteorite clearly originates in the feldspathic highlands, but someplace moderately contaminated, as is the Apollo 16 site, with Sm-rich material from the Procellarum KREEP Terrane.

Jiddat al Harasis 348 [¢]

JaH 348 is described as a 18.4 g "clast-rich, fragmental breccia with sparse vesicles (< 0.3 mm) that is dominated by many varieties of quench-textured impact-melt breccias and plagioclase fragments" (J. Wittke and T. Bunch, in Weisberg et al. 2009). Because in the classification system of Stöffler et al. (1980) fragmental breccias have a clastic matrix (shock compression) and JaH 348 has vesicles (melt matrix), I have identified it as a impact-melt breccia in Table 1. Texturally (Fig. 25) and compositionally (e.g., Figs. 5 and 7), the meteorite is similar to paired stones Dhofar 1436 and Dhofar 1443 collected 143 km away (Fig. 2). The differences between the meteorites are that JaH 348 has lower concentrations of ITEs (0.7–0.8×), lower concentrations of Na and Eu (0.94×, Fig. 29; indicating a slight difference in mean anorthite content of the plagioclase), lower concentrations of siderophile elements (0.7× and 0.6×, Ni and Ir), and lower Cr/Sc (0.91×, Fig. 5) and Mg' (0.95×, Fig. 6). JaH 348 is also considerably less contaminated with terrestrial Sr and Ba (Fig. 10). These various differences are not so great that the possibility of launch pairing can be dismissed. These two breccias may well contain the same lithologic components, but in different proportions.

Sayh al Uhaymir 169 [© and ®]

Sayh al Uhaymir ("slightly reddish plain," A. Al-Kathiri, pers. comm.) 169 (206 g) is unusual among lunar meteorites in being dilithologic, consisting mainly of a large clast of crystalline impact-melt breccia [symbol © in Fig. 3] with minor attached regolith breccia [®] of distinctly different composition (Gnos et al. 2004; Al-Kathiri et al. 2007; Korotev et al. 2009). The impact-melt breccia has the highest concentrations of ITEs of any meteorite and nearly all KREEP-rich impact-melt breccias of the Apollo collection. It is, however, indistinguishable in composition (Korotev et al. 2011b) and crystallization age (3920 ± 13 Ma; Liu et al. 2012) from an uncommon variety of impact-melt breccia found as small fragments in the Apollo 12 regolith (3914 ± 7; Liu et al. 2012). Lin et al. (2012) report Pb–Pb ages of zircon and baddeleyite that have a major peak at 3921 ± 3 but also a minor peak at 4016 ± 6 Ma. They also report the presence of clasts of "very-high-K KREEP" with 2.7% K_2O and concentrations of light REE that are two times that of the impact-melt breccia.

Other than the fact that both breccia lithologies of SaU 169 are rich in KREEP, there is little evidence that they are related in that the melt-breccia lithology is not a major component of the regolith-breccia lithology (Al-Kathiri et al. 2007; Korotev et al. 2009b). With some of the lowest concentrations of siderophile elements among regolith breccias studied here (Fig. 17), the regolith represented by SaU 169 is immature (Korotev et al.

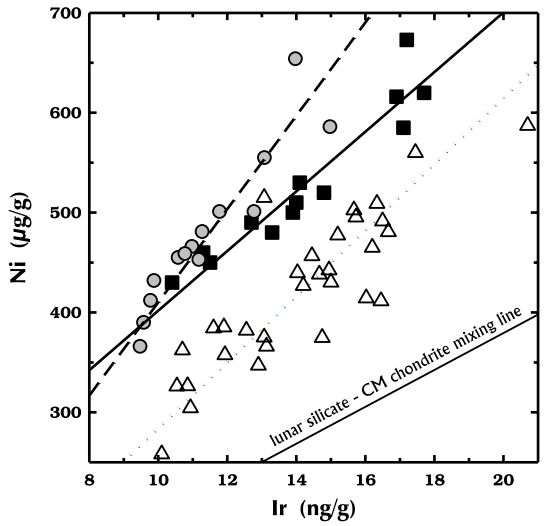

Fig. 28. Like Fig. 27, but for siderophile elements. The lunar silicate–CM mixing line is the same as in Fig. 26d. The other lines are least-squares fits to the plotted data points. Two points for NWA 4936 (Korotev et al. 2009) that plot off scale at 50 and 57 ng g^{-1} Ir have considerably lower Ni/Ir ratios and were not included in the regression. The metal components of the two meteorites and the Apollo 16 regolith have greater Ni/Ir ratios than do chondrites.

2009). It does, however, contain trapped solar wind gases (Gnos et al. 2004; Lorenzetti et al. 2005). The terrestrial age is 9.7 ± 1.3 kyr (Gnos et al. 2004), the lowest value reported for an Omani lunar meteorite.

Sayh al Uhaymir 300 [S]

SaU 300 is a 153 g breccia that was originally classified as a regolith breccia (R. Bartoschewitz et al., in Connolly et al. 2007; Hsu et al. 2007), but was later recognized to be a crystalline impact-melt breccia (Hudgins et al. 2007; Hsu et al. 2008). Concentrations of solar wind gases are low, as expected for impact-melt breccias (Bartoschewitz et al. 2009). With 64% normative plagioclase, it is distinct in being at the mafic end of the range of feldspathic lunar meteorites, yet there is no compositional evidence and only trace petrographic evidence that it contains mare basalt or KREEP-bearing components (Hudgins et al. 2007; Hsu et al. 2008), which are common in other lunar meteorites of intermediate iron concentration (Korotev et al. 2009). It has the lowest concentration of Eu among the Omani meteorites (Fig. 29), a feature due to its lack of KREEP and "low" abundance of plagioclase. The meteorite is uniform in composition and the compositional results of Korotev et al. (2009) agree well with those of Hsu et al. (2008). With Mg' of 67, the composition is consistent with derivation from a ferroan anorthositic norite precursor, although Hudgins et al. (2007) observed two populations of olivine mineral clasts, $Fo_{67–91}$ and $Fo_{63–72}$, suggesting the presence of a magnesian lithologic component in the breccia. SaU 300 is substantially contaminated with terrestrial Sr, but is not enriched in Ba (Fig. 9).

Sayh al Uhaymir 449 [V]

SaU 499 (16.5 g) was originally classified as a feldspathic impact-melt breccia (M. Ivanova and N. Kononkova, in Connolly et al. 2007), but Zeigler et al. (2010) prefer a classification of glassy-matrix regolith breccia. Table 3 reports major-element data for SaU 449 that were not presented in Korotev et al. (2009). As with the trace lithophile elements and siderophile elements, major-element concentrations are all but identical to those of Dhofar 925 and 960. SaU 449 is either a launch pair or a transported terrestrial pair to the Dhofar 925/960/961 meteorite (Korotev et al. 2009; Zeigler et al. 2010). The reported find locations of the two meteorites are 340 km apart (incorrectly stated as 212 km in Korotev et al. 2009). SaU 449, as well as Dhofar 925 and 960, has concentrations of K_2O that are 1.8 times greater than expected on the basis of the correlation between K and Sm among feldspathic lunar meteorites from Antarctica (Fig. 13). This apparent enrichment may not be a result of terrestrial weathering, but instead may reflect the composition of the lunar rocks in the region of the Moon from which the meteorite derives (Korotev et al. 2009).

Shişr 160 [#]

Shişr 160 (101 g) is an undescribed feldspathic regolith breccia (Figs. 24 and 30). It was found in the most westerly location of the Omani lunar meteorite field (Fig. 1). With $Mg' = 61.7$, it is among the most ferroan of the feldspathic meteorites studied here (Table 3; Fig. 6). It bears some compositional similarity to Shişr 162 and Shişr 166 in being similarly feldspathic and low in ITEs (Fig. 4), but it has a distinctly different Eu concentration (Fig. 29) and texture (Fig. 30). Both texturally (Figs. 14 and 30) and compositionally, however, it is most similar to Dhofar 1428 collected 122 km away. The main differences are that Dhofar 1428 is slightly more mafic (Sc, Cr, and Fe concentration are 1.06–1.12 times greater), is more magnesian (66.4 compared with 61.7), has higher concentrations of ITEs (1.4–1.6 times greater), and has lower concentrations of siderophile elements (0.85× and 0.72× for Ni and Ir), on average. These differences are not great and the meteorites might be launch pairs. Shişr 160 is not highly contaminated with Sr and Ba, but is moderately contaminated with terrestrial U and highly contaminated

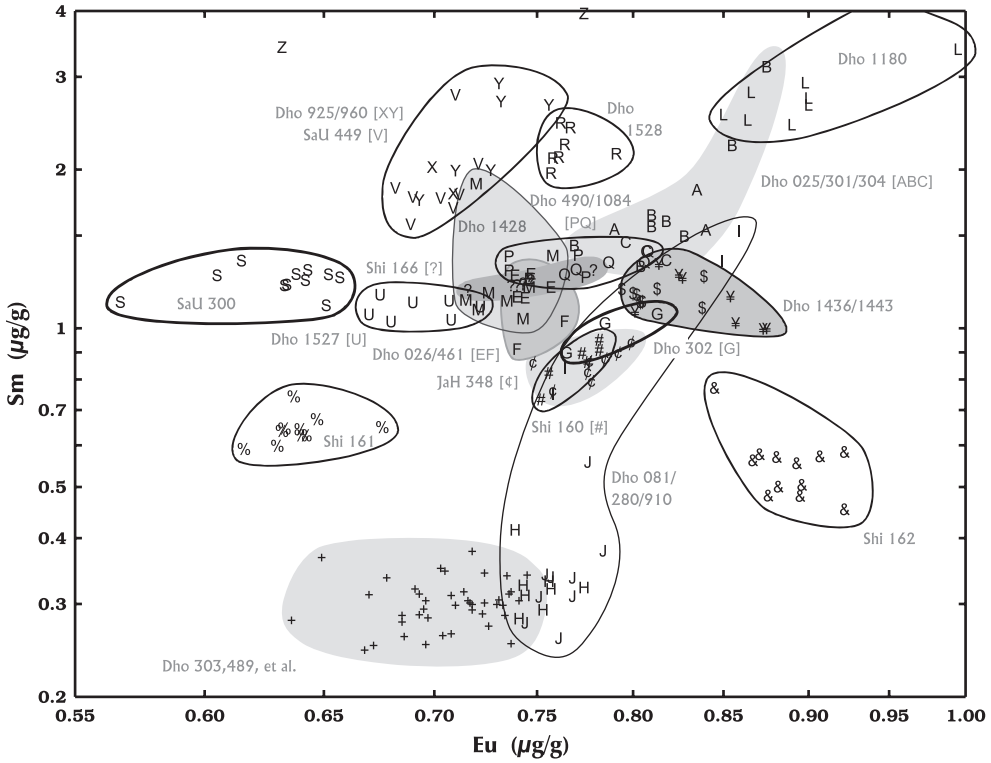

Fig. 29. Sm and Eu data for subsamples. This plot separates, for example, Shişr 162 from Shişr 160 and Dhofar 1528 from Dhofar 025 et al., which overlap on Fig. 4. Plotting off the scale of the figure are Dhofar 287 (basalt), Dhofar 733 (Eu-rich), most of the Dhofar 961 subsamples (Sm- and Eu-rich), Dhofar 1442 (Sm- and Eu-rich), Dhofar 1627 (Sm- and Eu-rich), and SaU 169 (Sm- and Eu-rich). See Fig. 3 for symbol key.

with P compared with other lunar meteorites from Oman (Figs. 9, 12, and 13). It does not show the Na and Zn enrichment of Dhofar 1428.

Shişr 161 [%]

Shişr 161 (57 g; Fig. 30), a regolith breccia (Foreman et al. 2009), is at the mafic end of the range of feldspathic lunar meteorites from Oman (Fig. 3). It contains lithic clasts of granulitic breccia, fragmental breccia, impact-melt breccia, and rare mare basalt (Foreman et al. 2009). Shişr 161 is compositionally distinct (Figs. 4, 5, and 7), but bears some resemblance to JaH 348, although it is more magnesian (Fig. 6). It has the lowest Sm/Sc, 0.049, among meteorites studied here. This value is even lower than the plutonic anorthositic norite of Apollo 16 sample 67513, 0.057 (Jolliff and Haskin 1995), indicating that the meteorite is effectively uncontaminated with KREEP. Concentrations of siderophile elements are low for a regolith breccia (Fig. 17). Because it has low concentrations of ITEs, it is one of the most highly contaminated, in a relative sense, with terrestrial U (Fig. 12). It also appears to be contaminated with Na and K (Figs. 8 and 13).

Shişr 162 [&]

At 5.525 kg, Shişr 162 (Fig. 30) is the largest lunar meteorite from Oman. It is the most feldspathic of the four Shişr lunar stones and among the most feldspathic of the Omani lunar meteorites (e.g., Fig. 29). Except for Dhofar 733, it is richer in Na_2O and Eu than any Omani meteorite of otherwise similar composition (Figs. 8 and 29), but has a normal Na/Eu ratio (Fig. 7). It is unusual, however, in having a concentration of K_2O almost eight times that expected on the basis of its Sm concentration (Fig. 13). This enrichment is almost certainly the result of some unidentified chemical weathering component, or perhaps a contamination by clay, because Ba correlates with K in lunar feldspars and Ba is not unusually high in Shişr 162 (Fig. 9b). The rock was found partially buried, unlike the smaller meteorites discussed here (Bartoschewitz, personal communication). The sample analyzed here derives from near the surface of the large stone and may be more contaminated than material from the interior.

Shişr 166 [?]

Shişr 166 is a 129 g vesicular impact-melt breccia that is visibly contaminated with terrestrial sulfates

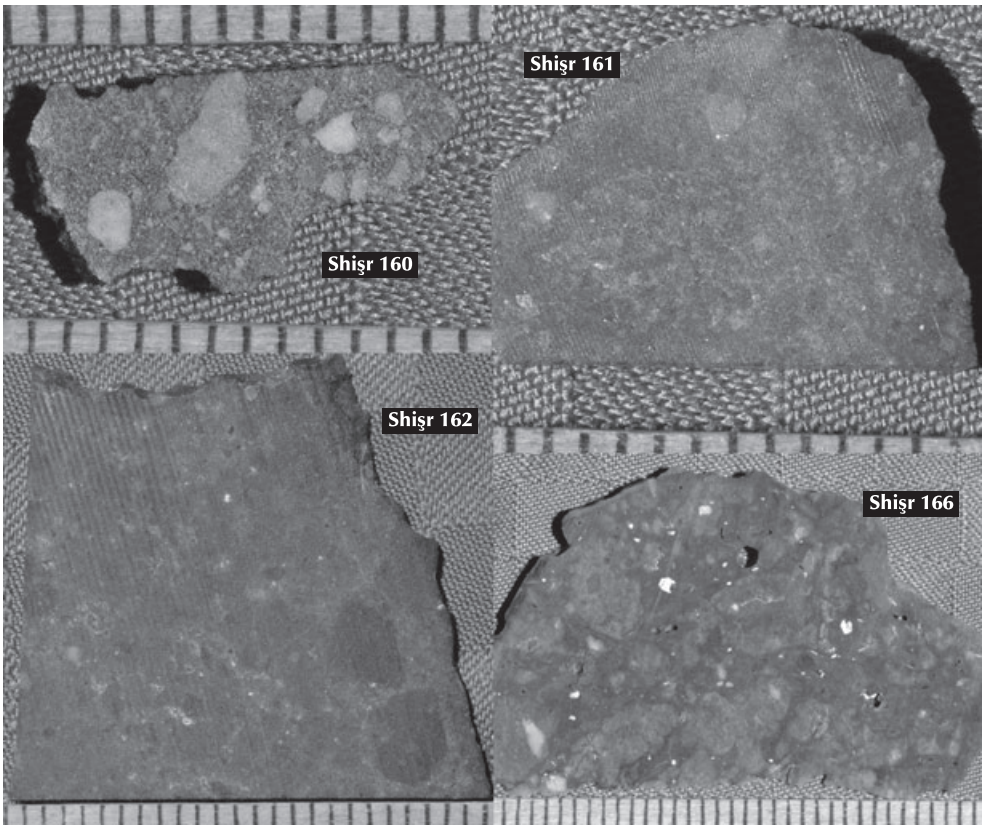

Fig. 30. The four Shişr meteorites are compositionally and texturally distinct from each other. Some vesicles in Shişr 166 are filled with Sr and Ba sulfates.

(Fig. 30). For lithophile elements, it is compositionally identical to paired stones Dhofar 026 and Dhofar 457–468 (Figs. 4, 5, 7, and 29). Ni, Ir, and Au concentrations are each 71–73% as great, however. Dhofar 026 was found 12 km east of its pairs, Dhofar 457–468 (Warren et al. 2005), but Shişr 166, which differs greatly in texture (Figs. 14 and 30), was found 33 kilometers north of Dhofar 457–468 (Fig. 2, inset). Shişr 166 is distinctly reddish from hematite staining, whereas the Dhofar 026 and Dhofar 457–468 stones are not. No CRE data are available.

DISCUSSION AND SUMMARY

Pairings

Above, the lunar meteorite stones from Oman are grouped under 24 subheadings, a number that reflects the author's working hypothesis for the number of meteorite falls represented. The number may be as high as 25 if Dhofar 489 is not paired with Dhofar 303 et al. (23 km separation; Table 4). The lower limit is more difficult to establish. It could be as low as 17 if (1) JaH 348 is terrestrially paired with Dhofar 1436/1443 (similar composition and texture, but 143 km separation; Table 4), (2) Shişr 160 is terrestrially paired with Dhofar 1428 (similar composition and texture, but 122 km separation; Table 4), (3) Dhofar 302 is paired with either Dhofar 081 et al. or Dhofar 303 et al. (proximity, Table 4), (4) Dhofar 025 and Dhofar 287 are paired (proximity), (5) Dhofar 1180 and 1428 are paired (proximity), (6) SaU 449 is terrestrially paired with Dhofar 925/960/961 (similar composition and petrography, but 340 km separation), and (7) Shişr 166 is paired with Dhofar 026 and its small pairs (similar composition, but 33 km separation).

Among the lunar meteorites from Oman, similarities in bulk composition suggest possible launch pairing (one impact on the Moon delivering more than one meteorite to Oman) for SaU 449 with Dhofar 925/960/961 (Korotev et al. 2009), JaH 348 with Dhofar 1436/1443, Shişr 160 with Dhofar 1428, and Shişr 166 with Dhofar 026/457–368. Compositional similarities can only suggest launch pairings and compositional differences provide only weak evidence against launch pairings, thus other launch pairings may exist. For example, to first order, Dhofar 025 et al., Dhofar 026 et al., Dhofar 490/1084, Dhofar 1428, Shişr 160, and Shişr 166 are all similar in

Table 4. Pairing truth table for lunar meteorites from Oman.

					Evidence for pairing					*N* meteorites	
S/N	Name	Grams	Paired with	Distance (km)	Prox.	CRE	Petr.	Text.	comp.	Min	Max
1	Dho 025	751	–	–	–	–	–	–	–	1	1
2	Dho 026	148	–	–	–	–	–	–	–	1	1
3	Dho 081	174	–	–	–	–	–	–	–	1	1
4	Dho 280	251.2	Dho 081	0.3	1	1	1	1	1	0	0
5	Dho 287	154	Dho 025?	0.5	1	X	0	0	0	0	1
6	Dho 301	9	Dho 025	0.4	1	X	1	1	1	0	0
7	Dho 302	3.83	Dho 303?	0.3	1	X	1	0	0	0	1
8	Dho 303	4.15	–	0.1	–	–	–	–	–	1	1
9	Dho 304	10	Dho 025	0.2	1	X	1	1	1	0	0
10	Dho 305	34.11	Dho 303	0.1	1	X	1	1	1	0	0
11	Dho 306	12.86	Dho 303	0.2	1	X	1	1	1	0	0
12	Dho 307	50	Dho 303	0.2	1	X	1	X	1	0	0
13	Dho 308	2	Dho 025	0.2	1	X	1	X	1	0	0
14	Dho 309	81.3	Dho 303	0.7	1	X	1	1	1	0	0
15	Dho 310	10.8	Dho 303	0.5	1	X	1	1	1	0	0
16	Dho 311	4	Dho 303	0.3	1	X	1	X	1	0	0
17	Dho 457	1.64	Dho 026	11.9	0	X	1	1	1	0	0
18	Dho 458	1	Dho 457	0.09	1	X	1	X	1	0	0
19	Dho 459	1.68	Dho 457	0.19	1	X	1	X	1	0	0
20	Dho 460	9.16	Dho 457	0.61	1	X	1	X	1	0	0
21	Dho 461	3.03	Dho 457	0.57	1	X	1	1	1	0	0
22	Dho 462	1.97	Dho 457	0.19	1	X	1	X	1	0	0
23	Dho 463	2.85	Dho 457	0.19	1	X	1	X	1	0	0
24	Dho 464	1.17	Dho 457	0.78	1	X	1	X	1	0	0
25	Dho 465	2.58	Dho 457	0.51	1	X	1	X	1	0	0
26	Dho 466	2.17	Dho 457	0.59	1	X	1	X	1	0	0
27	Dho 467	1.17	Dho 457	0.61	1	X	1	X	1	0	0
28	Dho 468	0.91	Dho 457	1.35	1	X	1	X	1	0	0
29	Dho 489	34.4	Dho 303?	23.1	0	1	1	1	1	0	1
29	Dho 489	34.4	Dho 925	3.1	1	X	1	1	1	0	0
30	Dho 490	34.05	–	–	–	–	–	–	–	1	1
31	Dho 730	108	Dho 303	1.0	1	X	1	X	1	0	0
32	Dho 731	36	Dho 303	1.3	1	X	1	X	1	0	0
33	Dho 733	98	–	–	–	–	–	–	–	1	1
34	Dho 908	245	Dho 303	0.3	1	1	X	1	1	0	0
35	Dho 909	3.9	Dho 303	0.4	1		X	X	X	0	0
36	Dho 910	142	Dho 081	0.5	1	1	1	1	1	0	0
37	Dho 911	194	Dho 303	0.8	1	1	X	1	1	0	0
38	Dho 925	49	–	–	–	–	–	–	–	1	1
39	Dho 950	21.7	Dho 303	0.5	1	X	1	X	1	0	0
40	Dho 960	35.4	Dho 925	0.5	1	X	1	1	1	0	0
41	Dho 961	21.6	Dho 925	0.2	1	X	1	1	0	0	0
42	Dho 1084	90	Dho 490	1.3	1	X	1	1	1	0	0
43	Dho 1085	197	Dho 303	0.6	1	1	X	1	1	0	0
44	Dho 1180	115.2	–	0.9	–	–	–	–	–	1	1
45	Dho 1224	4.57	Dho 081	1.0	1	X	1	X	X	0	0
46	Dho 1428	213	Dho 1180?	2.7	1	X	0	0	0	0	1
47	Dho 1436	24.2	–	–	–	–	–	–	–	1	1
48	Dho 1442	106.5	–	–	–	–	–	–	–	1	1
49	Dho 1443	36.7	Dho 1436	0.8	1	X	1	1	1	0	0
50	Dho 1527	42.6	–	–	–	–	–	–	–	1	1
51	Dho 1528	213.2	–	–	–	–	–	–	–	1	1
52	Dho 1627	86.14	–	–	–	–	–	–	–	1	1
53	JaH 348	18.4	Dho 1436?	143	0	X	0	1	1	0	1

Table 4. *Continued*. Pairing truth table for lunar meteorites from Oman.

					Evidence for pairing					*N* meteorites	
S/N	Name	Grams	Paired with	Distance (km)	Prox.	CRE	Petr.	Text.	comp.	Min	Max
54	SaU 169	206.45	–	–	–	–	–	–	–	1	1
55	SaU 300	152.6	–	–	–	–	–	–	–	1	1
56	SaU 449	16.5	Dho 925?	340	0	X	1	1	1	0	1
56	SaU 449	16.5	SaU 300	4.2	1	X	0	0	0	0	0
57	Shişr 160	100.86	Dho 1428?	122	0	X	X	1	1	0	1
58	Shişr 161	57.2	–	–	–	–	–	–	–	1	1
59	Shişr 162	5525	–	–	–	–	–	–	–	1	1
60	Shişr 166	128.8	Dho 026?	33.5	0	X	0	0	1		1
	Sum									17	25

Parameters: prox = proximity, distance < 5 km; CRE = cosmic-ray exposure data; petr. = petrology (microscope, EPMA); text. = macroscopic texture and color; comp = composition. Truth: 0 = parameter inconsistent with pairing, 1 = parameter consistent with pairing, X = no data. Rows with dashes represent unpaired stones or the lowest-numbered stone of a potential pair group.

composition (Figs. 4, 5, 7, and 29). They also overlap in composition, however, with Dar al Gani 262, NWA (Northwest Africa) 482, NWA 2200, NWA 6481, NWA 6578, Allan Hills 81005, Larkman Nunataks 06638, MacAlpine Hills 88015, Miller Range 090034, and Queen Alexandra Range 93069 (Fig. 20). The similarities are not necessarily because these meteorites are all paired or launch paired, they merely reflect that these meteorites are all typical of the feldspathic highlands and that their compositions reflect the typical composition of the surface of the lunar highlands, that is, 27–30% Al_2O_3, 4–5% FeO, 6–10 μg g^{-1} Sc, 0.7–1.7 μg g^{-1} Sm, and 0.2–0.6 μg g^{-1} Th (Korotev et al. 2006). Nevertheless, both texturally and compositionally, Dhofar 1428 is very similar to MacAlpine Hills 88105 (Fig. 31) and these two meteorites are good candidates for a two-continent launch pair.

Siderophile Elements

Iridium concentrations vary by a factor of 100 among the brecciated meteorites studied here (Fig. 17). Most lunar meteorites have concentrations of Ir and Ni consistent with a mixture of lunar crustal rocks having essentially zero Ir and low Ni (Fig. 17a) and CM chondrites, the type of meteorite that most closely accounts for siderophile-element ratios in the lunar regolith (Wasson et al. 1975). A chondritic component accounts for Ni/Ir for most of the meteorites studied here (see also Warren et al. 2005). The exceptions are informative. For Dhofar 081 et al., Ni/Ir of the meteoritic component is either subchondritic or the Ni concentration of the feldspathic material is unusually low (< 10 μg g^{-1}; Fig. 17). Most of the Ni-rich meteorites have Ni/Ir ratios that deviate from the CM ratio because they contain FeNi metal that probably derives from iron meteorites. Two of the three metal-rich meteorites, Dhofar 1527 and Dhofar 1627, are impact-melt breccias and the metal may derive from the impactor that formed the breccia. Dhofar 961 is a regolith breccia, but it contains a large component of metal-rich impact-melt-breccia clasts. Dhofar 1442, a regolith breccia, is rich in siderophile elements that appear to derive from an H-chondrite. FeNi metal grains are not as large as they are in Dhofar 961, 1527, and 1627. There is no correlation between siderophile-element abundances and breccia type (regolith, fragmental, impact-melt, or granulitic; Fig. 17b). Both regolith breccias and impact-melt breccias span most of the range in siderophile-element concentrations.

Chemical Alteration

In lunar meteorites from Oman, the most obvious chemical effect of exposure to the terrestrial environment is the heavy contamination with Sr and Ba, mainly in the form of the sulfates, celestite and barite (Korotev et al. 2003, 2009; Nazarov et al. 2004; Warren et al. 2005; Fig. 9). The Sr and Ba derive from the local soil (Al-Kathiri et al. 2005; Zurfluh et al. 2011) and are deposited in the meteorites by evaporation following rainfall. Although rain is rare at the annual scale, reported terrestrial ages of the meteorites are long, ranging from 10 kyr to at least 500 kyr (Nishiizumi and Caffee 2001; Gnos et al. 2004). Also, there have been several pluvial periods associated with variation in Indian Ocean monsoons over the past half-million years (Burns et al. 2001; Al-Kathiri et al. 2005). As a consequence, Sr and Ba concentrations in the meteorites increase with the terrestrial age (Nazarov et al. 2003; Al-Kathiri et al. 2005; Zurfluh et al. 2011). There may also be a geographic effect in that all of the lunar meteorites most contaminated with Sr (> 1000 μg g^{-1} excess, Fig. 10) are Dhofar stones (Fig. 1). Al-Kathiri et al. (2005) conclude that Ba and Sr sulfates found in ordinary chondrites derive their sulfur at least in part from the weathering of

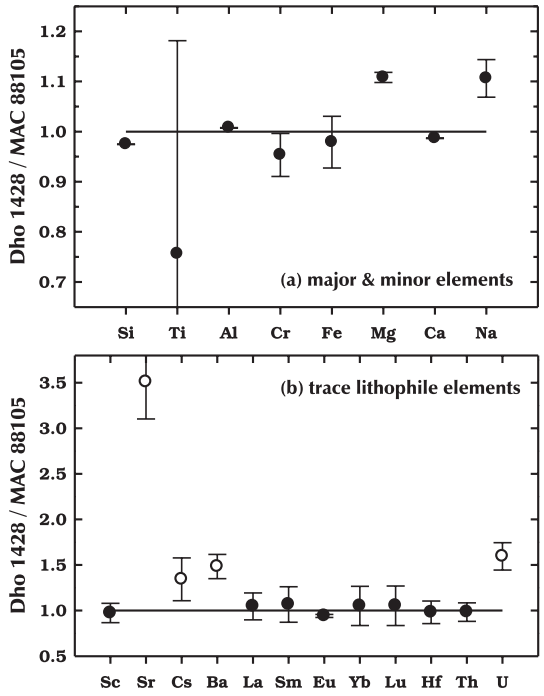

Fig. 31. Comparison of Dhofar 1428 to MAC 88105. Error bars represent 95% confidence limits on the concentration ratios based on the subsample data for Dhofar 1428 ($N = 8$, Table 1). (a) For major elements, the two meteorites are nearly identical except that Dhofar 1428 is 11% richer in MgO and Na_2O. (b) Trace lithophile elements are also essentially identical, except for those elements (open circles) enriched in hot-desert meteorites from weathering processes. For elements not plotted (e.g., Mn, K, Ni, Ir), error bars are large. MAC 88105 data from Jolliff et al. (1991), Koeberl et al. (1991); Lindstrom et al. (1991), Palme et al. (1991), Warren and Kallemeyn (1991), and Joy et al. (2010).

troilite. However, feldspathic lunar rocks contain much less troilite than do chondrites, yet many lunar meteorites are contaminated to a much greater degree with Sr and Ba than are the chondrites (Fig. 10), thus the sulfates in the lunar meteorites must derive from the local soil. Al-Kathiri et al. (2005) note that 50 of 54 ordinary chondrites they dated by ^{14}C had terrestrial ages of <47 kyr, yet the two Omani meteorites with the oldest ages are lunar Dhofar 025 (500–600 kyr; Nishiizumi and Caffee 2001) and shergottite Dhofar 019 (360 kyr; Nishiizumi et al. 2002). Thus one possible explanation for why some lunar meteorites have much higher concentrations of Sr and Ba than do the chondrites is that chondrites do not survive as long in the desert as do the achondrites, which contain much less metallic iron.

Dhofar 490/1084 is severely contaminated with calcite (Fig. 21) and some of the meteorites are contaminated with Na, K, P, Zn, As, Se, Br, Sb, and U (Figs. 12, 13, and 32). Sr and Ba concentrations in the meteorites are not strongly correlated with each other in the meteorites, and concentrations of other elements associated with terrestrial alteration also do not correlate with Sr (Figs. 12 and 32), thus the process of chemical weathering is not simple. None of the Omani lunar meteorites are so severely contaminated, however, that their bulk compositions are not useful for making certain kinds of inferences about the Moon.

Mass Distribution and Flux

The number of lunar meteorites from Oman (24) is similar to the number from Antarctica (20) and northern Africa (28; Fig. 33). The mass from Oman (10.62 kg) is twice that from Antarctica (5.43 kg); however one meteorite, Shişr 162 (5.5 kg), accounts for more than half the mass from Oman. The mass distribution is otherwise similar for the two regions (Fig. 33). The mean mass of lunar meteorites from Antarctica is small because no large meteorites have been found there, and the systematic nature of searching in Antarctica (e.g., Cassidy et al. 1992) leads to recovery of some very small meteorites. Lunar meteorites from Africa tend to be larger than those from Oman for reasons unknown to the author (Fig. 33).

The Shişr, Dhofar, and Jiddat al Harasis lunar meteorites define an area of 10.7×10^3 km^2 (Fig. 1). A total of 10.24 kg of lunar meteorites has been found in the area leading to a concentration of 0.95 g km^{-2}. The oldest terrestrial age for a meteorite from this area is 0.5–0.6 Myr for Dhofar 025 (Nishiizumi and Caffee 2001). Assuming that the rocks were found where they landed, these values lead to a mass flux of 0.97 kg yr^{-1} of lunar rocks in the 1 g to 10 kg size range reaching the surface of the Earth. This is the same calculation done by Nazarov et al. (2004). The new value is four times greater, however, because of the numerous new lunar meteorite finds in the past several years. The value is, however, still an underestimate. Among lunar meteorites from Oman for which CRE ages have been measured, the youngest terrestrial ages are 9.7 ± 1.3 kyr for SaU 169 (Gnos et al. 2004) and 40 ± 20 kyr for paired stones Dhofar 081, 280, and 910 (Nishiizumi et al. 2004; Nishiizumi and Caffee 2006). These are the only lunar meteorites from Oman on which fusion crusts have been described (Greshake et al. 2001; Nazarov, in Grossman and Zipfel 2001; Gnos et al., in Russell et al. 2003; Bunch and Wittke, in Connolly et al. 2007). On older meteorites, the crusts and underlying material have ablated away from wind erosion. Mass loss of at least 50% is evident on some stones (Fig. 34).

Compositional and Lithologic Types

Lunar meteorites from Oman cover most of the range of lunar meteorite compositions and extend it in some directions (Fig. 20). Among lunar meteorites, the

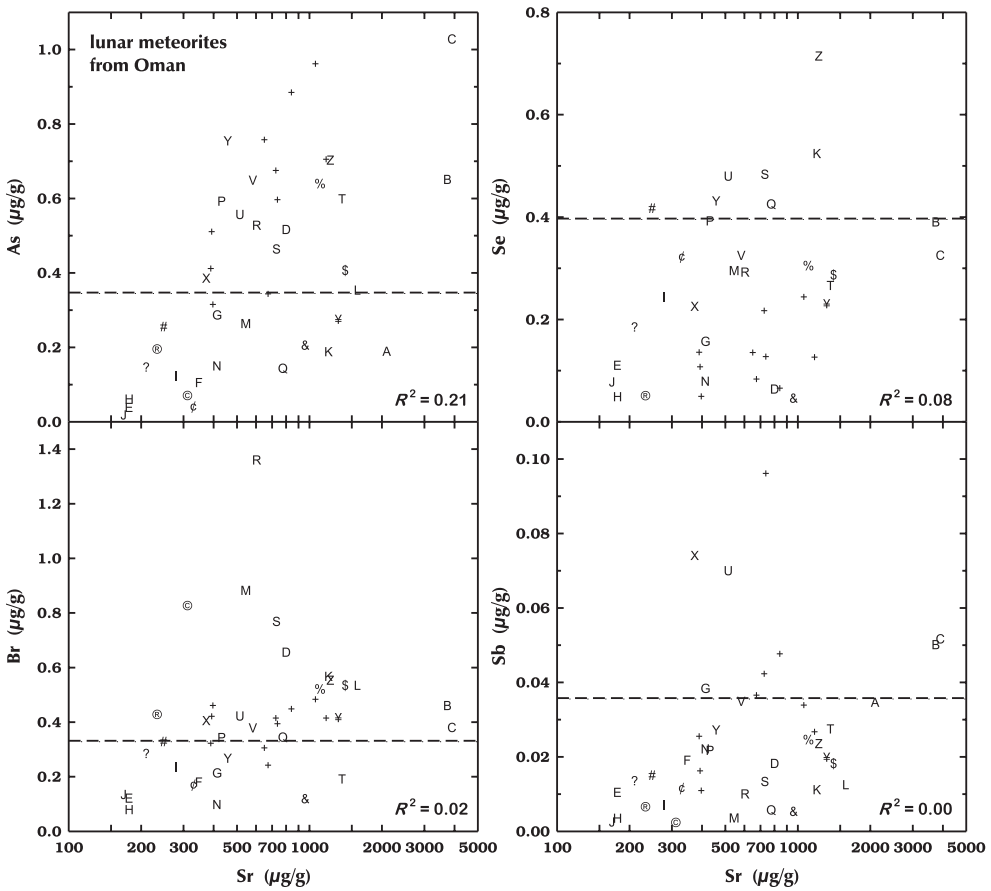

Fig. 32. In Apollo samples, As, Se, Br, and Sb are below INAA detection limits, which are given approximately by the dashed lines (3σ). Each point represents the mass-weighted mean concentration of all subsamples of a stone (Table 1). A number of the meteorites are enriched in one or more of these four elements as a result of terrestrial weathering effects. There are no correlations with Sr enrichment for these elements. See Fig. 3 for symbol key.

two with the highest concentrations of ITEs, Dhofar 1442 and SaU 169, are from Oman. Six of the low-Sm, feldspathic lunar meteorites from Oman have $Mg' > 70$ (Fig. 6). From elsewhere, only Allan Hills 81005, Graves Nunataks 06157, and NWA 5744 are similar. These meteorites demonstrate that some regions of the feldspathic highlands are dominated by magnesian anorthosites (Korotev et al. 2003; Takeda et al. 2006; Treiman et al. 2010). Curiously, only one lunar meteorite from Oman is a basalt, Dhofar 287, and only one is a breccia with a significant component of mare basalt, Dhofar 1180 (Fig. 20), yet basaltic meteorites are moderately common among lunar meteorites from Antarctica and Africa. In detail, both Dhofar 287 and Dhofar 1180 Oman are unique among lunar meteorites.

Feldspathic Lunar Meteorites

Some of the most feldspathic of the lunar meteorites are from Oman (Fig. 20). Of the 12 most feldspathic Omani lunar meteorites (lowest Sc), only Dhofar 1627 is moderately rich in ITEs (Fig. 35) and a candidate for originating in the feldspathic highlands somewhere near the Procellarum KREEP Terrane. The low concentrations of ITEs in the other 11 meteorites, however, do not necessarily provide strong evidence that they originate from the farside or other points distant from the Apollo landing sites or the Procellarum KREEP Terrane (Korotev et al. 2006). There are many small feldspathic rocks in the regoliths of Apollo 16, Apollo 17, and even Apollo 11 with similarly low concentrations of elements associated with KREEP (Fig. 35a).

Except for some granulitic breccias from Apollo 16 and 17 (Lindstrom and Lindstrom 1986), magnesian feldspathic breccias with low concentration ITEs are not as common among 10–100 g Apollo rocks as they are among the Omani lunar meteorites. There may be a size bias, however, in that Cr/Sc ratios for small feldspathic lithic fragments in Apollo regoliths are, on average, the same as that for the lunar meteorites (Fig. 35b), suggesting that Mg' is also the same (Fig. 6b). Thus, high

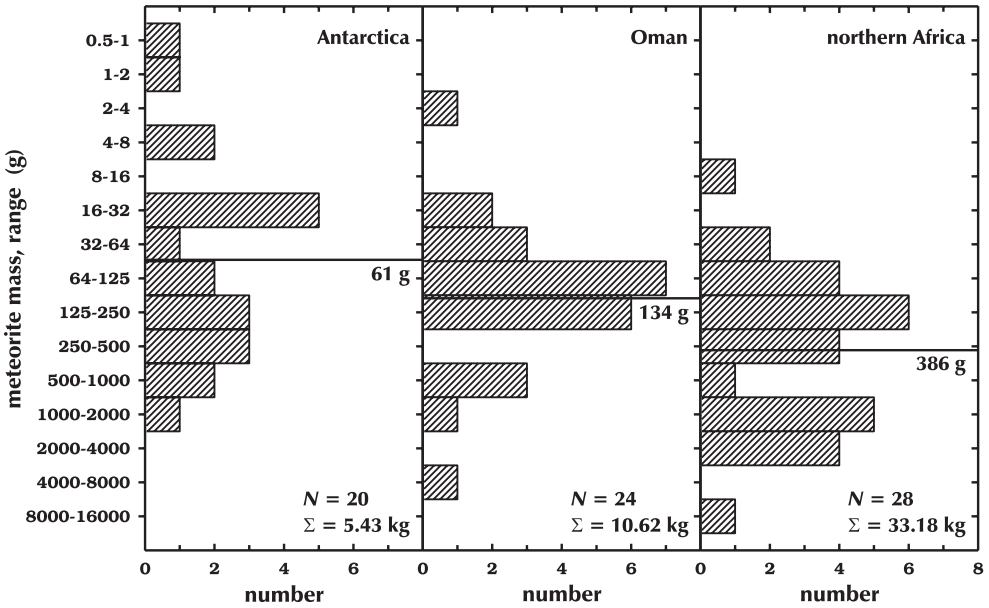

Fig. 33. Comparison of mass distributions of lunar meteorites from Antarctica, Oman, and northern Africa. The African data do not include the largest lunar meteorite, Kalahari 008 and 009 (14.1 kg) from Botswana (Sokol et al. 2008). The horizontal lines represent the geometric mean masses. The masses are sums of all stones of a pair group. Pairing relationships are those inferred in this paper and Korotev (2005), Korotev and Zeigler (2007), and Korotev et al. (2008, 2009a, 2011a, 2012). Pairing relationships are not well established for those from northern Africa. Mass data are from the Meteoritical Bulletin Database (2012).

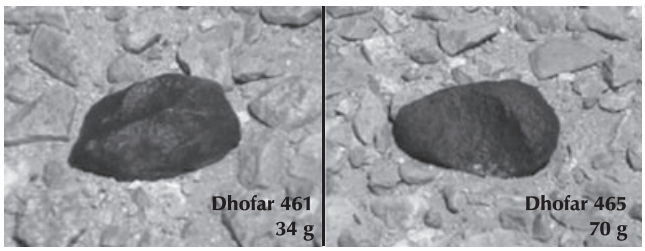

Fig. 34. Lunar-meteorite ventifacts in the field. These stones have clearly lost a substantial portion of their immediate postfall mass. Photos by Luc Labenne.

Mg' for a feldspathic lunar meteorite is not compelling evidence for origination from the far side of the Moon; similar material occurs at the Apollo sites.

Warren et al. (2005) noted that among "KREEP-poor highlands regoliths" (two Apollo samples and five lunar meteorites, including one from Oman, Dhofar 025) Mg' increases with decreasing Al_2O_3 concentration or, by inference, increasing Sc concentration. This trend is seen in Fig. 6a (× symbols). Data for three additional feldspathic regolith breccias (Dhofar 1428, Shişr 160, and Shişr 161) largely conform to the same trend. However, there is little evidence in the lunar meteorites for existence of a mafic, magnesian component. Lithic clasts of mafic, magnesian rocks are rare in the meteorites (Korotev 2005). Three of the four most magnesian of the Omani lunar meteorites (impact-melt and granulitic breccias Dhofar 489 et al. [+], Dhofar 302 [G], and Dhofar 733 [N]; Fig. 6a) are more feldspathic than any of the regolith breccias.

Availability

Except for SaU 169, none of the meteorites discussed here would have been available to scientists were it not for private collectors who are inspired to find them so that they can sell them at prices ranging from 800 to 4500 dollars per gram (this is the range I paid). Of the 60 named stones, I was able to obtain a sample of only one, SaU 169, by request to the museum holding the type specimen. I made requests to museums holding the type specimens for samples in the 0.06–0.3 g mass range of 22 other stones and was refused or ignored. I obtained samples of 8 meteorites from the type specimens as part of the classification process. Samples of another 8 were donated by collectors. I had to purchase samples of 26 stones and I have been unable to obtain samples of 17 of the stones. The availability of these meteorites is ephemeral and the window of opportunity for some of them has been only a week or so. At this writing, it would be challenging to obtain samples of as many as 20 of them.

Acknowledgments—The author thanks Rainer Bartoschewitz, Ted Bunch, Norbert Classen, Don

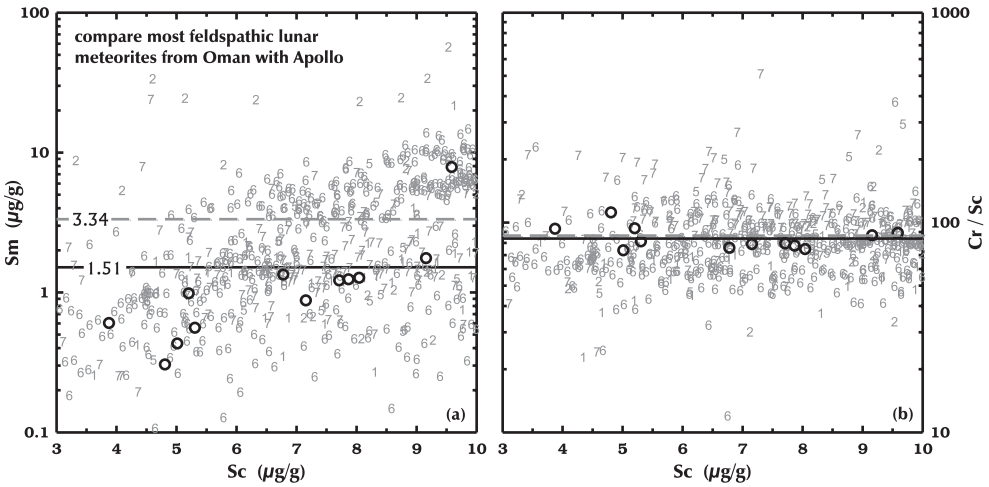

Fig. 35. Comparison of the 12 lowest-Sc lunar meteorites from Oman (circles) with samples of similar Sc concentrations (3–10 μg g^{-1} Sc, or 27.5–32% Al_2O_3, Fig. 3) from the Apollo missions. Each circle represents the mean composition of a meteorite. The Apollo data are from the Apollo reference suite of Korotev et al. (2009). Each point represents a lithic fragment from the 2–4 mm grain-size fraction of regolith from Apollo 11 (symbol 1, $N = 40$), Apollo 12 (2, $N = 22$), Apollo 14 (4, $N = 5$), Apollo 15 (5, $N = 13$), Apollo 16 (6; $N = 408$), and Apollo 17 (7, $N = 119$). The horizontal lines represent the means of each data set. (a) The high-Sm meteorite is Dhofar 1627 (7.7 μg g^{-1} Sm). On average, the Apollo samples are richer in Sm by a factor of 2.2, but many Apollo samples have low Sm similar to the lunar meteorites. (b) Mean Cr/Sc for the two data sets are essentially identical and correspond to a mean Mg' of 69 for the meteorites and 70 for the Apollo samples (Fig. 6b).

Edwards, Jim Haklar, Tony Irving, Luc Labenne, Phil Mani, and an anonymous finder for providing and donating samples. He greatly appreciates reviews of manuscript by Allan Treiman and Cari Corrigan and discussions with Ali Al-Kathiri, Rainer Bartoschewitz, Beda Hofmann, Brad Jolliff, Luc Labenne, Axel Wittmann, and Ryan Zeigler. Also, many thanks to Ryan Zeigler for preparing samples and doing the EMPA analyses of Table 3. This work was funded by NASA grants NNX07AI44G, NNX10AI44G, and NNX11AB26G.

Editorial Handling—Dr. A. J. Timothy Jull

REFERENCES

Al-Kathiri A., Hofmann B. A., Jull A. J. T., and Gnos E. 2005. Weathering of meteorites from Oman: Correlation of chemical and mineralogical weathering proxies with ^{14}C terrestrial ages and the influence of soil chemistry. *Meteoritics & Planetary Science* 40:1215–1239.

Al-Kathiri A., Gnos E., and Hofmann B. A. 2007. The regolith portion of the lunar meteorite Sayh al Uhaymir 169. *Meteoritics & Planetary Science* 42:2137–2152.

Anand M., Taylor L. A., Misra K. C., Demidova S. I., and Nazarov M. A. 2003. KREEPy lunar meteorite Dhofar 287A: A new lunar mare basalt. *Meteoritics & Planetary Science* 38:485–499.

Arai T., Takeda H., Yamaguchi A., and Ohtake M. 2007. Dhofar 489 et al. as ground truth of the lunar farside crust (abstract). Proceedings of the 31st Symposium on Antarctic Meteorites. pp. 3–4.

Baedecker P. A., Chou C.-L., Sundberg L. L., and Wasson J. T. 1972. Extralunar materials in Apollo 16 soils and the decay rate of the extralunar flux 4.0 Gyr ago. *Earth and Planetary Science Letters* 17:79–83.

Bartoschewitz R., Park J., Nagao K., Okazaki R., and Kurtz T. 2009. Lunar meteorite SaU 300—Noble gas record (abstract #5101). *Meteoritics & Planetary Science* 44(Suppl):A30.

Basaltic Volcanism Study Project (BVSP). 1981. Lunar mare basalts. In *Basaltic volcanism on the terrestrial planets*. New York: Pergamon Press. pp. 236–267.

Bischoff A. 2001. Fantastic new chondrites, achondrites, and lunar meteorites as the result of recent meteorite search expeditions in hot and cold deserts. *Earth, Moon and Planets* 85–86:87–97.

Bunch T. E., Wittke J. H., and Korotev R. L. 2006. Petrology and composition of lunar feldspathic breccias NWA 2995, Dhofar 1180 and Dhofar 1428 (abstract #5254). *Meteoritics & Planetary Science* 41(Suppl):A31.

Burns S. J., Fleitmann D., Matter A., Neff U., , and Mangini A. 2001. Speleothem evidence from Oman for continental pluvial events during interglacial periods. *Geology* 29:623–626.

Cahill J. T., Floss C., Anand M., Taylor L. A., Nazarov M. A., and Cohen B. A. 2004. Petrogenesis of lunar highlands meteorites: Dhofar 025, Dhofar 081; Dar al Gani 262, and Dar al Gani 400. *Meteoritics & Planetary Science* 39:503–530.

Cassidy W., Harvey R., Schutt J., Delisle G., and Yanai K. 1992. The meteorite collection sites in Antarctica. *Meteoritics* 27:490–525.

Cohen B. A., James O. B., Taylor L. A., Nazarov M. A., and Barsukova L. D. 2004. Lunar highland meteorite Dhofar 026 and Apollo sample 15418: Two strongly shocked, partially melted, granulitic breccias. *Meteoritics & Planetary Science* 39:1419–1447.

Connolly H. C., Jr., Zipfel J., Folco L., Smith C., Jones R. H., Benedix G., Righter K., Yamaguchi A., Chennaoui Aoudjehane H., and Grossman J. N. 2007. The

Meteoritical Bulletin, No. 91. *Meteoritics & Planetary Science* 42:413–466.

Demidova S. I., Nazarov M. A., Taylor L. A., and Patchen A. 2003a. Dhofar 304, 305, 306 and 307: New lunar highland meteorites from Oman (abstract #1285). 34th Lunar and Planetary Science Conference. CD-ROM.

Demidova S. I., Nazarov M. A., Anand M., and Taylor L. A. 2003b. Lunar regolith breccia Dhofar 287B: A record of lunar volcanism. *Meteoritics & Planetary Science* 38:501–514.

Demidova S. I., Nazarov M. A., Kurat G., Brandstätter F., and Ntaflos T. 2005. New lunar meteorites from Oman: Dhofar 925, 960 and 961, meteorite (abstract #1607). 36th Lunar and Planetary Science Conference. CD-ROM.

Demidova S. I., Nazarov M. A., Lorenz C. A., Kurat G., Brandstätter F., and Ntaflos T. 2007. Chemical composition of lunar meteorites and the lunar crust. *Petrology* 15:386–407.

Fagan T. J., Taylor G. J., Keil K., Bunch T. E., Wittke J. H., Korotev R. L., Jolliff B. L., Gillis J. J., Haskin L. A., Jarosewich E., Clayton R. N., Mayeda T. K., Fernandes V. A., Burgess R., Turner G., Eugster O., and Lorenzetti S. 2002. Northwest Africa 032: Product of lunar volcanism. *Meteoritics & Planetary Science* 37:371–394.

Fernandes V. A., Anand M., Burgess R., and Taylor L. A. 2004. Ar-Ar studies of Dhofar clast-rich feldspathic highland meteorites: 025, 026, 280, 303 (abstract #1514). 35th Lunar and Planetary Science Conference. CD-ROM.

Foreman A. B., Korotev R. L., Jolliff B. L., and Zeigler R. A. 2008. Petrography and geochemistry of Dhofar 733—An unusually sodic, feldspathic lunar meteorite (abstract #1853). 39th Lunar and Planetary Science Conference. CD-ROM.

Foreman A. B., Korotev R. L., Zeigler R. A., Wittmann A., Kring D. A., Irving A. J., and Kuehner S. M. 2009. Petrographic and geochemical analysis of feldspathic lunar meteorite Shisr 161 (abstract #2304). 40th Lunar and Planetary Science Conference. CD-ROM.

Gnos E., Hofmann B. A., Al-Kathiri A., Lorenzetti S., Eugster O., Whitehouse M. J., Villa I., Jull A. J. T., Eikenberg J., Spettel B., Krähenbühl U., Franchi I. A., and Greenwood G. C. 2004. Pinpointing the source of a lunar meteorite: Implications for the evolution of the Moon. *Science* 305:657–659.

Greshake A., Schmitt R. T., Stöffler D., Pätsch M., and Schultz L. 2001. Dhofar 081: A new lunar highland meteorite. *Meteoritics & Planetary Science* 36:459–470.

Grossman J. N. 2000. The Meteoritical Bulletin, No. 84. *Meteoritics & Planetary Science* 35:A199–A225.

Grossman J. N. and Zipfel J. 2001. The Meteoritical Bulletin, No. 85. *Meteoritics & Planetary Science* 36:A293–A322.

Haloda J., Týcová P., Korotev R. L., Fernandes V. A., Burgess R., Thöni M., Jelenc M., Jakeš P., Gabzdyl P., and Košler J. 2009. Petrology, geochemistry, and age of low-Ti mare-basalt meteorite Northeast Africa 003-A: A possible member of the Apollo 15 mare basaltic suite. *Geochimica et Cosmochimica Acta* 73:3450–3470.

Haskin L. A. and Warren P. H. 1991. Lunar chemistry. In *Lunar sourcebook*, edited by Heiken G., Vaniman D., and French B. M. Cambridge: Cambridge University Press. pp. 357–474.

Hidaka Y., Yamaguchi A., and Ebihara M. 2009. Geochemistry and petrology of lunar meteorite Dhofar 1428 (abstract #5329). *Meteoritics & Planetary Science* 44:A91.

Hidaka Y., Yamaguchi A., and Ebihara M. 2010a. Trace element characteristics of a lunar meteorite Dhofar 1428 (abstract #5308). *Meteoritics & Planetary Science* 45(Suppl):A81.

Hidaka Y., Yamaguchi A., and Ebihara M. 2010b. Chemical compositions of lunar meteorite Dhofar 1428 (abstract). Proceedings of the 33rd Symposium on Antarctic Meteorites. pp. 19–20.

Hofmann B. A., Gnos E., Eggenberger U., Zurfluh F. J., Boschetti S., and Al-Rajhi A. 2011. The Omani-Swiss meteorite search project—Recent campaigns and outlook (abstract #5441). *Meteoritics & Planetary Science* 46(Suppl):A97.

Hsu W., Zhang A., Guan Y., Ushikubo T., and Bartoschewitz R. 2007. Sayh al Uhaymir 300: Petrology, mineralogy, and trace element geochemistry (abstract #1149). 38th Lunar and Planetary Science Conference. CD-ROM.

Hsu W., Zhang A., Bartoschewitz R., Guan Y., Ushikubo T., Krähenbühl U., Niedergesaess R., Pepelnik R., Reus U., Kurtz T., and Kurtz P. 2008. Petrography, mineralogy, and geochemistry of lunar meteorite Sayh al Uhaymir 300. *Meteoritics & Planetary Science* 43:1363–1381.

Hudgins J. A., Walton E. L., and Spray J. G. 2007. Mineralogy, petrology, and shock history of lunar meteorite Sayh al Uhaymir 300: A crystalline impact-melt breccia. *Meteoritics & Planetary Science* 42:1763–1779.

Hudgins J. A., Spray J. G., Kelley S. P, Korotev R. L., and Sherlock S. C. 2008. A laser probe $^{40}Ar/^{39}Ar$ and INAA investigation of four Apollo granulitic breccias. *Geochimica et Cosmochimica Acta* 72:5799–5818.

Hudgins J. A., Kelley S. P., Korotev R. L., and Spray J. G. 2011. Mineralogy, geochemistry, and $^{40}Ar—^{39}Ar$ geochronology of lunar granulitic breccia Northwest Africa 3163 and paired stones: Comparisons with Apollo samples. *Geochimica et Cosmochimica Acta* 75:2865–2881.

Jolliff B. L. and Haskin L. A. 1995. Cogenetic rock fragments from a lunar soil: Evidence of a ferroan noritic–anorthosite pluton on the Moon. *Geochimica et Cosmochimica Acta* 59:2345–2374.

Jolliff B. L., Korotev R. L., and Haskin L. A. 1991. A ferroan region of the lunar highlands as recorded in meteorites MAC 88104 and MAC 88105. *Geochimica et Cosmochimica Acta* 55:3051–3071.

Jolliff B. L., Korotev R. L., and Haskin L. A. 1993. Lunar basaltic meteorites Yamato-793169 and Asuka-881757: Samples of the same low-Ti mare-lava? Eighteenth Symposium on Antarctic Meteorites. pp. 214–217.

Jolliff B. L., Rockow K. M., Korotev R. L., and Haskin L. A. 1996. Lithologic distribution and geologic history of the Apollo 17 site: The record in soils and small rock particles from the highlands massifs. *Meteoritics & Planetary Science* 31:116–145.

Joy K. H., Crawford I. A., Russell S. S., and Kearsley A. T. 2010. Lunar meteorite regolith breccias: An in situ study of impact melt composition using LA-ICP-MS with implications for the composition of the lunar crust. *Meteoritics & Planetary Science* 45:917–946.

Koeberl C., Kurat G., and Brandstätter F. 1991. MAC 88105—A regolith breccia from the lunar highlands: Mineralogical, petrological, and geochemical studies. *Geochimica et Cosmochimica Acta* 55:3073–3087.

Korochantseva E. V., Trieloff M., Hopp J., Buykin A. I., and Korochantsev A. V. 2009. ^{40}Ar-^{39}Ar dating of solar gas-rich lunar meteorite Dhofar 1436 (abstract #5226). *Meteoritics & Planetary Science* 44:A113.

Korotev R. L. 1982. Comparative geochemistry of Apollo 16 surface soils and samples from cores 64002 and 60002 through 60007. 13th Lunar and Planetary Science Conference, in *Journal of Geophysical Research* 87:A269–A278.

Korotev R. L. 1987. Mixing levels, the Apennine Front soil component, and compositional trends in the Apollo 15 soils. 17th Lunar and Planetary Science Conference, in *Journal of Geophysical Research* 92:E411–E431.

Korotev R. L. 1996. On the relationship between the Apollo 16 ancient regolith breccias and feldspathic fragmental breccias, and the composition of the prebasin crust in the Central Highlands of the Moon. *Meteoritics & Planetary Science* 31:403–412.

Korotev R. L. 1997. Some things we can infer about the Moon from the composition of the Apollo 16 regolith. *Meteoritics & Planetary Science* 32:447–478.

Korotev R. L. 2005. Lunar geochemistry as told by lunar meteorites. *Chemie der Erde* 65:297–346.

Korotev R. L. 2006. New geochemical data for a some poorly characterized lunar meteorites (abstract #1404). 37th Lunar and Planetary Science Conference. CD-ROM.

Korotev R. L. and Morris R. V. 1993. Composition and maturity of Apollo 16 regolith core 60013/14. *Geochimica et Cosmochimica Acta* 57:4813–4826.

Korotev R. L. and Zeigler R. A. 2007. Keeping up with the lunar meteorites (abstract #1340). 38th Lunar and Planetary Science Conference. CD-ROM.

Korotev R. L., Jolliff B. L., and Rockow K. M. 1996. Lunar meteorite Queen Alexandra Range 93069 and the iron concentration of the lunar highlands surface. *Meteoritics & Planetary Science* 31:9–24.

Korotev R. L., Jolliff B. L., Zeigler R. A., Gillis J. J., and Haskin L. A. 2003a. Feldspathic lunar meteorites and their implications for compositional remote sensing of the lunar surface and the composition of the lunar crust. *Geochimica et Cosmochimica Acta* 67:4895–4923.

Korotev R. L., Jolliff B. L., Zeigler R. A., and Haskin L. A. 2003b. Compositional constraints on the launch pairing of three brecciated lunar meteorites of basaltic composition. *Antarctic Meteorite Research* 16:152–175.

Korotev R. L., Zeigler R. A., and Jolliff B. L. 2006. Feldspathic lunar meteorites Pecora Escarpment 02007 and Dhofar 489: Contamination of the surface of the lunar highlands by post-basin impacts. *Geochimica et Cosmochimica Acta* 70:5935–5956.

Korotev R. L., Irving A. J., and Bunch T. E. 2008. Keeping up with the lunar meteorites—2008 (abstract #1209). 39th Lunar and Planetary Science Conference. CD-ROM.

Korotev R. L., Zeigler R. A., Irving A. J., and Bunch T. E. 2009a. Keeping up with the lunar meteorites—2009 (abstract #1137). 40th Lunar and Planetary Science Conference. CD-ROM.

Korotev R. L., Zeigler R. A., Jolliff B. L., Irving A. J., and Bunch T. E. 2009b. Compositional and lithological diversity among brecciated lunar meteorites of intermediate iron composition. *Meteoritics & Planetary Science* 44:1287–1322.

Korotev R. L., Jolliff B. L., and Carpenter P. K. 2011a. Miller Range feldspathic lunar meteorites (abstract #1999). 42th Lunar and Planetary Science Conference. CD-ROM.

Korotev R. L., Jolliff B. L., Zeigler R. A., Seddio S. M., and Haskin L. A. 2011b. Apollo 12 revisited. *Geochimica et Cosmochimica Acta* 75:1540–1573.

Korotev R. L., Irving A. J., and Bunch T. E. 2012. Keeping up with the lunar meteorites—2012 (abstract #1152). 44th Lunar and Planetary Science Conference. CD-ROM.

Kuehner S. M., Irving A. J., Gellissen M., and Korotev R. L. 2010. Petrology and composition of lunar troctolitic granulite Northwest Africa 5744: A unique recrystallized, magnesian crustal sample (abstract #1552). 41st Lunar and Planetary Science Conference. CD-ROM.

Leont'eva E. M., Matukov D. I., Nazarov M. A., Sergeev S. A., Shukolyukov Y. A., and Brandstaetter F. 2005. First determination of the isotopic age of a lunar meteorite by the uranium-lead zircon method. *Petrology* 13:193–196.

Lin Y., Shen W., Liu Y., Xu L., Hofmann B. A., Mao Q., Tang G. Q., Wu F., and Li X. H. 2012. Very high-K KREEP-rich clasts in the impact melt breccia of the lunar meteorite SaU 169: New constraints on the last residue of the Lunar Magma Ocean. *Geochimica et Cosmochimica Acta* 85:19–40.

Lindstrom M. M. and Lindstrom D. J. 1986. Lunar granulites and their precursor anorthositic norites of the early lunar crust. 16th Lunar and Planetary Science Conference, in *Journal of Geophysical Research* 91:D263–D276.

Lindstrom M. M., Wentworth S. J., Martinez R. R., Mittlefehldt D. W., McKay D. S., Wang M.-S., and Lipschutz M. J. 1991. Geochemistry and petrography of the MacAlpine Hills lunar meteorites. *Geochimica et Cosmochimica Acta* 55:3089–3103.

Liu Y., Zhang A., and Taylor L. A. 2009. Fragments of asteroids in lunar rocks (abstract #5434). *Meteoritics & Planetary Science* 44(Suppl): A123.

Liu D., Jolliff B. L., Zeigler R. A., Korotev R. L., Wan Y., Xie H., Zhang Y., Dong C., and Wang W. 2012. Comparative zircon U-Pb geochronology of impact melt breccias from Apollo 12 and lunar meteorite SaU 169, and the age of the Imbrium impact. *Earth and Planetary Science Letters* 319–320:277–286.

Lorenzetti S., Busemann H., and Eugster O. 2005. Regolith history of lunar meteorites. *Meteoritics & Planetary Science* 40:315–327.

McKay D. S., Bogard D. D., Morris R. V., Korotev R. L., Johnson P., and Wentworth S. J. 1986. Apollo 16 regolith breccias: Characterization and evidence for early formation in the mega-regolith. 16th Lunar and Planetary Science Conference, in *Journal of Geophysical Research* 91(B4): D277–D303.

Meteoritical Bulletin Database. 2012. http://www.lpi.usra.edu/meteor/metbull.php. Accessed February 1, 2012.

Nazarov M. A., Demidova S. I., Patchen A., and Taylor L. A. 2002. Dhofar 301, 302 and 303: Three new lunar highland meteorites from Oman (abstract #1293). 33rd Lunar and Planetary Science Conference. CD-ROM.

Nazarov M. A., Demidova S. I., and Taylor L. A. 2003. Trace element chemistry of lunar highland meteorites from Oman (abstract #1636). 34th Lunar and Planetary Science Conference. CD-ROM.

Nazarov M. A., Badyukov D. D., Lorents K. A., and Demidova S. I. 2004. The flux of lunar meteorites onto the Earth. *Solar System Research* 38:49–58.

Neal C. R., Taylor L. A., and Lindstrom M. M. 1988. Apollo 14 mare basalt petrogenesis: Assimilation of KREEP-like components by a fractionating magma.

Proceedings, 18th Lunar and Planetary Science Conference. pp. 139–153.
Nishiizumi K. and Caffee M. W. 2001. Exposure histories of lunar meteorites Dhofar 025, 026, and Northwest Africa 482 (abstract #5411). *Meteoritics & Planetary Science* 36:A148.
Nishiizumi K. and Caffee M. W. 2006. Constraining the number of lunar and Martian meteorite falls (abstract #5368). *Meteoritics & Planetary Science* 41(Suppl):A133.
Nishiizumi K., Okazaki R., Park J., Nagao K., Masarik J., and Finkel R. C. 2002. Exposure and terrestrial history of Dhofar 019 Martian meteorite (abstract #1366). 33rd Lunar and Planetary Science Conference. CD-ROM.
Nishiizumi K., Hillegonds D. J., McHargue L. R., and Jull A. J. T. 2004. Exposure and terrestrial histories of new lunar and Martian meteorites (abstract #1130). 35th Lunar and Planetary Science Conference. CD-ROM.
Nyquist L. E., Shih C.-Y., Reese Y. D., Park J., Bogard D. D., Garrison D. H., and Yamaguchi A. 2010. Lunar crustal history recorded in lunar anorthosites (abstract #1383). 41st Lunar and Planetary Science Conference. CD-ROM.
Palme H., Spettel B., Weckwerth G., and Wänke H. 1983. Antarctic meteorite ALHA81005, a piece from the ancient lunar crust. *Geophysical Research Letters* 10:817–820.
Palme H., Spettel B., Jochum K. P., Dreibus G., Weber H., Weckwerth G., Wänke H., Bischoff A., and Stöffler D. 1991. Lunar highland meteorites and the composition of the lunar crust. *Geochimica et Cosmochimica Acta* 55:3105–3122.
Rambaldi E. R. 1977. Trace element content of metals from H- and LL-group chondrites. *Earth and Planetary Science Letters* 36:347–358.
Russell S. S., Zipfel J., Grossman J. N., and Grady M. M. 2002. The Meteoritical Bulletin, No. 86. *Meteoritics & Planetary Science* 37:A157–A184.
Russell S. S., Zipfel J., Folco L., Jones R., Grady M. M., McCoy T., and Grossman J. N. 2003. The Meteoritical Bulletin, No. 87. *Meteoritics & Planetary Science* 38:A189–A248.
Russell S. S., Folco L., Grady M. M., Zolensky M., Jones R., Righter K., Zipfel J., and Grossman J. N. 2004. The Meteoritical Bulletin, No. 88. *Meteoritics & Planetary Science* 39(Suppl):A215–A272.
Russell S. S., Zolensky M., Righter K., Folco L., Jones R., Connolly H. C., Jr., Grady M. M., and Grossman J. N. 2005. The Meteoritical Bulletin, No. 89. *Meteoritics & Planetary Science* 40:A201–A263.
Shih C.-Y., Nyquist L. E., Reese Y., Wiesmann H., Nazarov M. A., and Taylor L. A. 2002. The chronology and petrogenesis of the mare basalt clast from lunar meteorite Dhofar 287: Rb-Sr and Sm-Nd isotopic studies (abstract #1344). 33rd Lunar and Planetary Science Conference. CD-ROM.
Shukolyukov Y. A., Nazarov M. A., Pätsch M., and Schultz L. 2001. Noble gases in three lunar meteorites from Oman (abstract #1502). 32nd Lunar and Planetary Science conference. CD-ROM.
Shukolyukov Y. A., Nazarov M. A., and Ott U. 2004. Noble gases in new lunar meteorites from Oman: Irradiation history, trapped gases, and cosmic-ray exposure and K-Ar ages. *Geochemistry International* 42:1001–1017.
Sokol A. K., Fernandes V. A., Schulz T., Bischoff A., Burgess R., Clayton R. N., Münker C., Nishiizumi K., Palme H., Schultz L., Weckwerth G., Mezger K., and Horstmannaan M. 2008. Geochemistry, petrology and ages of the lunar meteorites Kalahari 008 and 009: New constraints on early lunar evolution. *Geochimica et Cosmochimica Acta* 72:4845–4873.
Stöffler D., Knöll H.-D., Marvin U. B., Simonds C. H., and Warren P. H. 1980. Recommended classification and nomenclature of lunar highlands rocks—A committee report. In *Proceedings of the Conference on the Lunar Highlands Crust*, edited by Papike J. J. and Merrill R. B. New York: Pergamon Press. pp. 51–70.
Takeda H., Yamaguchi A., Bogard D. D., Karouji Y., Ebihara M., Ohtake M., Saiki K., and Arai T. 2006. Magnesian anorthosites and a deep crustal rock from the farside crust of the moon. *Earth and Planetary Science Letters* 247: 171–184.
Takeda H., Arai T., Yamaguchi A., Otuki M., and Ishii T. 2007. Mineralogy of Dhofar 309, 489 and Yamato-86032 and varieties of lithologies of the lunar farside crust (abstract #1607). 38th Lunar and Planetary Science Conference. CD-ROM.
Takeda H., Arai T., Yamaguchi A., Otsuki M., and Ohtake M. 2008. Granulitic lithologies in Dhofar 307 lunar meteorite and magnesian, Th-poor terrane of the northern farside crust (abstract #1574). 39th Lunar and Planetary Science Conference. CD-ROM.
Takeda H., Karouji Y., Ogawa Y., Otsuki M., Yamaguchi A., Ohtake M., Arai T., Matsunaga T., and Haruyama J. 2009. Iron contents of plagioclases in Dhofar 307 lunar meteorite and surface materials of the farside large basins (abstract #1565). 40th Lunar and Planetary Science Conference. CD-ROM.
Takeda H., Kobayashi S., Yamaguchi A., Otsuki M., Ohtake M., Haruyama J., Morota T., Karouji Y., Hasebe N., Nakamura R., Ogawa Y., and Matsunaga T. 2010. Olivine fragments in Dhofar 307 lunar meteorite and surface materials of the farside large basins (abstract #1572). 41st Lunar and Planetary Science Conference. CD-ROM.
Terada K., Sasaki Y., Anand M., Sano Y., Taylor L. A., and Horie K. 2008. Uranium–lead systematics of low-Ti basaltic meteorite Dhofar 287A: Affinity to Apollo 15 green glasses. *Earth and Planetary Science Letters* 270:119–124.
Treiman A. H., Maloy A. K., Shearer C. K., Jr., and Gross J. 2010. Magnesian anorthositic granulites in lunar meteorites Allan Hills A81005 and Dhofar 309: Geochemistry and global significance. *Meteoritics & Planetary Science* 45:163–180.
Warren P. H. and Kallemeyn G. W. 1991. The MacAlpine Hills lunar meteorite and implications of the lunar meteorites collectively for the composition and origin of the Moon. *Geochimica et Cosmochimica Acta* 55:3123–3138.
Warren P. H., Ulff-Møller F., and Kallemeyn G. W. 2005. "New" lunar meteorites: Impact melt and regolith breccias and large-scale heterogeneities of the upper lunar crust. *Meteoritics & Planetary Science* 40:989–1014.
Wasson J. T., and Kallemeyn G. W. 1988. Compositions of chondrites. *Philosophical Transactions of the Royal Society of London A* 325:535–544.
Wasson J. T. and Kallemeyn G. W. 2002. The IAB iron-meteorite complex: A group, five subgroups, numerous grouplets, closely related, mainly formed by crystal segregation in rapidly cooled melts. *Geochimica et Cosmochimica Acta* 66:2445–2473.
Wasson J. T., Boynton W. V., Chou C.-L., and Baedecker P. A. 1975. Compositional evidence regarding the influx of interplanetary materials onto the lunar surface. *The Moon* 13:121–141.

Weisberg M. K., Smith C., Benedix G., Folco L., Righter K., Zipfel J., Yamaguchi A., and Chennaoui Aoudjehane H. 2009. The Meteoritical Bulletin, No. 95. *Meteoritics & Planetary Science* 44:429–462.

Zeigler R. A., Korotev R. L., Jolliff B. L., and Haskin L. A. 2005. Petrology and geochemistry of the LaPaz icefield basaltic lunar meteorite and source-crater pairing with Northwest Africa 032. *Meteoritics & Planetary Science* 40:1073–1102.

Zeigler R. A., Korotev R. L., and Jolliff B. L. 2007. Petrography, geochemistry, and pairing relationships of basaltic lunar meteorite stones NWA 773, NWA 2700, NWA 2727, NWA 2977, and NWA 3160 (abstract #2109). 38th Lunar and Planetary Science Conference. CD-ROM.

Zeigler R. A., Jolliff B. L., and Korotev R. L. 2010. Petrography and pairing relationships of lunar meteorites Sayh al Uhaymir 449 and Dhofar 925, 960, and 961 (abstract #1985). 41st Lunar and Planetary Science Conference. CD-ROM.

Zeigler R. A., Korotev R. L., and Jolliff B. L. 2011. Petrography and geochemistry of lunar meteorite Dhofar 1442 (abstract #1012). 42nd Lunar and Planetary Science Conference. CD-ROM.

Zhang A. and Hsu W. 2009. Petrography, mineralogy, and trace element geochemistry of lunar meteorite Dhofar 1180. *Meteoritics & Planetary Science* 44:1265–1286.

Zhang A. C., Hsu W. B., Liu Y., and Taylor L. A. 2009. Petrography and mineralogy of Dhofar 1428 lunar highland regolith breccia (abstract #5096). *Meteoritics & Planetary Science* 44:A226.

Zhang A.-C., Hsu W.-B., Li X.-H., Ming H.-L., Li Q.-L., Liu Y., and Tang G.-Q. 2011. Impact melting of lunar meteorite Dhofar 458: Evidence from polycrystalline texture and decomposition of zircon. *Meteoritics & Planetary Science* 46:103–115.

Zurfluh F. J., Hofmann B. A., Gnos E., Eggenberger U., Villa I. M., Greber N. D., and Jull A. J. T. 2011. New insights into the strontium contamination of meteorites outlook (abstract #5229). *Meteoritics & Planetary Science* 46(Suppl):A264.

SUPPORTING INFORMATION

Additional supporting information may be found in the online version of this article.

Data S1. INAA data for 280 subsamples of lunar meteorites from Oman.

Please note: Wiley-Blackwell is not responsible for the content or functionality of any supporting materials supplied by the authors. Any queries (other than missing material) should be directed to the corresponding author for the article.